A positron lifetime study of properties of light particles in liquids

Jacobsen, F.M.

Publication date:
1981

Document Version
Publisher's PDF, also known as Version of record

Risø-R-433

RISØ

Risø-R-433

A Positron Lifetime Study of Properties of Light Particles in Liquids

Finn M. Jacobsen

Risø National Laboratory, DK-4000 Roskilde, Denmark
April 1981

RISØ-R-433

A POSITRON LIFETIME STUDY OF PROPERTIES OF LIGHT PARTICLES IN LIQUIDS

Finn M. Jacobsen
Chemistry Department

Abstract. The positron lifetime technique has been used for studying the behaviour of the three light particles: the positron, positronium (Ps) (a bound state of an electron and positron), and excess electron in non-polar liquids. A brief introduction to the subject and a short description of the experimental techniques are given. Further, the principles of the data analyses are discussed in some detail. Positron lifetime measurements have been performed on the liquids: SF_6, neopentane, hexane, and two viscoelastic organic liquids. The experiments have been performed as function of temperature, e.g., from just above the melting point to above the critical point in the cases of liquid SF_6 and neopentane. In all of the liquids the experimental results show that Ps is formed. The analyses of the lifetime spectra show that the Ps yields as well as the state of Ps in these liquids change with temperature. A detailed discussion of the

(continue on next page)

April 1981
Risø National Laboratory, DK 4000 Roskilde, Denmark

state of Ps in liquids is given. The present results can be explained fairly well in terms of the Ps bubble model. In liquid SF_6 the experimental results strongly indicate that ortho-Ps can annihilate from two different states. The longest-lived ortho-Ps state seems to be similar to that observed in most liquids while the shortest-lived state seems not to have been observed in any other liquids before. A detailed discussion of the measured Ps yield in liquid neopentane and hexane is given. The Ps yield is interpreted by means of the positron spur model.

INIS descriptors: 2-2-DIMETYLPROPANE; ANNIHILATION; BUBBLES; EXPERIMENTAL DATA; GLASS; HEXANE; LIFETIME; LIQUIDS; PHASE TRANSFORMATIONS; POSITRONIUM; POSITRONS; SPURS; SULFUR FLUORIDES; TEMPERATURE DEPENDENCE; TIME RESOLUTION; VISCOSITY.

UDC 539.124.6 : 539.189.2 : 546.22'161-14

ISBN 87-550-0758-9
ISSN 0106-2840

Risø Repro 1981

CONTENTS

1. INTRODUCTION

1.1. How the positron "entered" into the world of physics

One of the strangest and at the same time most fascinating consequences of the theory of quantum electrodynamics is that it has led to the acknowledgment that matter and anti-matter exist together in the Universe. To every particle there exists an anti-particle and, as shown by experiments and theory, particle-anti-particle pairs can be created from photons or they can annihilate into photons and/or other similar pairs.

As early as 1905 Einstein showed in his work on the special theory of relativity that the energy, ε, of a particle is related to its momentum, p, as

$$\varepsilon^2 = p^2c^2 + m^2c^4 \qquad (1)$$

where m is the mass of the particle and c the speed of light in vacuo. The derivation of (1) is based only on the single experimental observation that the speed of light does not depend on the inertial frame of the observer (Michelson and Morley, 1887). In the special case of p = 0, we obtain from Eq. (1) the famous relation

$$\varepsilon = mc^2 \qquad (2)$$

which expresses the equivalence between energy and mass.

In the first decades of the 20th century the understanding of the detailed behaviour of electrons in atoms/molecules came about through a self-consistent theory, quantum mechanics. However, the theory of quantum mechanics was able to describe the motion of electrons only as long as their velocities were well below that of light. That is, the theory of quantum mechanics does not include relativistic effects. In 1926 Gordon, Klein, and Fock formulated a relativistic quantum mechanical theory by

using the operators for energy and momentum as developed in the non-relativistic quantum mechanics, together with the relativistic relation between energy and momentum given by Einstein (Eq. (1)). However, two principal problems were associated with their equation of motion: 1) It contained the second derivative with respect to time, and 2) it gave solutions with both positive and negative energies. The former inferred that the probability density of the particle coordinates could take either positive, negative, or zero values.

In 1928, Dirac succeeded in constructing a relativistic equation of motion which contained only the first derivative with respect to time. Dirac started from the requirement that the equation of motion should lead to a positive probability of charge density. In doing so Dirac obtained a four component wave-equation. However, the solutions of the equation still contained both positive and negative values of the energy. Due to the requirement of a positive probability of charge density, the solutions with negative energies could be associated with positive particles and Dirac tried to combine these solutions with the properties of the proton. It was soon shown, however, that these solutions had to be connected to particles with mass close to that of the electron. It should be remembered that the proton and the electron were the only elementary particles known at that time. Then, in 1930, Dirac postulated his famous "hole" theory in which the "negative energy electron states" were normally all occupied. However, by exciting an electron from the "negative energy states" to the positive states a positive hole would be created which could be associated with the possible existence of a positive electron. Two years later the existence of the positive electron was experimentally verified by Anderson (1932). After a careful analysis of a photographic plate showing the tracks of high-energy cosmic radiation in a magnetic field, Anderson came to the conclusion that one of these tracks must be associated with a positive particle with mass close to that of the electron. Anderson did not know Dirac's theory. It was not until 1933, when Blackett and Occhialini gave further experimental evidence of the existence of positive electrons, that it was demonstrated that the experimentally observed properties of the new particle

were those predicted by Dirac. Thus, the existence of the positive electron, or positron, was established completely independently from theoretical and experimental work.

In 1934, Mohorovicic suggested that an electron and positron might form a hydrogen-like bound state. In 1945, the bound state of an electron and a positron was named positronium (Ruark, 1945). From that time the properties of the positronium atom were extensively investigated from a theoretical point of view (Wheeler (1946), Pirenne (1947), Berestetzkii (1949), and Ferrell (1951)). In 1951, Deutsch discovered the positronium atom experimentally. He measured the positron lifetime decay spectra in various gases and observed that a small addition of NO to e.g. N_2 caused a very rapid annihilation of the positrons compared to pure N_2. This enhancement of the decay rate was interpreted as convertion of ortho-Ps into para-Ps by an electron exchange with the unpaired electron in NO.

1.2. Physical properties of the positron and the positronium atom

In Dirac's theory it was shown that an electron and a positron can annihilate together. Dirac visualized this behaviour of an electron-positron system by saying that an electron with positive energy may fall down in a hole in the "negative energy electron states". The energy released in such a transition is given by Eq. (1). In a non-relativistic approximation the "annihilation energy" is:

$$\varepsilon = 2m_e c^2 + E_+ + E_- \qquad (3)$$

where $m_e c^2$ is the rest mass energy of the electron (0.511 MeV) and E_+ and E_- are the kinetic energy of the positron and the electron, respectively. The "annihilation energy" or transition energy is normally emitted as photons.

The number and properties of the annihilation photons depend upon the state of the electron-positron system through the usual conservation rules. Thus, knowledge of the properties of the

annihilation photons provides information of the electron-positron state. The number of photons emitted depends on the conservation of the charge parity and momentum. The charge parity of an electron-positron system is given by $P_c = P_i P_\ell P_\sigma$ (Akhiezer and Berestetzkii, 1965), where P_i, P_ℓ, and P_σ are the internal parity (= -1 for a particle - anti-particle system), the spatial parity (= $(-1)^\ell$), and the spin parity (= $-(-1)^\sigma$), respectively. The charge parity of a system consisting of n photons is $P_c = (-1)^n$. In the case of $\ell = 0$ the charge parity of a positron-electron state is given by $P_c = (-1)^\sigma$. Thus, if the spins of the electron and the positron are anti-parallel ($\sigma = 0$) then $P_c = 1$ and hence an even number of photons must be emitted in the annihilation process. If the two spins are parallel ($\sigma = 1$) then $P_c = -1$ and the annihilation process must be accompanied by emission of an odd number of photons.

The probability of emitting n photons in an annihilation process decreases roughly as α^n, where α is the fine-structure constant ($\alpha = e^2/(4\pi\varepsilon_o hc) = 1/137$). Hence, in the annihilation process of an electron-positron system the emission of the lowest number of photons will be dominant, in agreement with the conservation of the charge parity. On the other hand, the emission of a single photon requires that a third body takes part in the process in order to conserve the momentum. The involvement of a third body in the annihilation process, however, reduces the annihilation probability further by a factor roughly equal to α^3. Thus, the most significant annihilation channels are those in which two ($\sigma = 0$), and three photons ($\sigma = 1$) are emitted. The cross-section, $\sigma_{2\gamma}$, for 2-photon annihilation of a free positron and free electron was calculated by Dirac (1930) as:

$$\sigma_{2\gamma} = 2\pi r_e^2/(\tau\gamma)\{(\gamma+8(\tau-1))\ln(\tau/2-1+\tfrac{1}{2}\sqrt{\gamma})-(\tau+4)\sqrt{\gamma}\} \qquad (4)$$

where $\tau = 2(1+\varepsilon_-/m_e c^2)$, $\gamma = \tau(\tau-4)$, and r_e is the classical radius of the electron. In Eq. (4) we have assumed the positron to be at rest. Thus, ε_- represents the total energy of the electron (Eq. (1)). In a non-relativistic approximation $\tau \to 4$ and $\gamma \to 4\,(v/c)^2$. Hence, in the case of $v \ll c$ Eq. (4) reduces to:

$$\sigma_{2\gamma} = \pi r_e^2 (c/v) \tag{5}$$

For free positrons to a very good approximation three-photon annihilation can be neglected. Hence, the annihilation rate of free positrons, λ_f, can be calculated from Eq. (5) as:

$$\lambda_f = nv\sigma_{2\gamma} = \pi r_e^2 nc \tag{6}$$

where n is the density of electrons at the positron.

Let us consider a two-photon annihilation process. The conservation of energy and momentum can be expressed through the four-vectors of momentum of the partieles, $\tilde{p} = (p^o, \bar{p})$ and the photons $\hbar\tilde{k} = \hbar(k^o, \bar{k})$ as:

$$\tilde{p}_- + \tilde{p}_+ = \hbar(\tilde{k}_1 + \tilde{k}_2) \tag{7}$$

where $\bar{p}$ is the usual three-dimensional momentum vector, and $\bar{k}$ the three-dimensional wave vector, while p^o and k^o are, respectively, ε/c and ω/c, where ε is given by Eq. (1) and ω the angular frequency; and $|\bar{k}| = \omega/c$. Recalling the definition of a scalar product of two four-vectors: $\tilde{p}_\alpha \tilde{p}_\beta = p_\alpha^o p_\beta^o - \bar{p}_\alpha \bar{p}_\beta$ we obtain by squaring Eq. (7):

$$m_e^2c^2 + m_e^2c^2\{1 + 1/(m_e^2c^2)[|\bar{p}_+|^2 + |\bar{p}_-|^2] + 1/(m_e^4c^4)|\bar{p}_-|^2|\bar{p}_+|^2\}^{\frac{1}{2}}$$
$$-\bar{p}_-\bar{p}_+ = (\hbar/c)^2\omega_1\omega_2(1 - \cos(\theta)) \tag{8}$$

where θ is the angle between the directions of the emission of the two annihilation photons. Until now no approximations have been introduced. However, in many cases of experimental interest the kinetic energies of the positrons and "annihilation electrons" will be much less than $m_e c^2$. Hence, the square root on the LHS of Eq. (7) is approximately equal to: $(1 + x)^{\frac{1}{2}} \approx 1 + \frac{1}{2}x$ Thus, by using the above and Eq. (8) we have:

$$4m_e^2c^2 + |\bar{p}_+|^2 + |\bar{p}_-|^2 + (m^2c^2)^{-1}|\bar{p}_+|^2|\bar{p}_-|^2 - 2\bar{p}_+\bar{p}_-$$
$$= 2(\hbar/c)^2\omega_1\omega_2(1 - \cos(\theta)) \tag{9}$$

By expressing the energy of the two photons as: $\hbar\omega_1 = m_e c^2 + \delta_1$ and $\hbar\omega_2 = m_e c^2 + \delta_2$ we obtain in a non relativistic approximation: $(2m_e)^{-1}(|\bar{p}_-|^2 + |\bar{p}_+|^2) = \delta_1 + \delta_2$ and hence to first order in δ_1, δ_2: $\hbar^2\omega_1\omega_2 = m_e^2c^4 + c^2/2(|\bar{p}_-|^2+|\bar{p}_+|^2)$. Thus, by using the above we can express Eq. (9) as:

$$2m_e^2c^2 + (m_e^2c^2)^{-1}|\bar{p}_+|^2|\bar{p}_-|^2 - 2\bar{p}_+\bar{p}_- = -(2m_e^2c^2 + |p_+|^2 + |p_-|^2)\cos(\theta) \tag{10}$$

The RHS and the bracket on the LHS are close to $2m_ec^2$, and hence $\cos(\theta) = -1$. Thus, by using $\cos(\theta) = -1 + \frac{1}{2}(\theta - \pi)^2$ we finally obtain:

$$\begin{aligned}(\bar{p}_+ + \bar{p}_-)^2 - (m_e^2c^2)^{-1}|\bar{p}_+|^2|\bar{p}_-|^2 \\ = m_e^2c^2(\theta - \pi)^2 + \tfrac{1}{2}(|\bar{p}_+|^2 + |\bar{p}_-|^2)(\theta - \pi)^2 \\ (\theta - \pi) = \pm (m_ec)^{-1}|\bar{p}_+ + \bar{p}_-| = \pm (m_ec)^{-1}|\bar{p}_c|\end{aligned} \tag{11}$$

where $\bar{p}_c$ is the center-of-mass momentum. Hence, the deviation from π of the angle between the direction of the emission of the two annihilation photons is proportional to the center-of-mass momentum.

In a centre-of-mass frame, viz $\bar{p}_c = 0$, the two annihilation photons are emitted in exactly opposite directions with an equal energy of $\hbar\omega_o = m_ec^2$. Assuming that the centre-of-mass momentum in a laboratory frame is equal to $\bar{p}_c$, then the relation between the energy of the photons in the centre-of-mass frame and the laboratory frame can be expressed as:

$$E_{lab} = (1 - (v_c/c)^2)^{-\frac{1}{2}}(E_{cm} \pm E_{cm}(v_c/c)) \tag{12}$$

where v_c is the centre-of-mass velocity in the laboratory frame, viz $v_c = (E_c/m_e)^{\frac{1}{2}}$. To first order in v_c/c we obtain from Eq. (10):

$$E_c = (\hbar\Delta\omega)^2/m_ec^2 \text{ or } |\bar{p}_c| = 2\hbar\Delta\omega/c \tag{13}$$

which relates the Doppler shift to the center-of-mass energy of the annihilating electron-positron pair.

The above discussion of the properties of an electron-positron system and of the properties of the annihilation photons indicates the types of experimental techniques which can be applied in order to obtain information about the behaviour of a positron-electron system. The basic connection between theory and experiment is given by Eq. (6), (11), and (13). Hence, the potential experimental techniques consist of determinations of the positron lifetime, angular correlation of the annihilation photons, and Doppler shift of one of the annihilation photons. It should be emphasized that the positron lifetime depends on the state of the positron throughout its lifetime, whereas the angular correlation of the annihilation photons and the Doppler shift of one of the annihilation photons depend only on the final state of the positron prior to annihilation. The experimental techniques will be discussed further in Section 2.

Let us now discuss the properties of a bound state of an electron-positron pair, viz. the positronium atom (Ps). The quantum-mechanical treatment of Ps is very similar to that of the hydrogen atom. However, due to the replacement of the proton by the positron the reduced mass of the electron becomes half of that in the hydrogen atom. Further, due to the low mass of the positron compared to the proton, the spin-spin interaction becomes more significant in the Ps atom. The binding energy of Ps in the ground state is $E_B = 6.8$ eV, the average distance of the positron and the electron is double the Bohr radius r_b. Thus, the diameter of Ps is equal to that of hydrogen, ≈ 1 Å.

The Ps atom may be formed in two different states: one in which the two spins of the electron and the positron have opposite direction, para-Ps, or in which the two spins have the same direction, ortho-Ps. The total spin of ortho-Ps is $\sigma = 1$ and the spin component along an arbitrary direction can take the values $m_z = 1, 0, -1$. The total spin of para-Ps is $\sigma = 0$. Due to the number of spin states of para-Ps and of ortho-Ps in general it is believed that the probability of an electron and a positron forming ortho-Ps is three times the probability that they form para-Ps. From the discussion of the conservation rules connected to the annihilation process, we have that the significant annihila-

tion channels of Ps are those in which para-Ps and ortho-Ps annihilate into two and three photons, respectively. The intrinsic lifetime of para-Ps can be calculated from Eq. (6) simply by replacing n with the value of the electron probability density function at the positron and in addition by multiplying the right-hand side of Eq. (6) by four in order to remove the spin average condition, which, of course, is meaningless in the case of Ps. Eq. (6) only takes 2γ anninilation into account; however, the probability that a free positron interacts with an electron having the same spin direction is three times that of opposite spin direction. The calculation yields a para- Ps lifetime τ_s = 0.125 nsec. The intrinsic lifetime of ortho-Ps is close to 140 nsec. In Table I the intrinsic properties of the positron and Ps are summarized.

Table I. Intrinsic properties of the positron and the positronium atom (Ps)

Property	positron	para-Ps	ortho-Ps
mass	m_e	$2m_e$	$2m_e$
charge	+e	neutral	neutral
spin	1/2	0	1; m_z=-1,0,1
"radius"	r_e	r_b	r_b
intrinsic lifetime	∞	0.125 nsec	140 nsec
decay mode	-	2-γ	3-γ
binding energy	-	6.8 eV	6.8 eV
probability of formation	-	0.25 P	0.75 P

m_e; electron mass, r_e; classical electron radius, r_b; Bohr radius, P; total yield of Ps

1.3. The behaviour of light particles in fluids

Previous studies of the three light particles, the electron, positron and Ps atom in fluids strongly indicate that the behaviour of light particles in fluids is influenced mainly by quantum mechanical phenomena. Thus, in studies of light particles in fluids it is important to be aware of phenomena such as:

1) zero-point motion, 2) delocalization/localizatio., 3) tunneling, etc. Perhaps the quantum-mechanical nature of light particles in fluids can best be illustrated by considering the available information on the behaviour of the excess electrons in fluids. In Fig. 1 the mobility of excess electrons in some "typical" liquids are shown (references may be found in the list under the label "mobility data"). The most stricking feature of Fig. 1 is the enormous range of mobilities of excess electrons in liquids. By selecting the liquid the excess electron mobility can be changed over nearly seven decades. As reference, the mobilities of electrons in Ge and Cu are also shown in Fig. 1. A closer inspection of this figure shows that the mobility of ex-

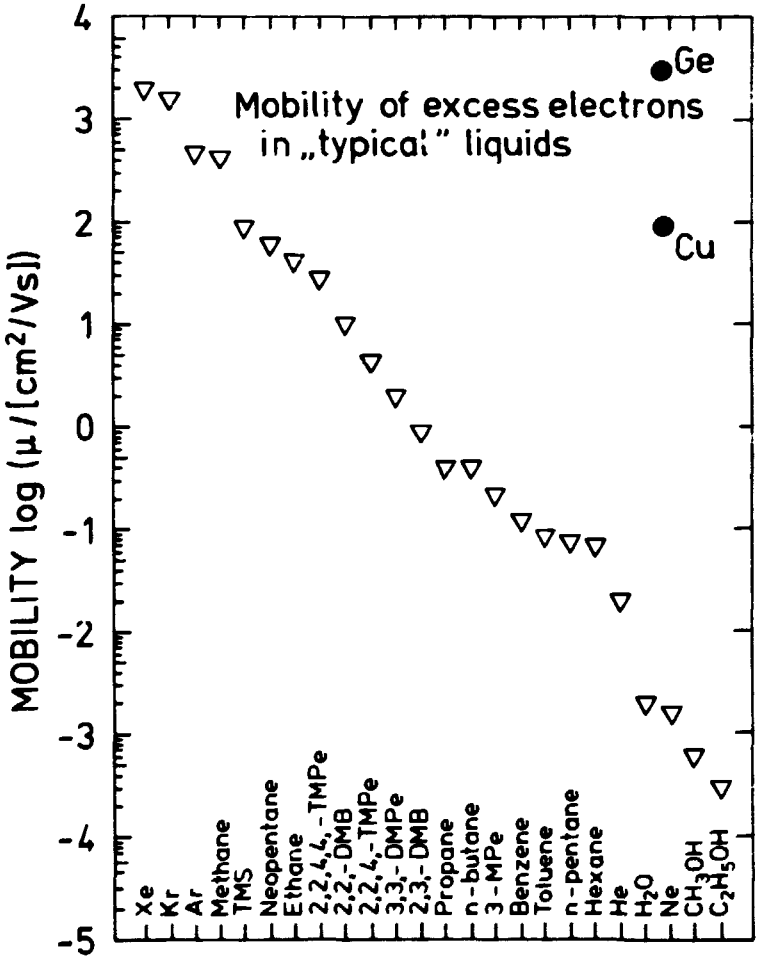

Fig. 1. Mobility of excess electrons in some "typical" selected liquids. In addition the electron mobility in Ge and Cu is also shown.

cess electrons increases with increasing degree of spherical shape, and simplicity of the molecules constituting the liquid; exceptions are liquid He and Ne (see below). The mobility of excess electrons in fluids is governed by the nature of the interaction between the excess electrons and liquid molecules.

The mobility of electrons in fluids can be limited by several types of interactions between the electron and the fluid such as: 1) single scattering processes, 2) multi-scattering processes, and/or 3) various degrees of self-trapping of the electron. The self-trapped electron states include 1) solvation of the electron in the liquid, 2) formation of a negative ion state with one of the solvent molecules in electron-attaching liquids, 3) electron bubble formation, etc. The electron bubble state, in which the electron is localized in a microscopic cavity, is formed as a result of the zero-point motion of the electron in liquids where the interaction potential between the electron and the molecules is essentially determined by the repulsive Coulomb and exchange interaction. The electron bubble state has been observed in liquid He (Jortner, Kestner, Rice and Cohen, 1965), and liquid Ne (Loveland, LeComber and Spear, 1972). The electron bubble formation in liquid He and Ne explains the low mobility of excess electrons in these two liquids.

In a simple picture we can express the mobility of excess electrons in fluids as:

$$\mu = P_c \mu_c + (1 - P_c)\mu_t \qquad (14)$$

where μ_c and μ_t are the mobility of the excess electrons in the conduction band and in the trapped state, respectively. P_c is the probability of finding the electron in the conduction band. P_c is determined by factors such as the cross section of inelastic scattering in the conduction band and energy difference of the electron in the conduction band compared with the trapped state. μ_c is determined mainly by elastic scattering processes, whereas μ_t is determined by factors such as the probability that the electron can tunnel from one trap to a nearby one, the dynamics of the liquid molecules which may open up channels between

Table II. Light particle states in liquids.

Definition	Physical state of liquids	Light particle states	Examples
1 Quasi-free $\mu > 10^{2}cm^{2}/Vs$	unperturbed	extended	e^{-},e^{+}(?) in all liquids short time; e^{-} in Ar,Kr,Xe, neopentane(?),TMS(?)
2 Quasi-localized $0.1<\mu<10cm^{2}/Vs$	unperturbed	localized(Anderson model)? or extended	e^{-} in some hydrocarbons e^{+} in some hydrocarbons?
3 Self-trapped by small density and/or structural fluctuation $0.1<\mu<10cm^{2}/Vs$	small configurational changes	localized	e^{-} in some hydrocarbons; hexane. e^{+} in some hydrocarbons
4 Localized by pre-existing traps $\mu < 0.1cm^{2}/Vs$	unperturbed	localized	Ps in all liquids short time? Ps in high viscosity liquids e^{-},e^{+} in polar liquids
5 Localized by bubble formation $\mu < 10^{-2}cm^{2}/Vs$	formation of a microscopic cavity, large configurational changes	localized	Ps in all low viscosity liquids e^{-} in H_2,He,Ne
6 Localized by large local configurational changes $\mu \approx 10^{-3}cm^{2}/Vs$	Radial and configurational changes induced by charged particles	localized	solvated e^{-} and e^{+} in polar liquids

traps, etc. Since we usually have $\mu_c >> \mu_t$, the mobility of excess electrons can be taken as a measure of how free the electrons are in a liquid.

According to the mobility of excess electrons in liquids, Jortner and Gaathon (1977) suggested a classification of the states of excess electrons. They distinguish between six different electronic states: 1) quasi-free electrons, and 2) quasi-localized electrons plus four different trapped states of the electrons. However, as the electron is merely a special type of light particle we have extended their classification to include also the two other light particles, viz. the positron and positronium. The classification of light particles is shown in Table II. Although the classification given in this table is somewhat arbitrary with respect to mobility we recommend its use as long as it is not in conflict with experimental facts. The use of the classification in Table II may avoid some misunderstandings in discussing the states of light particles in liquids. It should be emphasized that the present knowledge of the positron in liquids does not allow one to be too certain as far as the state of the positron in various liquids is concerned; this explains the question marks used in describing the state of the positron in the various examples given in Table II. The properties of the positron and Ps in liquids will be discussed further below and in Section 5.

1.4. Positronium formation in liquids

When energetic positrons ($\sim$0.2 MeV) are injected into a liquid a certain fraction may form Ps prior to annihilation. The formation of Ps in liquids is normally explained in terms of one of the following two models: 1) the Ore model (Ore, 1949), or a modified version of it, or 2) the spur reaction model (Mogensen, 1974). The basic difference between the two models is that in the first Ps is assumed to be formed by epithermal positrons of energies about 3-10 eV, whereas in the spur model Ps is assumed to be formed by a reaction between a mainly thermalized positron and one of the excess electrons created during the slow-down of

the positron. In the former model other processes, e.g. hot Ps reactions, must also be used in order to explain the measured results (Lévay, 1979 and Goldanskii, 1968). Apparently, the spur model is the most used model today, although the Ore model combined with hot Ps reactions cannot be disproved at present because of the many unknown processes which are invoked in it. Recent new experimental results tend to strongly favour the spur model (Lévay, 1979, Mogensen, 1979, and Lévay and Mogensen, 1980). Thus, in the present paper, we shall use the spur model in interpreting the measured Ps yields in liquids.

In the spur model it is assumed that when the positron loses the last part of its kinetic energy (100-200 eV) it will become thermalized in a fairly localized region, called the positron spur, consisting of a number of excess electrons, corresponding positive ions, and maybe some radicals. Typical values of the positron spur size in liquid hydrocarbons are 40-200 Å. Figure 2 visualizes a positron spur at the time of its formation. Typical reactions which may take place in the spur are:

$X^+ + e^- \rightarrow X$	recombination	
$e^+ + e^- \rightarrow Ps$	Ps formation	
$e^- + A \rightarrow A^-$	electron attachment	(15)
$e^+ + A^- \rightarrow Ps + A$	Ps formation	
$e^+ + A^- \rightarrow [e^+, A^-]$	positron bound state	

Hence, Ps is formed in competition with processes such as recombination of the excess electrons and the positive ions, electron attachment to solvent/solute molecules, positron bound-state formation, out-diffusion of the electrons/positron of the spur, solvation of the electrons/positron, etc. The electron attachment to solvent/solute molecules can influence the Ps yield in two ways depending on whether the positron is able to pick-off the electron from the solvent/solute anion or not. In the former case the electron attachment process merely competes with the recombination process and providing the mobility of the positron exceeds that of the positive ion, the electron attachment process may work in the direction of increasing the Ps yield.

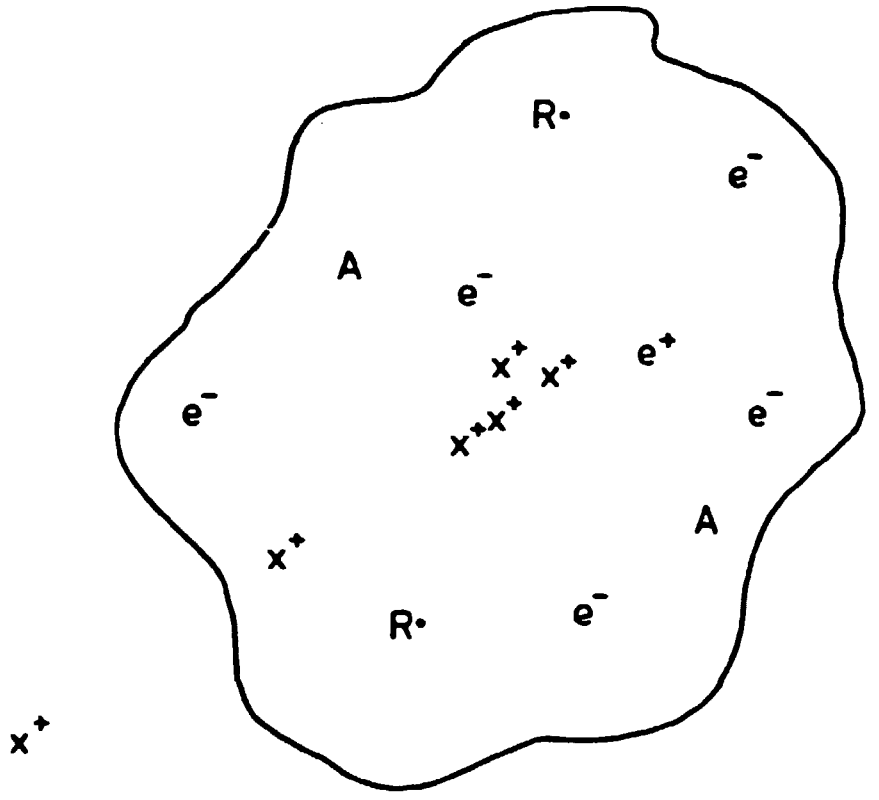

Fig. 2. Positron spur at its formation (t=0).

Due to the lack of detailed experimental information of the state of the excess electrons and the positron as a function of space and time it is not possible at present to calculate the Ps yield in liquids. However, by using the limited available information of the properties of the excess electrons in various liquids and solutions it is in many cases possible to predict the Ps yield in a qualitative way by using the spur model. For typical experimental cases which illustrate the power of the spur model very well see Mogensen and Lévay, 1980.

1.5. Positron annihilation experiments in liquids

Detailed studies of the behaviour of positrons and Ps in condensed matter are usually made by performing measurements of positron lifetime spectra and/or 2-γ angular correlation distri-

butions (see e.g. Lévay, 1979, West, 1973, Merrigan. Green and Tao, 1972, Goldanskii, 1968, and Gray, Cook, and Sturm, 1968). A typical lifetime spectrum obtained in a pure liquid is usually believed to consist of three exponentially decaying lifetime components attributed to the separate decay of para-Ps, free positrons, and ortho-Ps (Lévay, 1979, and Goldanskii, 1968). Typical lifetimes of para-Ps, free positrons, and ortho-Ps in pure liquids are 0.12 nsec, 0.3-0.5 nsec, and 1-10 nsec, respectively (Lévay, 1979, Goldanskii, 1968, Gray et al., 1968, and Jansen and Mogensen, 1977). As mentioned in Section 1.2 the yield of ortho-Ps is generally believed to be three times that of para-Ps. In a positron lifetime experiment the total Ps yield is determined from the intensity of ortho-Ps, whereas in an angular correlation experiment it is determined from the intensity of the narrow component associated with para-Ps.

The intrinsic lifetime of ortho-Ps is 140 nsec. However, in condensed matter ortho-Ps decays mainly by the pick-off mechanism, by which the positron in ortho-Ps annihilates with an electron of opposite spin on the surrounding molecules. In liquids the lifetime of ortho-Ps is usually explained in terms of the Ps bubble model in which it is assumed that Ps is localized in a microscopic cavity, the Ps bubble, in its equilibrium state. The nature of the Ps bubble state is analogous to that of the electron bubble state, briefly discussed in Section 1.3. Due to the charge of the electron, the electron bubble state is, however, formed only in liquids (He, H_2, Ne) consisting of molecules having a low polarizability together with a negligible dipole moment. However, due to the neutrality of Ps, the Ps bubble state is believed to be formed in nearly all low viscosity liquids (Lévay, 1979). Thus, it is much easier to study the Ps bubble state than the corresponding electron state. By varying the liquid, temperature, viscosity, pressure, etc., many different Ps bubble states can be prepared.

The "radii" of the Ps bubble are roughly 2-3 Å in water, 4-6 Å in typical liquid hydrocarbons at room temperature, and 10-20 Å in liquid noble gases. The size of the Ps bubble is determined by the inward pressure of the surface tension and the vapour

pressure balanced by the outward pressure caused by the zero-point motion of Ps. The overlap between the Ps wave function and the molecules decreases with increasing size of the Ps bubble; hence, the lifetime of ortho-Ps increases with increasing size of the Ps bubble. The Ps bubble was first suggested by Ferrell (1957) in order to explain the abnormally long lifetime of ortho-Ps in liquid He.

In Section 2 the experimental techniques will be described, while in Section 3 we will describe the experimental conditions and the data analyses related to the present experiments. The experimental results are shown in Section 4 and Section 5 contains a discussion of the results. A summary and conclusions are given in Section 6.

2. EXPERIMENTAL TECHNIQUES

2.1. Introduction

From the discussion in Section 1.2 of the properties of an electron-positron system and those of the annihilation photons it was indicated that the experimental methods of obtaining information on the behaviour of the positron (electron) in a medium consist of measuring 1) the positron lifetimes, 2) the momentum distribution of the annihilating electron-positron pairs, and/or 3) the Doppler shift of one of the annihilation photons. In the subsections that follow we shall give a short description of each of the experimental techniques.

The positron can be obtained from a number of radioactive isotopes such as ^{22}Na, ^{58}Co, ^{64}Cu, ^{68}Ge, etc. The positron source most frequently used is ^{22}Na. The decay scheme of ^{22}Na is shown in Fig. 3. The half-life of ^{22}Na is 2.6 years and the maximum energy of the positrons in the main decay (90%) is 0.5 MeV corresponding to a maximum range of roughly 0.16 gcm^{-2}. Apart from

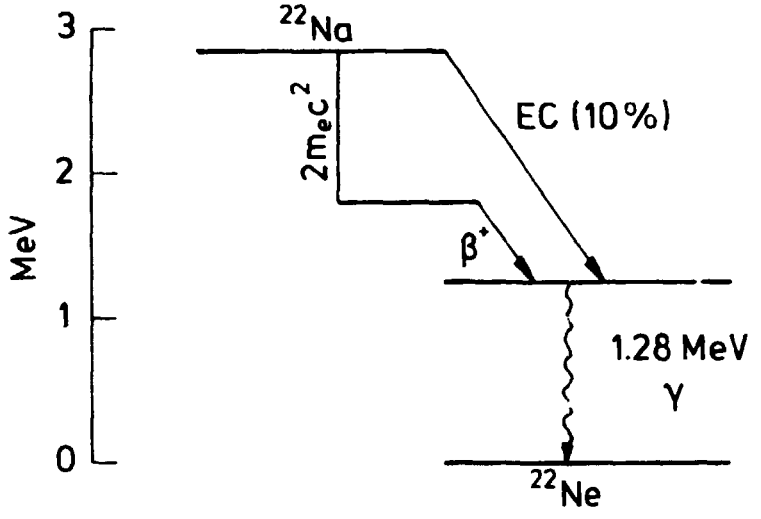

Fig. 3. Decay scheme of ^{22}Na.

the long half-life, the main advantage of using ^{22}Na is that the emission of the positron is followed by a simultaneous (< 10^{-11} sec) emission of a 1.28 MeV photon. Such a positron lifetime can be measured by determining the time interval between the detection of the 1.28 MeV photon and one of the two 0.511 MeV annihilation photons. In an angular correlation experiment the main advantage of using ^{22}Na as the positron emitter is its long half-life.

2.2. Positron lifetime technique

In Fig. 4 a typical diagram of a fast-fast coincidence system for measuring positron lifetimes is shown. The lifetime apparatus used at Risø has been developed by S.J.G. Lund (1978). The system consists of two identical detectors (D), two identical constant-fraction timing discriminators (CFTD), a time to amplitude converter (TAC), and a multi-channel analyser (MCA) in which the data also are stored. The two detectors (D) consist of a 1.5" x 1.5" Pilot U plastic scintillator mounted on the top of a fast photomultiplier tube (Philips XP2020). The signal from the photomultiplier tube is taken from the anode. The constant-fraction timing discriminator consists of three parts: 1) a single-

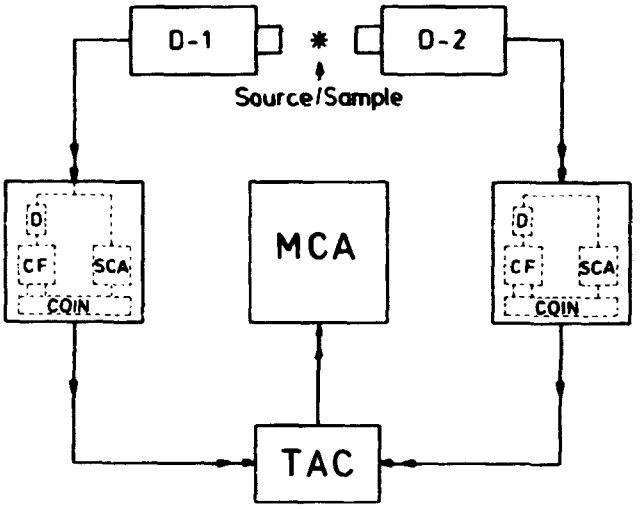

Fig. 4. A positron lifetime spectrometer using the fast-fast coincidence method.

channel analyser (SCA) which provides an output only if the input signal is within a preselected range of amplitudes, 2) a constant-fraction unit (CF) responsible for the determination of the time of an event in the detector (see below), and 3) a coincidence unit (COIN), which ensures that the CFTD provides an output only if the detector signal is within the preselected range set by the SCA. The delay in the front of the CF unit ensures that its output always appears later than that of the SCA for the same event. Thus, the time at which the output appears on the CFTD is determined solely by the CF unit (for pileup phenomena, see below). The time-to-amplitude converter (TAC) provides an output pulse whose amplitude is proportional to the time difference between the two input signals. The output of the TAC is analysed and stored in a multi-channel analyser (MCA) in such a way that the channel number in the MCA becomes proportional to the amplitude of the output pulse from the TAC, within a certain interval. In this way the channel number in the MCA becomes proportional to the time interval between the detection of two events satisfying the separate conditions set by the SCA in the two CFTD's. Thus, the way the system is set up for measurements of positron lifetimes is by adjusting the SCA in one of the CFTD in a way such that an output pulse can appear only

as a result of detecting a 1.28 MeV photon, whereas the SCA in the other CFTD is adjusted to accept pulses which can result from the detection of an annihilation photon (0.511 MeV). The output from the former CFTD is connected to the start input of the TAC while the output from the other is connected to the stop input. In order to be in the linear range of the TAC it is usually necessary to have a delay of several nsec between the CFTD detecting the annihilation photons and the stop terminal on the TAC.

The energy absorbed by the Pilot U scintillator mounted on the photomultiplier is not the total energy of the detected photon, but only the energy transferred to an electron in a single Compton process. Hence, the signal amplitude resulting from a detection of one photon may vary from essentially zero to a value corresponding to the Compton edge. For this reason the SCA in the CFTD arranged to detect the 1.28 MeV photons is adjusted to give output pulses when the input signals are between what corresponds to well above the Compton edge of the 0.511 MeV and the Compton edge of the 1.28 MeV. The SCA in the CFTD for detecting the annihilation photons is adjusted to give output pulses when the input signals are between the Compton edge of 0.511 MeV and some lower value determined by a compromise between a good time resolution and a good counting efficiency. The time resolution, FWHM, in each of the detectors roughly varies as $E^{-\frac{1}{2}}$, where E is the energy. Also noise from the photomultiplier and backscattering from one detector to the other may put a lower limit on the minimum amplitude of the signals which can be used. In Fig. 5 a typical set-up of the two SCA windows is shown.

The most critical part of the CFTD is the circuit (CF) determining the time at which the output pulse appears during the detection of an event. The main problem arising is that in order to obtain a reasonable counting efficiency it is necessary to use pulses of quite a large range of amplitudes (see Fig. 5). The timing discriminator most used indicating the "birth" and the "death" of the positron is the constant fraction discriminator (CF). In principle the constant fraction discriminator produces an output signal at a fixed time after the input pulse reaches

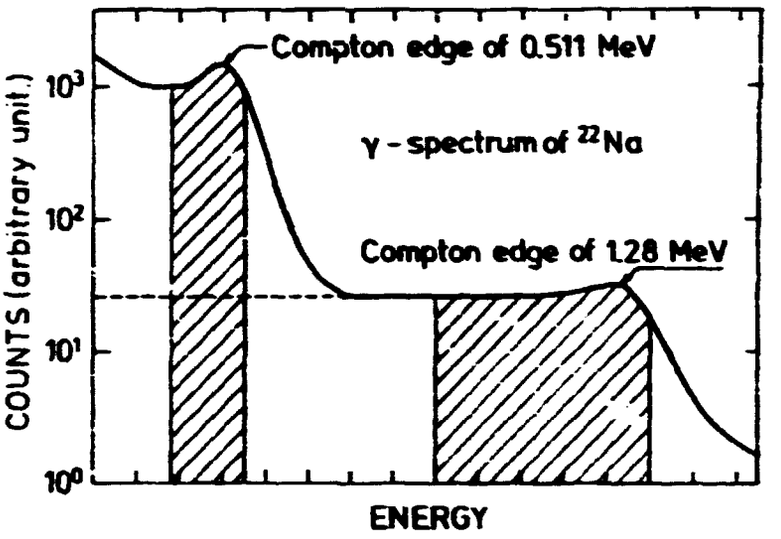

Fig. 5. The γ-energy spectrum of ^{22}Na source, the hatched areas show the setup of the two SCA windows.

a certain preselected fraction of its amplitude. Compared to other types of timing discriminators (e.g., the leading-edge discriminator) the constant fraction discriminator has greatly reduced the problem of time walk, viz. the pulse-amplitude dependence of detecting the time of a Compton event in a scintillator. The principle of the constant fraction discriminator is to convert the negative anode signal into a zero-crossing signal. In the input circuit of the timing discriminator (CF) the anode signal is divided into two parts. One of the signals is inverted and delayed while the other is attenuated. The two signals are added together to produce the zero-crossing pulse. We have now obtained a pulse of which the time of zero-crossing is independent of the amplitude of the signal from the photomultiplier tube (see Fig. 6). After an appropriate amplification the zero-crossing pulse is fitted into a zero-crossing detector which sends out a standard pulse when the zero-crossing point is detected. In order to be able to use the zero-crossing point as the trigger time of the coincidence unit it is necessary to divide the constant fraction pulse into two pulses, one of which is inverted and delayed. In Fig. 7 the arrival of the two constant-fraction pulses from the CF-unit together with the output pulse from the

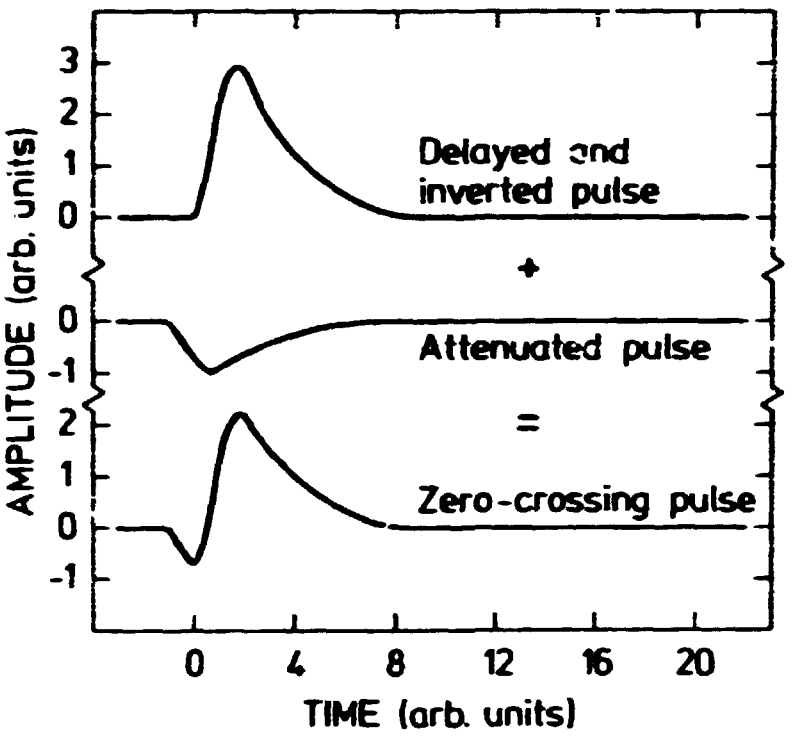

Fig. 6. The principles of converting the negative anode signal into a zero-crossing signal.

SCA is shown. The dashed line indicates the trigger level of the coincidence circuit, and the output goes high when all three signals are below the trigger level. By setting in the DC-level of the "timing pulse" the discriminator can be adjusted to produce negative, positive, or zero time walk. This possibility could seem a bit meaningless. However, in addition to what we could call the "geometrical walk" other kinds of time walk will exist in the electronics. In discriminators using logical electronics (e.g. a norgate) to produce the output pulse the inputs on such a device have to be changed from logical 1 to logical 0. This will produce positive time walk by itself. Also, the presence of capacitors in the active devices causes time walk. It is probably not possible to estimate the effect of the above-mentioned walk sources (and those not mentioned?). However, by varying the DC-level of the "timing pulse' it is possible experimentally to adjust the discriminator such that no time walk takes place.

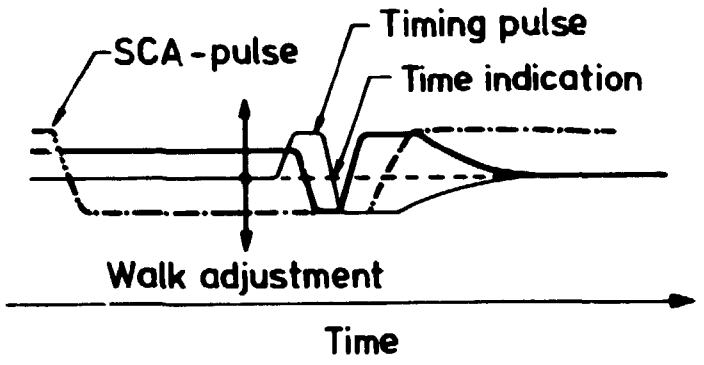

Fig. 7. The arrival time at the inputs of the coincidence unit of the pulses from, respectively, the SCA —— · —— and the constant fraction unit: timing pulse ————, condition pulse ————.

In the beginning of this section we mentioned another problem, viz. pile-up phenomena. Due to the use of very fast pulses it is probably impossible to avoid these problems following the normal techniques of pile-up rejection. In principle we can differentiate between three different types of pile-up phenomena. Suppose a real event is detected at a time, t, we can then have the following types of pile-up phenomena: 1) a non-real event is detected within the time $t-t_c < t' < t+t_c$, where t_c is comparable to the width of the CF-pulse, 2) a non-real event is detected at a time t''; $t-t_e+t_c < t'' < t-t_c$, where t_e is the time between the arrival of a "timing pulse" and the corresponding SCA pulse at the coincidence unit, and 3) a non-real event is detected at a time t'''; $t-t_e < t''' < t-t_e+t_c$. In the first case two pulses are added together, and providing the resulting pulse still satisfies the condition set by the SCA the time indication of the real event will differ from what it should be due to the pile-up. There is probably only one way of reducing this type of pile-up and that is to reduce the strength of the positron source. Since a non-real event can be detected with an equal probability within the time interval of interest the second type of pile-up just causes an enhancement of the background. Because we measure time intervals rather than absolute times this additional background will cover the time interval of roughly $t-t_e+t_c < t'' < t+t_e-t_c$. In the third case, it is the pulse of the SCA which sets the time

indication of the real event. Thus, this type of pile-up will produce a reduced lifetime spectrum on both sides of the real lifetime spectrum roughly a time distance $\pm t_e$ away. One way to come around this problem is to ensure that t_e is large enough such that these side spectra appear outside the time interval of interest.

Above we have briefly discussed some of the problems connected to the timing discriminator. However, the photomultiplier tubes and the properties of the light collecting process in the scintillators are also important for the time resolution of the whole system.

In order to increase the signal-to-noise ratio of the anode pulse it seems important to have the cathode at ground potential, particularly if magnetic shielding of the photomultiplier tubes is used. Due to the mechanical arrangement of the last dynode and the anode it seems that time resolution can be gained if the output is taken from the 9th or 10th dynode (for 12-stage tubes) (Bengtson, 1980).

Of course, the collecting time of the light from the scintillators has an influence on the resolving time. Several authors (see, e.g Kögel, 1979, and Dannefær, 1980) looked into this problem. A conclusion of their work seems to be that the shortest time of light collection is obtained for conical-shaped scintillators.

For a more detailed discussion of the positron lifetime technique we refer to a paper by Moszynski and Bengtson, 1979.

The constant-fraction timing discriminators used at Risø have been realized by the use of fast-emitter coupled-logic (ECL) devices. The best time resolution obtained with the lifetime spectrometer at Risø with 1½" x 1½" Pilot U scintillators and with normal ^{22}Na windows (see Fig. 5) is $\sim$ 300 psec at FWHM.

Finally, in Fig. 8 two typical examples of a positron lifetime spectrum as obtained in liquid SF_6 at the temperatures, -45°C and T_c, respectively, are shown.

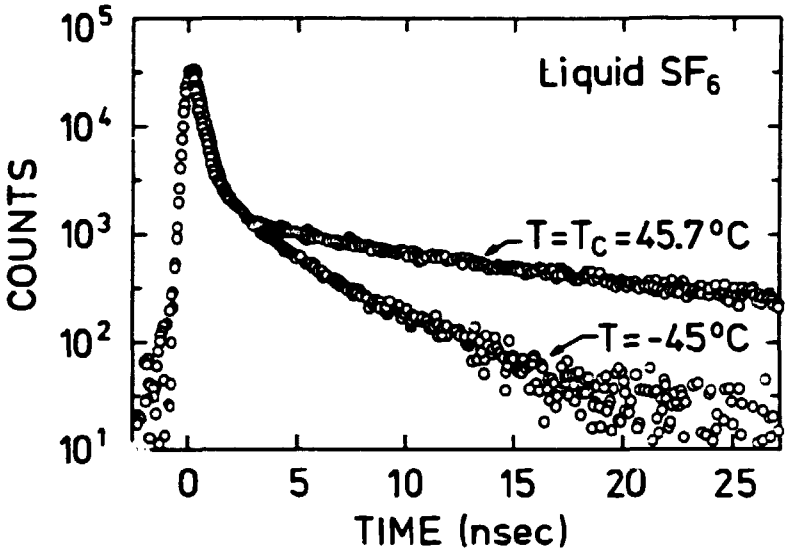

Fig. 8. Positron decay spectra as measured in liquid SF_6 at -45°C and T_c = 45.7°C. The two spectra are normalized to the same peak count. The lifetime of the long-lived component is ∿ 6 nsec (-45°C) and ∿ 17 nsec (T_c), respectively.

2.3. Two-photon angular-correlation technique

From the discussion of the properties of the annihilating electron-positron pairs and of the properties of the annihilation photons in Section 1.2, we saw that the momentum distribution of the annihilating electron-positron pairs can be determined by measuring the distribution of the deviations of the angle of the direction of the emission of the two annihilation photons from π (Eq. (11)). In Fig. 9 a diagram of a typical 2-γ angular correlation apparatus is shown. The system can be divided into two parts: a mechanical part, and an electronic part. Assume the two detectors to be in a position corresponding to the angle π. Then the position of the sample is arranged in a way such that most of the positrons are stopped in the same plane as the one containing the two detectors. The resolution of the apparatus is determined mainly by the mechanical dimensions of the set-up. Let ℓ be the distance between the sample and one of the two detectors and d the width of the collimators placed in the front of the detectors. The angular resolution is then roughly equal to $\theta_{\frac{1}{2}} \approx d/\ell$. Typical values of ℓ and d are 2 m and 0.5-2 mm, respectively, correspond-

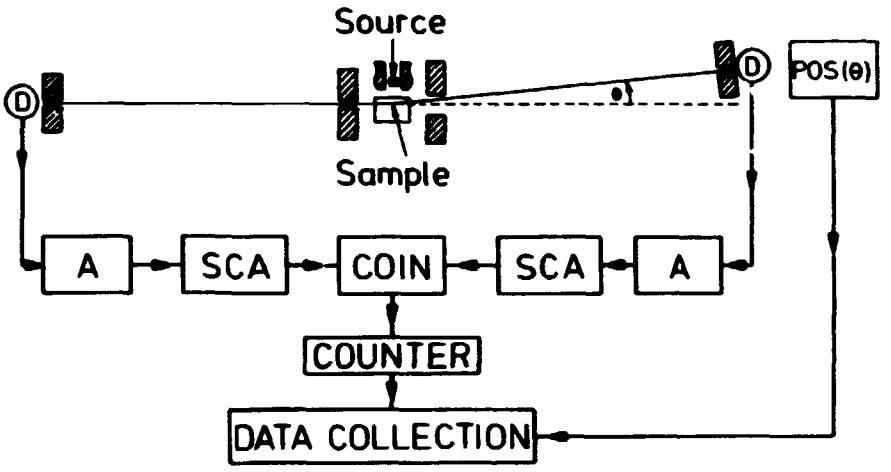

Fig. 9. A typical 2γ angular correlation apparatus.

ing to an angular resolution of ∿0.25-1 mrad. From Eq.(11) we have that 1 mrad corresponds to $E_c \simeq 0.13$ eV.

The two detectors consist of a NaI(Tl) scintillator mounted on top of a photomultiplier tube. After an appropriate shaping and amplification the signal from the anode is connected to the input of a single channel analyser (SCA), which sends out a standard pulse if the amplitude of the input signal is within a preselected range. The two SCA are adjusted such that only an output pulse can appear as a result of detection of a 0.511 MeV photon. The outputs of the two SCA are connected to the inputs of a coincidence unit which provide an output pulse if the two inputs are detected within a certain time (typically 50-100 nsec). In this way an angular correlation curve is measured by collecting the number of events from the coincidence unit in a fixed time interval as a function of a preselected number of angular positions. A typical angular correlation curve is measured within the interval of $\pm$ 15 mrad. In Fig. 10 an angular correlation curve obtained on liquid neopentane is shown.

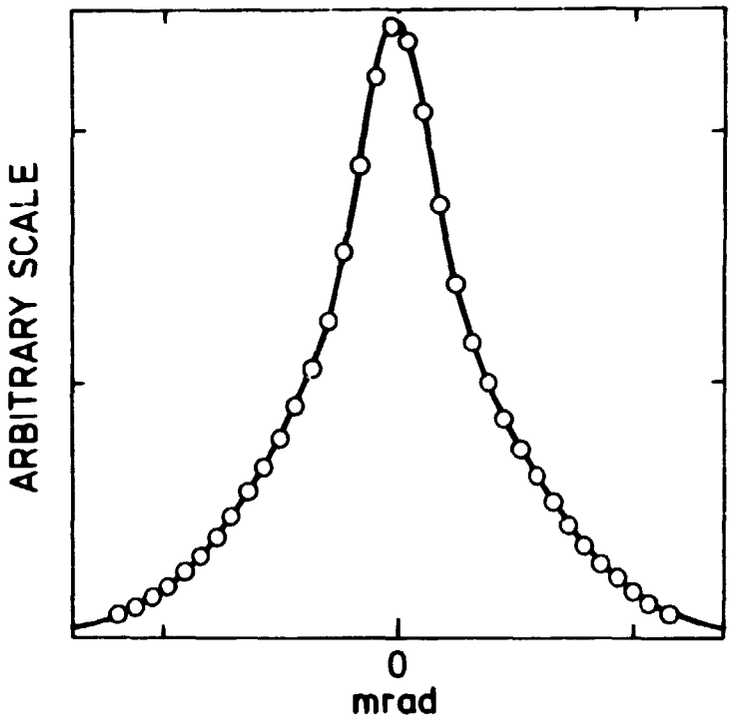

Fig.10. An angular correlation curve as measured in liquid neopentane at 23°C.

2.4. Doppler-broading technique

By measuring the distribution of the Doppler shift of the annihilation photons we obtain in principle the same information as obtained in an angular correlation experiment. However, the energy (or momentum) resolution is far away from what can be obtained in an angular correlation experiment. Typical energy resolution of an annihilation photon is ∿1.2 keV corresponding to E_c = 2.8 eV. The advantages of using the Doppler-broading technique are: 1) the simplicity of the apparatus, 2) positron sources of low activity can be used, 3) Doppler-broading measurements can easily be performed simultaneously with positron lifetime measurements, etc. In Fig. 11 a diagram of a Doppler-broading set-up is shown. The detector consists of a Ge(Li) detector. The signal from the detector (proportional to the photon energy) is amplified by a pre-amplifier placed close to the detector. The output signal from the pre-amplifier is further amplified by a spectro-

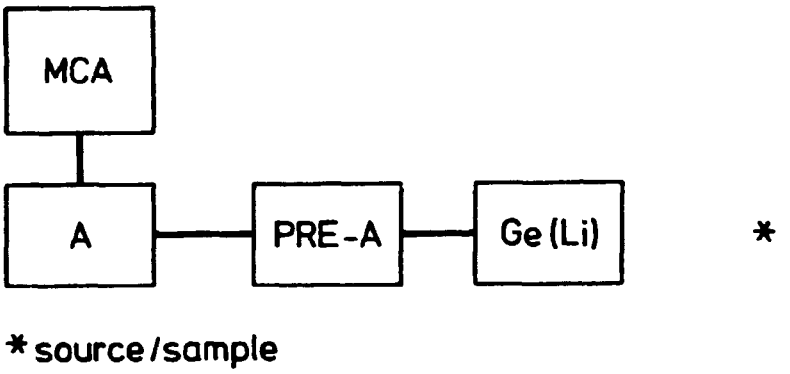

Fig.11. A typical Doppler-broading apparatus.

meter amplifier. The output of the spectrometer amplifier is analysed and stored in a multi-channel analyser (MCA) in such a way that the channel number becomes linearly dependent to the energy of the photons detected. A typical energy calibration is ∿ 0.1 keV/channel.

3. EXPERIMENTAL DETAILS

3.1. Introduction

The liquids chosen for positron lifetime studies as functions of temperature were: 1) two phenyl ethers, 2) liquid sulfurhexafluoride, 3) liquid neopentane, and 4) liquid hexane. The two phenyl ethers: m-phenoxy-phenyl-m-(m-phenoxyphenoxy)phenyl ether and bis(m-(m-phenoxyphenoxy)phenyl)ether designated 5PO and 6PO, respectively, have previously been studied extensively for their viscolastic properties (Eastwood, Cochrane, Harrison, Lamb, and Phillips, 1980). The structures of the two phenyl ethers are shown in Fig. 12.

The three other liquids have been studied through a broad temperature range: sulphur hexafluoride (-45°C to 71°C), neopentane

(23°C to 180°C), and hexane (-72°C to 160°C). The critical constants of these liquids are shown in Table III.

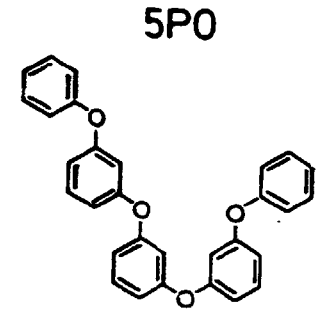

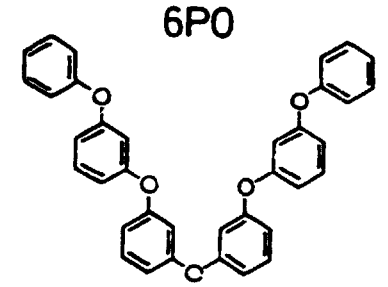

Fig.12. The structures of m-phenoxy-phenyl-m(m-phenoxyphenoxy) phenyl ether (5PO) and bis(m-(m-phenoxyphenoxy)phenyl) ether (6PO).

Table III. Critical constants of SF_6, neopentane and hexane.

Liquid	Pressure P_c	Temperature T_c	Volume V_c
SF_6	37.7 atm	45.65°C	199ml/mol
neopentane	31.3 atm	160.3°C	311ml/mol
hexane	29.9 atm	234.2°C	368ml/mol

3.2. Experimental conditions

All the liquids were degassed and sealed with an encapsulated positron source in a Pyrex tube or in an autoclave system of stainless steel. During positron lifetime measurements in the liquids at temperatures of low vapour pressure (< 2 atm), a Pyrex tube was used for containing the liquid, while at higher

temperatures the autoclave was used. The autoclave system was bought from Carl Roth KG, West Germany and modified slightly so it could fit onto a vacuum line during the sample preparation. The volume of the autoclave was 50 ml. The amount of liquid used in the autoclave was that which gave the critical density at the critical temperature.

The positron source used in the lifetime experiments was ^{22}Na in the form of NaCl sandwiched between two Kapton foils 1 mg/cm^2 thick. The source was always positioned such that all positrons were stopped and annihilated in the liquid phase (apart from a small fraction annihilating in the source). No positron reached the gas phase region. Above the critical temperature of the liquids all the positrons annihilated in the fluid phase. The strength of the positron source was roughly 20 μCi in the case where the liquids were sealed in Pyrex tubes, while a rather strong source of approximately 150 μCi was used in cases where the liquids were sealed in the autoclave.

The positron lifetimes were recorded by a spectrometer using the fast-fast coincidence method; see Section 2.2 (Lund, 1978, and Hardy and Lynn, 1976). The spectrometer included digital stabilisation of the spectrum peak position. The time resolution of the spectrometer during the period of the present experiments was characterised by its full width at half maximum (FWHM), 400-500 psec. A typical resolution curve is shown in Fig. 13. The time resolution was checked from time to time (at least once a week) during the experiments. The time calibration of the spectrometer corresponded to 0.077 nsec/channel in the MCA. For each lifetime spectrum at least 5 x 10^5 time events were collected at a count rate equal to roughly 25-35 sec^{-1}. However, a lifetime spectrum often contained the detection of several millions of time events.

The temperature was controlled by a proportional regulator using the resistance of a thermistor as feedback signal. The thermistor was placed at the same level as the positron source and on the outside of the Pyrex tube (autoclave). The temperature was read from a thermocouple placed just beside the thermistor. During

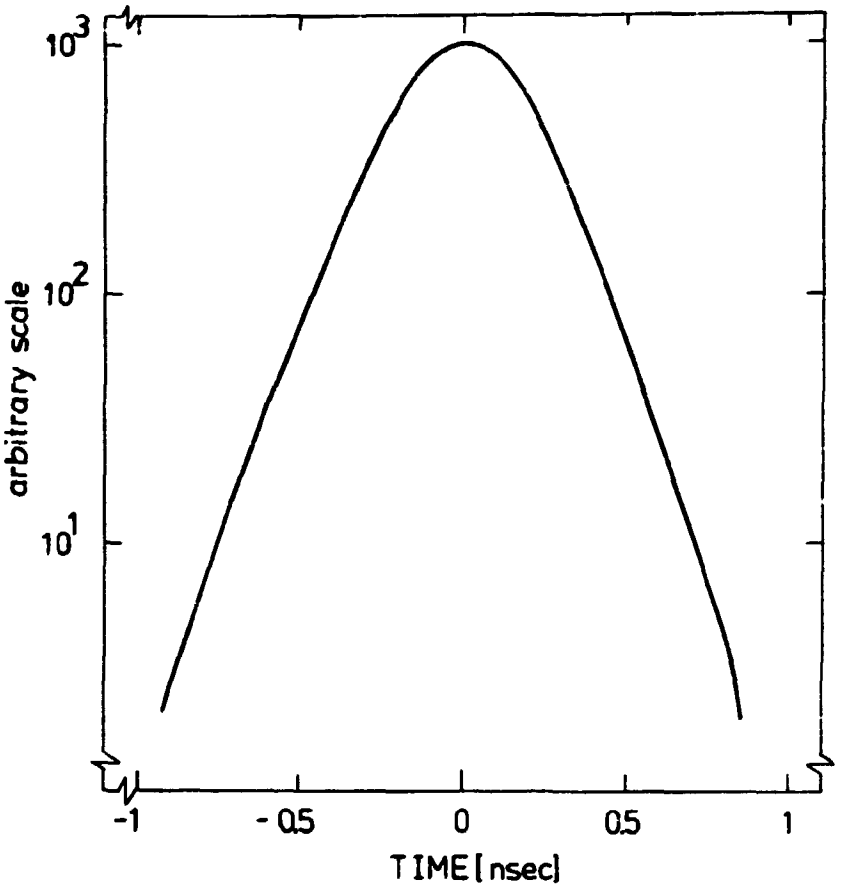

Fig.13. A typical time resolution curve.

the lifetime measurements below room temperature the autoclave (Pyrex tube) was placed in a simple flow cryostat using nitrogen as cooling gas. During the high-temperature measurements the liquids were heated in an electric furnace. The heat elements were arranged such that no magnetic field was produced across the liquids. The overall accuracy of the temperature was within $\pm$ 0.5°C.

3.3. Principles of the data analyses

All the positron lifetime spectra were analysed by assuming that a typical positron lifetime spectrum can be divided into a certain number of exponentially decaying lifetime components attributed to the separate decays of positrons from different

states in the liquids. Thus, in a medium in which the positrons can annihilate from n different states we can express the positron lifetime spectrum as:

$$T(t) = \Sigma\, I_i \lambda_i \exp -\lambda_i t \ , \ \Sigma\, I_i = 1 \ ; \ t \geq 0 \qquad (16)$$

where λ_i and I_i are the decay rate and the fraction of positrons annihilating from the i-state. By knowing the exact or theoretical positron lifetime spectrum the experimental spectrum E(t) can be calculated as

$$E(t) = \int_0^\infty R(t-t')T(t')dt' + B \qquad (17)$$

where R(t) is the time-resolution function of the spectrometer and B is a constant background.

The principle of the analysis of an experimental positron lifetime spectrum is as follows: By use of Eq. (17) an "experimental" spectrum is calculated from the free parameters - the I's and the λ's. By comparing the calculated to the measured spectrum the values of the λ's and the I's can be determined by imposing the choice of the number of lifetime components and that of the I's and the λ's to the principle of least squares.

All the positron lifetime spectra recorded in this work were analysed by using the computer programme POSITRONFIT EXTENDED (Kirkegaard and Eldrup, 1974, and Kirkegaard and Eldrup, 1972, and Kirkegaard, Eldrup, Mogensen and Pedersen, 1981). The input parameters to the programme can be divided into two sets of parameters:
1) parameters describing the experimental conditions, and
2) parameters used to extract information of the number and the properties of different positron lifetime components in the medium under investigation. The former parameters include the time calibration and the time resolution function of the spectrometer. The time resolution function is described as a sum of up to three gaussians of which widths, intensities, and centroid positions can be individually fixed. Furthermore, it is possible to specify the positron decay spectrum in the positron source and the fraction of positrons annihilating in the source. Before the

final analysis the positron source contribution is calculated and subtracted from the spectrum. Finally, the last two parameters connected to the experimental conditions, viz. the time zero (the time reference channel) and the background, can be treated either as fixed or fitting parameters. The input parameters specified in order to obtain information of the positron lifetime components in the medium under investigation are: 1) the number of lifetime components, and 2) initial guesses of the decay rates. Further, various constraints can be imposed on the fitting parameters such as fixed values of some of the decay rates and/or the intensities. In addition, linear combination of some of the intensities can be fixed to zero.

The programme uses an iterative method (Marquardt's technique, 1963) to determine the least-square values of the fitting parameters. Among the estimated values, including statistical uncertainties of the fitting parameters, the programme also gives as output the variance of the fit, Φ, and a correlation matrix (covariances) of the fitting parameters. The variance of the fit is defined as: $\Phi = (n-k)^{-1}\Sigma N_i^{-1}\Delta_i^2$, where N_i is the number of time events in the i'th channel (in the MCA) and Δ_i is the difference of the number of time events in the i'th channel and that calculated from Eq. (17). The sum is extended over n measuring points and k is the number of free parameters. It can be shown that Φ_{min} is normally distributed with a mean of 1 and a standard deviation of $(2(n-k))^{-\frac{1}{2}}$. Thus, in analyses of positron lifetime spectra the values of Φ_{min} can serve partly as an indicator of the validities of the models used, viz. number of lifetime components and the validity of possible constraints of the fitting parameters.

The time resolution function was determined by measuring the lifetime spectrum of the "Kapton source" placed between a number of Kapton foils (250 Kapton foils corresponding to 0.25 g/cm^2). The positron lifetime spectrum in Kapton consists of a single decaying lifetime component of $\lambda = 2.62 \cdot 10^9$ sec^{-1}. The lifetime spectrum was analysed by using the computer programme RESOLUTION (Kirkegaard, Eldrup, Mogensen and Pedersen, 1981). The working principles of this programme are very similar to that of POSITRONFIT

EXTENDED except that the parameters of the time resolution curve are treated as fitting parameters. The time resolution curve can be fitted as a sum of up to four gaussians of which the widths and centroid positions are treated as fitting parameters.

The positron lifetime spectrum in the positron source consists of positrons annihilating in the Kapton foils (1 mg/cm^2) plus those annihilating in the source material. The total source/foil correction is estimated to be 8.5%. The lifetime components of the source/foil spectrum are determined in the same experiment as the time resolution function by letting the RESOLUTION programme search for two lifetime components. A typical result from such an analysis gives: τ_1 = 0.381 nsec (Kapton), and τ_2 = 2 nsec with the intensities: I_1 = 99.5% and I_2 = 0.5%, respectively. Hence, a typical source correction spectrum would consist of τ_{s1} = 0.381 nsec (8%) and τ_{s2} = 2 nsec (0.5%).

All the positron lifetime spectra of the present work have been corrected for background and source/foil annihilations.

3.4. Discussion of the data analyses

One of the main problems during the analysis of an experimental positron lifetime spectrum is: How can we decide the number of exponentially decaying lifetime components that are included in a spectrum. It is quite clear that it is not possible by means of the variance of the fit alone to determine this number. By increasing the number of exponential functions in the fit the variance of the fit decreases and, hence, the goodness of the fit becomes better. One can argue that we know (for statistical reasons) that the variance of the fit should be close to 1 and then use this "fact" in the determination of the number of different lifetime components included in a spectrum. However, the use of such an argument implies that a positron lifetime spectrum can be divided into a certain number of purely exponentially decaying functions. Although, in many cases this may be a good description of the spectrum, there are no reasons to believe that such a description is other than an approximation of which

the goodness is usually not very well known. Also experimental uncertainties can probably influence the simple behaviour of the variance of the fit. To circumvent this problem we could, of course, allow the use of other types of functions in the fitting of a lifetime spectrum. However, to do so it would be necessary that the selection of these functions should be based on very detailed physical knowledge of the behaviour of the positrons in the medium investigated, since, otherwise, the inclusion of more complex functions in the fitting procedure will probably mean that the physics are turned into merely a mathematical exercise. In our opinion the present knowledge of the physical behaviour of positrons in condensed matter does not allow the use of complex functions to fit a decay spectrum of positrons in such a medium. So, although perhaps not strictly correct, the most reasonable way of describing a positron lifetime spectrum seems to be by the use of exponential functions. However, one should be aware that such a description is no more than an approximation. Perhaps the least subjective way in which to decide the number of exponential functions needed to fit a lifetime spectrum is, first, to consider the problem as one of pure mathematics. Using this point of view, we simply have to find the number of exponential functions that gives a reasonably low variance of the fit together with reasonably well-defined parameters of the exponential functions used in the fit. To bring physics into the problem we can use the available physical knowledge to judge the result and perhaps, in addition, place various types of constraints on the analysis. However, in the judgement of the lifetime components one should be aware that each of them does not necessarily represent the decay of positrons from single states, but could, e.g. be very well associated with the average decay rates of positrons from a number of different states.

For reasons which will become clear later we investigated whether or not it was possible to force the POSITRONFIT programme to extract four lifetime components from a spectrum containing only three. An "experimental" spectrum containing three purely exponentially decaying lifetime components was generated by means of a programme developed by Eldrup and Kirkegaard, 1973. The decay rates and intensities used were taken from a lifetime spectrum

obtained in liquid neopentane at T = 125°C and analysed into three components with no constraints. The time resolution function and the total number of time events were the same as for the real spectrum measured in neopentane. Furthermore, the spectrum was generated in accordance with the statistical scattering of the measured points as displayed by a measured spectrum. The values of the parameters of the lifetime components were: (τ_1, I_1) = (0.193, 29.486), (τ_2, I_2) = (0.848, 11.858), and (τ_3, I_3) = (9.533, 58.657), where the lifetimes and intensities are given in nsec and per cent, respectively. In the analyses of the generated spectrum the background was fixed to values between ~50% to 150% of the original value, and the FWHM of the time resolution function was changed from 90% to 110% of its original value. The spectrum was analysed in terms of four free lifetimes without any constraints, with one lifetime fixed to 0.125 nsec (the lifetime of para-Ps), and with the longest lifetime fixed to its original value. However, it was not possible by any means to obtain an extra lifetime component which could not be clearly associated with background corrections or with problems due to the incorrect time resolution function. Some typical results from the analyses are shown in Table IV. The conclusion of this computer experiment seems to be that a lifetime spectrum consisting of three purely exponentially decaying lifetime components with intensities and decay rates as used in the present case cannot be resolved into four components due to errors in the determination of the time resolution or background. Of course, in cases where the lifetime components do not display purely exponential behaviour or where a spectrum consists of lifetime components with other values of the decay rates and intensities, the results of such a computer experiment could be expected to turn out differently.

In the same computer experiment we also investigated the sensitivity of the lifetime components in a three-term fit to errors in the time resolution and background. The results are shown in Figs. 14 and 15. Qualitatively, the behaviour of the lifetime parameters are as expected.

Table IV. Results of four-term analyses performed on a lifetime spectrum known to consist of three purely exponentially decaying lifetime component.

background	time resolution	variance of fit	τ_1	I_1	τ_2	I_2	τ_3	I_3	τ_4	I_4
OK	OK	0.939	0.195	28.759	0.851	11.780	9.534	58.654	F0.125	0.804
20% lower	OK	1.474	0.289	17.854	1.223	9.003	10.526	59.156	F0.125	13.987
15% higher	OK	1.347	0.160	49.418	0.730	13.390	8.915	58.048	F0.125	-20.856
OK	90% FWHM	0.941	0.170	75.879	0.823	13.365	9.527	59.107	F0.125	-48.351
OK	110% FWHM	0.956	0.294	8.110	0.895	10.222	9.542	58.260	F0.125	23.408

τ and I are given in nsec and %, respectively. F indicate fixed parameter.

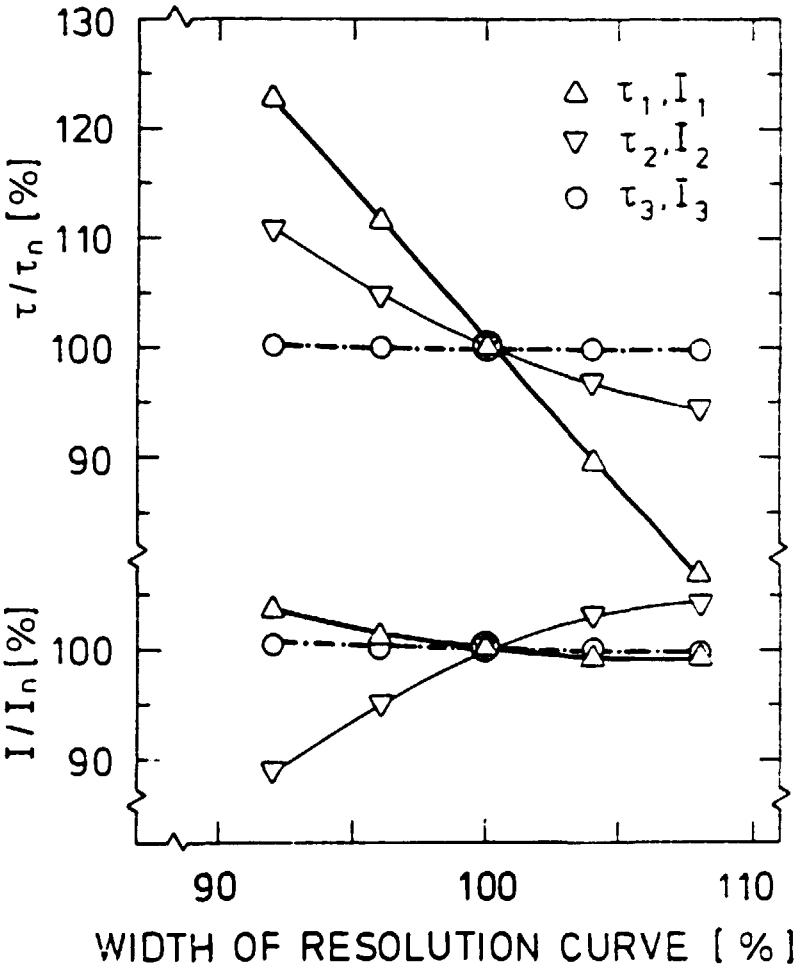

Fig.14. Changes of the lifetime parameters caused by errors in the time resolution curve (see text).

As mentioned in Section 1.5, a typical positron lifetime spectrum obtained in a pure liquid is usually believed to consist of three exponentially decaying lifetime components attributed to the separate decay of para-Ps, free positrons, and ortho-Ps (Lévay, 1979, and Goldanskii, 1968). In non-conducting condensed matter in which Ps is not formed, the positron decay spectra are usually well described by a single exponentially decaying lifetime component with a mean lifetime of the order of 0.3-0.5 nsec.

As the lifetime of free positrons in non-conducting matter depends on the extent to which the positrons can penetrate into the molecules (determined by factors such as polarisability of

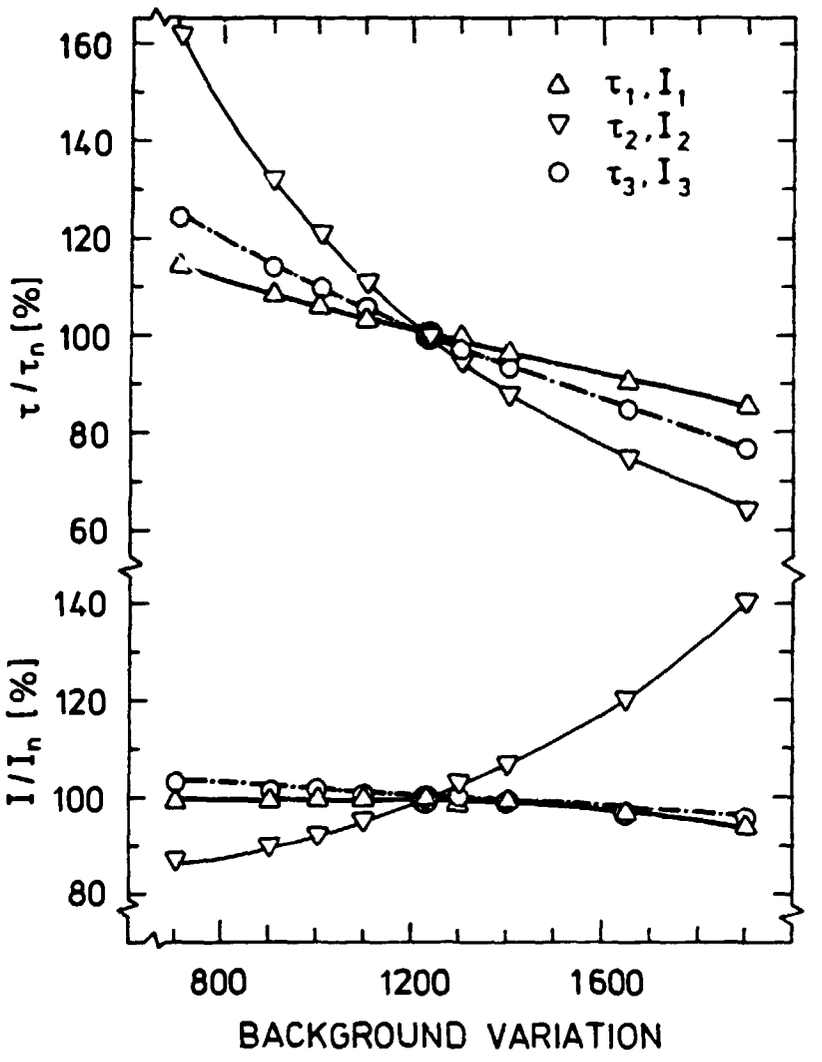

Fig.15. Changes of the lifetime parameters caused by errors in the determination of the background (see text).

the molecules, repulsion from the positive "core", and zeropoint motion of the positrons) it seems reasonable to believe that an upper limit of the lifetime of free positrons in condensed matter would not deviate much from 0.5 nsec. The spin average lifetime of Ps is 0.5 nsec. Thus, a positive indication of Ps formation is given if a lifetime spectrum contains lifetime components with a mean lifetime significantly longer than 0.5 nsec. In an angular correlation experiment a positive indication of Ps formation is provided if the curve contains a narrow component with a FWHM of the order of 3 mrad or less. Such a narrow component is associated with the intrinsic decay of para-Ps.

All of the lifetime spectra recorded in this work contained a long lifetime component with a mean lifetime we above what would be expected for free positrons, and are believed to contain at least three lifetime components due to the decay of para-Ps (0.125 nsec), free positrons (0.3-0.5 nsec), and ortho-Ps.

Short remarks on the specific analyses of the positron decay spectra obtained in the liquids investigated in this work are given in Section 4.

4. EXPERIMENTAL RESULTS

As mentioned in Section 3.2, all of the positron lifetime spectra have been corrected for background and source/foil annihilations.

In Figs. 16 and 17 the temperature dependence of τ_3 and I_3 of ortho-Ps in the liquids: m-phenoxy-phenyl-m-(m-phenoxyphenoxy)-phenyl ether (5PO) and bis(m-(m-phenoxyphenoxy)phenyl)ether (6PO) are shown. The structures of the two molecules are given in Fig. 12. The lifetime spectra were analysed in terms of three lifetime components without any constraints. The correlation between the two shortest lifetime components ($\tau_1 \approx 0.225$ nsec and $\tau_2 \approx 0.450$ nsec) was rather large, resulting in marked uncertainties in the intensities, I_1 and I_2. However, for the longest-lived component τ_3, I_3 separated out well at all temperatures. The uncertainties of τ_3 and I_3 are estimated to be 0.03 nsec and 0.5%, respectively. The lifetime spectra were taken alternately at high and low temperatures; no difference was detected in the form of the lifetime spectra, indicating no thermal hysteresis or long-term radiation damage effects.

These two liquids form glassy phases at low temperature and do not exhibit a first-order melt transition. At higher temperatures they have a low viscosity and behave similarly to normal liquids. On lowering the temperature the viscosity increases strongly

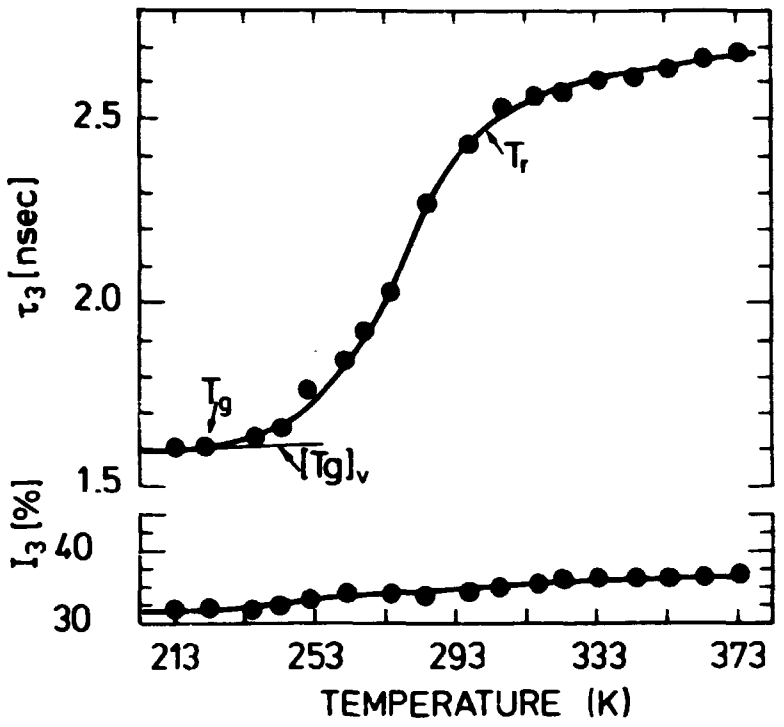

Fig.16. The temperature dependence of the ortho-Ps lifetime τ_3 and intensity I_3 in m-phenoxy-phenyl-m(m-phenoxyphenoxy) phenyl ether (5PO). $[T_g]_v$ is the glass transition temperature.

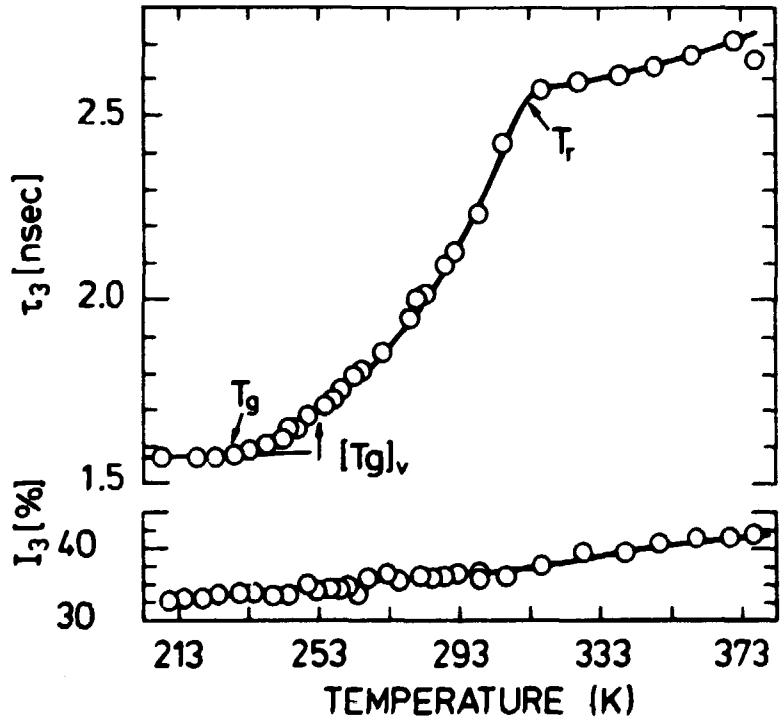

Fig.17. The temperature dependence of the ortho-Ps lifetime τ_3 and intensity I_3 in bis(m-(m-phenoxyphenoxy)phenyl)ether (6PO). $[T_g]_v$ is the glass transition temperature.

until at very low temperatures a glass is formed. The temperature dependence of the viscosity of the two liquids is shown in Fig. 18. The glass transition temperature has been determined to be -28°C and -20°C, respectively, for 5 PO and 6 PO (Barlow, Erginsav, and Lamb, 1969, and Cochrane and Harrison, 1972). The glass transition temperature is denoted as $[T_g]_v$ in Figs. 16 and 17.

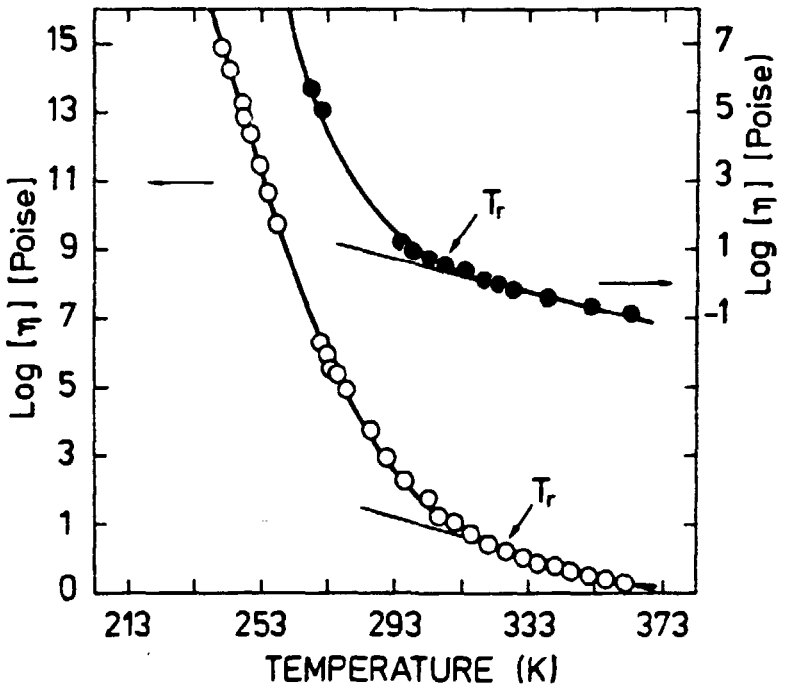

Fig.18. The temperature dependence of the viscosity of 6PO and 5PO, respectively.

The positron lifetime spectra obtained in liquid SF_6 as functions of temperature were resolved into four lifetime components. Since previous lifetime spectra obtained in various pure liquids have been resolved into only three lifetime components (and in some cases only two) (Lévay, 1979, Jansen and Mogensen, 1977 , Gray, Cook, and Sturm, 1968, and Goldanskii, 1968), we would like to discuss in some detail the reasons for using this form of analysis of the positron decay spectra in liquid SF_6. Table V lists three different types of analyses performed on a typical lifetime spectrum obtained in liquid SF_6 at room temperature. First, consider the free three-term analysis. The variance of the

fit (1.884) is significantly higher than expected from the experience of three-term fit performed on lifetime spectra obtained in various other liquids. The longest-lived component with a mean lifetime of ≈ 9.5 nsec clearly indicates that ortho-Ps is formed in liquid SF_6, and hence para-Ps as well. Thus, the two shortest-lived components could be associated with a mixture of the decays of para-Ps and free positrons. However, although a rather subjective argument, the lifetimes of the two shortest components seem to be larger than expected for a simple description of the decay of para-Ps (≈ 0.12 nsec) and free positrons (≈ 0.3-0.5 nsec). However, the variance of the fit itself is justification for one to be sceptical. It should be emphasized that several lifetime spectra have been obtained in liquid SF_6 at room temperature and the result of the three-term analysis of the one shown in Table V is not outstanding. The second example in Table V shows the results of a free four-term analysis. We observe a significant decrease in the variance of the fit compared to the three-term analysis. However, the parameters of the fit are (of course) not as well-defined as in the three-term analysis; but still the uncertainties are reasonably low.

As mentioned above, we expect the decay of para-Ps to be included in the lifetime spectrum. Due to the very fast intrinsic decay rate of para-Ps ($8 \cdot 10^9$ sec^{-1}) we do not expect the lifetime of para-Ps in liquid SF_6 to be very different from its intrinsic value (see Section 5). The determination of such a short-lived component is very difficult in a free four-term analysis. In order to obtain information about para-Ps as well, we decided to constrain the shortest lifetime to 0.125 nsec. The results of such an analysis are shown as the last example in Table V. We observe that the variance of the fit increases slightly compared to the free four-terms fit; however, the parameters of the fit are more well defined. In conclusion the constrained four-term analysis seems to give the best fit of the experimental lifetime spectra with respect to the balance between the variance of the fit and the uncertainties of the fitting parameters.

Table V. Results of three different types of analysis performed on a lifetime spectrum obtained on liquid SF_6 at 23°C.

Number of lifetimes	Number of constraints	Variance of the fit	τ_1 (nsec) $\pm\Delta\tau_1$	I_1 (%) $\pm\Delta I_1$	τ_2 (nsec) $\pm\Delta\tau_2$	I_2 (%) $\pm\Delta I_2$	τ_3 (nsec) $\pm\Delta\tau_3$	I_3 (%) $\pm\Delta I_3$	τ_4 (nsec) $\pm\Delta\tau_4$	I_4 (%) $\pm\Delta I_4$
3	0	1.884	0.285	40.8			1.250	16.4	9.486	42.9
			0.003	0.4			0.031	0.3	0.055	0.2
4	0	1.093	0.194	25.5	0.573	24.9	3.376	13.1	11.051	36.4
			0.010	1.5	0.026	1.2	0.272	0.9	0.288	1.2
4	1	1.203	0.125	17.2	0.453	31.5	2.544	12.3	10.478	39.0
				0.5	0.008	0.4	0.132	0.4	0.144	0.5

The values shown in Table V are not exactly those shown in figures 19 and 20 since the latter ones are average values of several measurements.

Above 51°C it was, in addition, necessary to use a fixed lifetime of τ_2. The constraint of τ_2 above 51°C will be discussed in Section 5.

The lifetime measurements have been performed as a function of the temperature in three runs with sufficient overlap between each run to ensure the reproducibility of the lifetime parameters at various temperatures. Furthermore, lifetime spectra at room temperature have been obtained several times during each run.

In Fig. 19 the temperature dependence of the lifetimes is shown. The critical temperature T_c is indicated by an arrow on the temperature scale. The full line without experimental points indicates the temperatures at which this lifetime has been fixed during the analyses. The intensities I_1, I_3, and I_4 are shown in

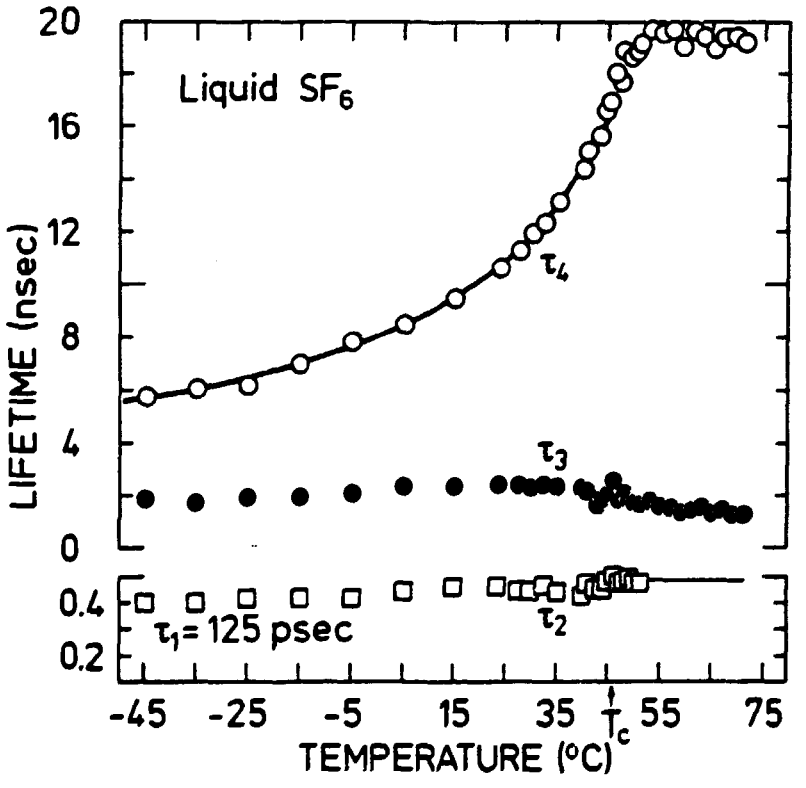

Fig.19. Temperature dependence of the positron lifetime in liquid SF_6 as obtained from lifetime spectra resolved into four components using a constant lifetime of para-Ps equal to 0.125 nsec. T_c is the critical temperature.

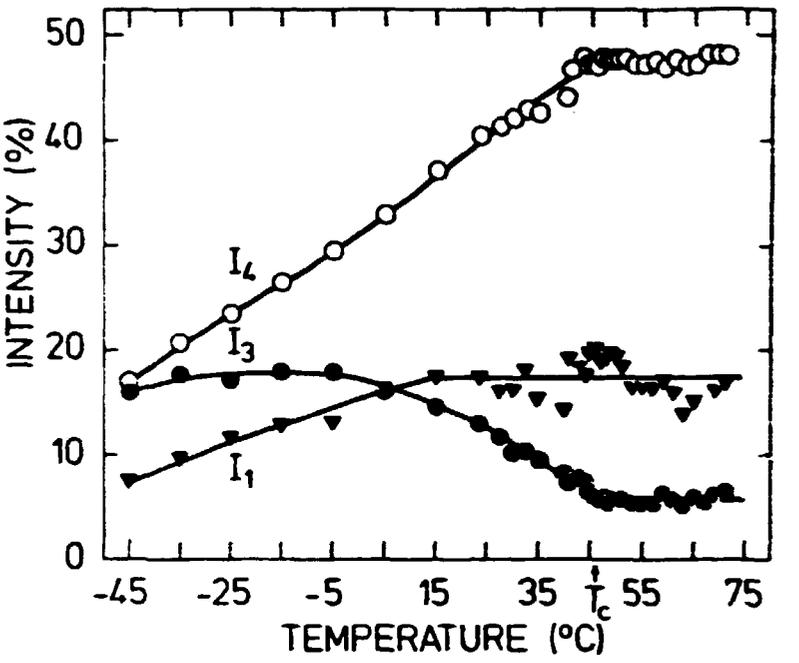

Fig.20. Temperature dependence of the intensities I_1, I_3, and I_4 in liquid SF_6. T_c is the critical temperature.

Fig. 20. The estimated uncertainties of the lifetime parameters including both the statistical and apparatus drift are: $\Delta\tau_2$ = 0.015 nsec, $\Delta\tau_3$ = 0.25 nsec, $\Delta\tau_4$ = 0.3 nsec, and $\Delta I_{1,2,3}$ = 1%, respectively.

The lifetime spectra obtained in liquid neopentane were resolved into three lifetime components with reasonably good variances of the fits. The temperature dependence of the lifetimes are shown in Fig. 21, while the corresponding intensities I_1 and I_3 are found in Fig. 22. The critical temperature is marked by an arrow on the temperature scale. In the temperature range from 23°C to 140°C, the lifetime spectra have been recorded in two runs, each with a temperature increment of 10°C between measurements. The measurements in the second run were performed at temperatures between those recorded in the first. At temperatures higher than 140°C it was very difficult to reproduce the intensity I_3 of the longest-lived component while the lifetime τ_3 itself was reasonably well reproduced. The values of I_3 displayed at these temperatures are those which seem most reliable in our opinion. How-

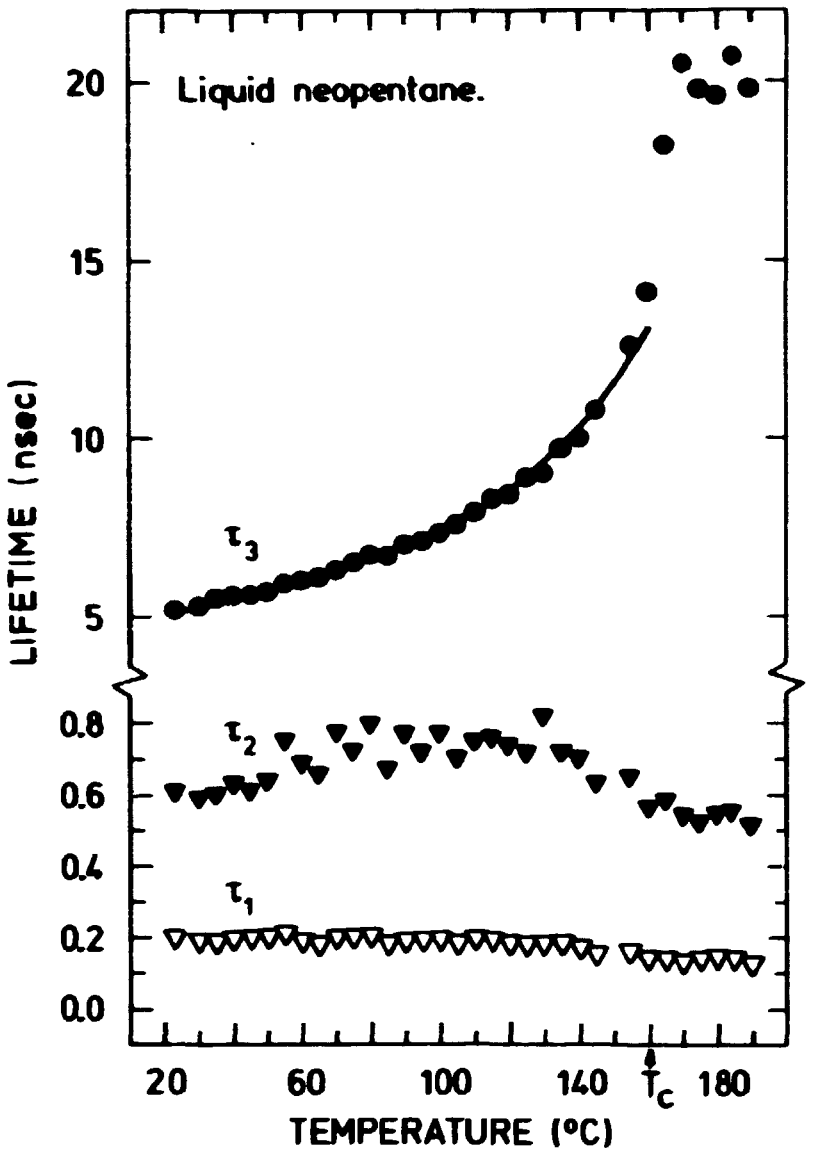

Fig.21. Temperature dependence of the positron lifetimes in liquid neopentane as obtained from lifetime spectra resolved into three components. T_c is the critical temperature.

ever, the characteristic decrease of I_3 at the critical point was qualitatively obtained in most of the measurements performed at these temperatures. In Section 5, we shall discuss possible reasons for the difficulties of the reproducibility of I_3 above 140°C.

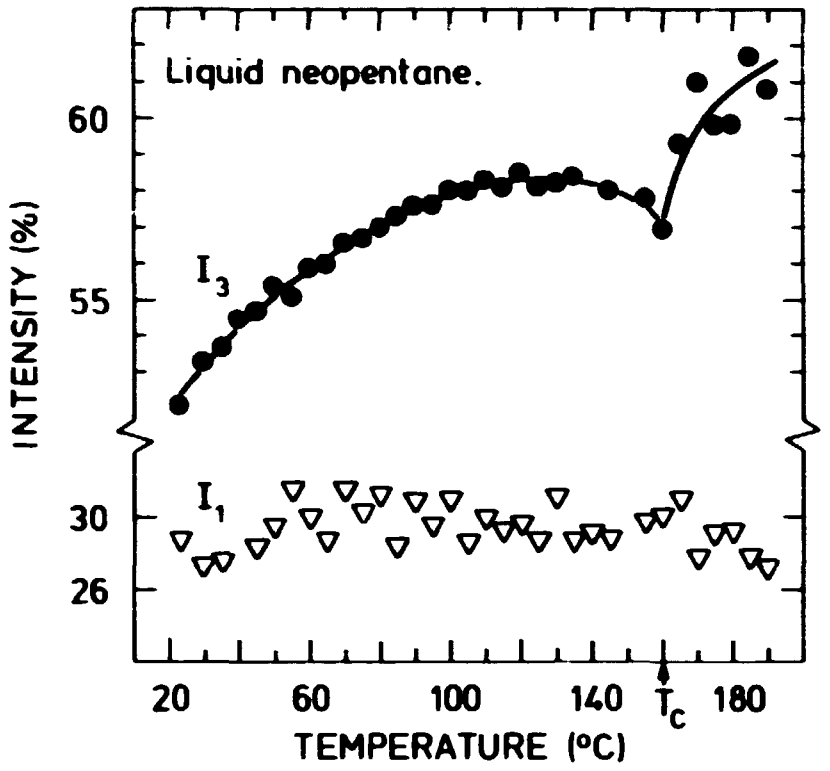

Fig.22. Temperature dependence of the intensities I_1 and I_3 in liquid neopentane. T_c is the critical temperature.

The uncertainties of the lifetime parameters at temperatures below 140°C are readable from the figures. The estimated uncertainties are $\Delta\tau_1$ = 0.05 nsec, $\Delta\tau_2$ = 0.1 nsec, $\Delta\tau_3$ = 0.05 nsec, $\Delta I_{1,2}$ = 1.5% and ΔI_3 = 0.2%, respectively.

Figure 23 shows the mobility of the excess electron in liquid neopentane as a function of temperature. The mobility measurements have been performed by Dodelet and Freeman, 1977. In Section 5 we shall discuss the influence of the behaviour of the excess electrons on the Ps yield.

In Figs. 24 and 25 the lifetimes and the intensities as obtained in liquid hexane as functions of temperature in the range from -72°C to 160°C are given. The lifetime spectra have been resolved into three lifetime components without any constraint and with reasonably good variances of the fits. The critical temperature

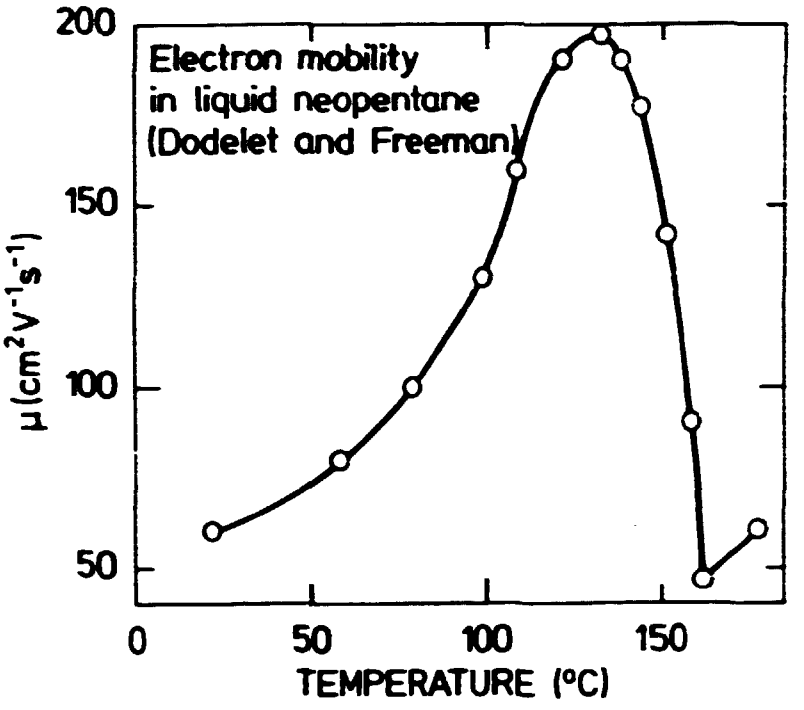

Fig.23. Temperature dependence of the excess electron mobility in liquid neopentane (Dodelet and Freeman, 1977).

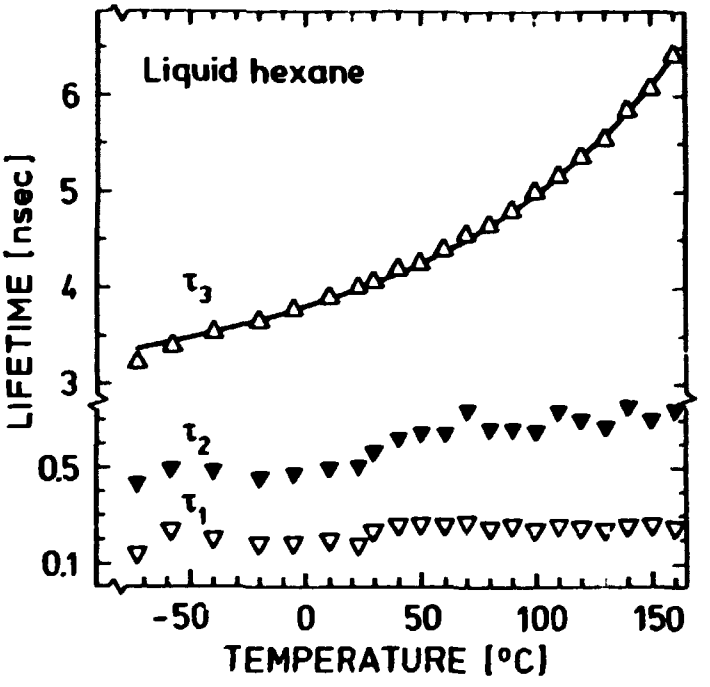

Fig.24. Temperature dependence of the positron lifetimes in liquid hexane as obtained from lifetime spectra resolved into three components.

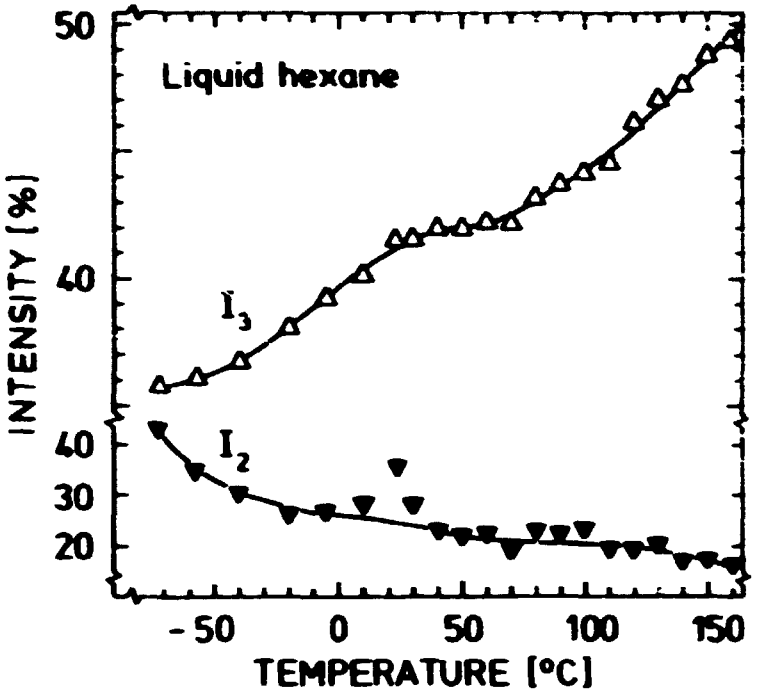

Fig.25. Temperature dependence of the intensities I_2 and I_3 in liquid hexane.

of hexane is T_c = 234.7°C. The spectra have been obtained in two runs of which one covered the temperature range from 23°C to 160°C, while the second covered the range from -72°C to 23°C. The estimated uncertainties of the lifetime parameters are: $\Delta\tau_1$ = 0.05 nsec, $\Delta\tau_2$ = 0.1 nsec, $\Delta\tau_3$ = 0.05 nsec, $\Delta I_{1,2}$ = 4%, and ΔI_3 = 0.5%. Figure 26 shows the mobility of the excess electrons in liquid hexane as a function of temperature as determined by Huang and Freeman, 1978. The behaviour of the excess electron will be related to the Ps yield in the discussion section below.

Before closing the presentation of the experimental results attention should be drawn to a few characteristics of the lifetime components as obtained in the various liquids investigated in this work.

The temperature dependence of τ_3 in the two liquids: 5PO and 6PO (Figs. 16 and 17) can be divided into three regions. Below a temperature designated T_g (not far from the glass transition

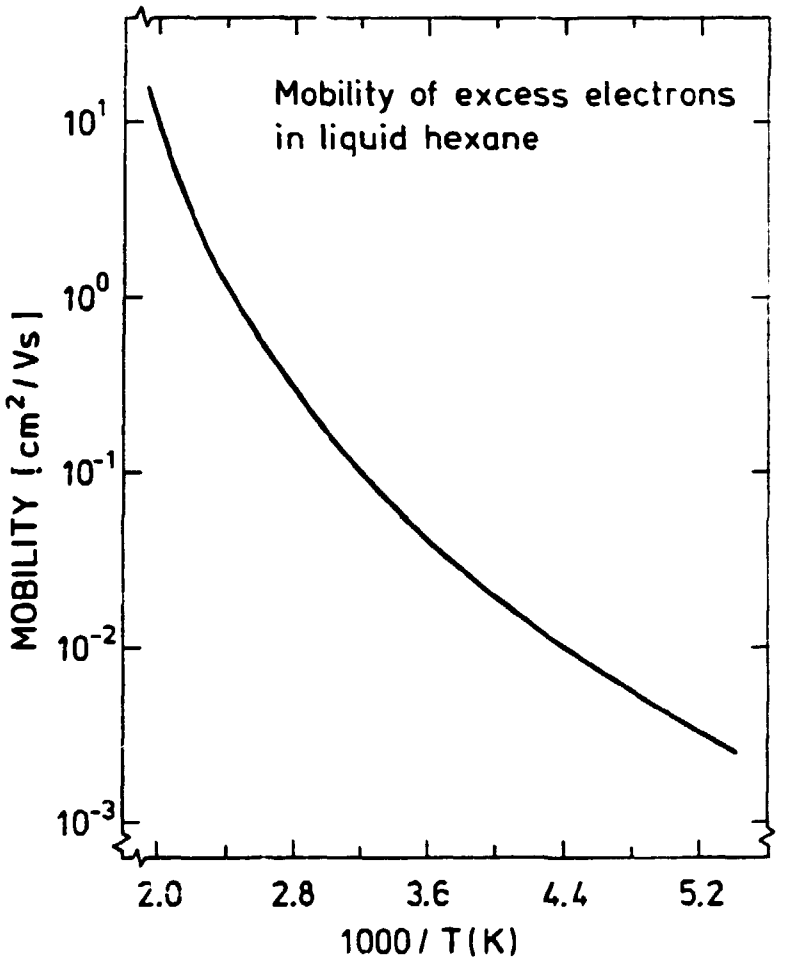

Fig.26. Temperature dependence of the excess electron mobility in liquid hexane (Huang and Freeman, 1978).

temperature) τ_3 is almost insensitive to temperature changes, while above the temperature denoted T_r τ_3 increases slightly with increasing temperature. At temperatures between T_g and T_r, τ_3 shows a strong temperature dependence.

The most surprising result appearing in the lifetime experiments performed on liquid SF_6 was that the analyses strongly indicated that all the lifetime spectra recorded at various temperatures contained two lifetime components with lifetimes in the nsec region. This result has to be compared with that of previous lifetime measurements performed on various other liquids which yielded only one lifetime in the nsec region (Lévay, 1979, Jansen

and Mogensen, 1977, and Gray, Cook and Sturm, 1968). The lifetime τ_3 of the new component is essentially constant in the main part of the temperature range studied, indicating that the state giving rise to this component is temperature independent.

The lifetime τ_4 shows a strong temperature dependence and increases from 5.7 nsec at -45°C to 19.5 nsec at 53°C. The temperature dependence of the longest-lived component τ_3 in neopentane seems to be similar to that of τ_4 in SF_6. Taking into consideration that the measurements in liquid hexane have been performed at lower temperatures compared to the critical temperature, it seems that τ_3 in hexane behaves very similar to the longest lifetime in SF_6 and neopentane.

In liquid SF_6 the intensities I_3 and I_4 depend quite strongly on the temperature below the critical point. The intensity I_4 increases from 16.9% at -45°C to 47.2% at the critical temperature, while I_3 decreases from 16% to 6.4% in this range. The intensity I_3 of the longest-lived component in liquid neopentane increases from 52% at 23°C to a maximum of 58.5% at 120°C. Above 120°C I_3 decreases to a minimum of 57% at the critical point. Above the critical temperature, I_3 increases with rising temperature. In liquid hexane the intensity of the longest-lived component increases with increasing temperature within the temperature range studied.

5. DISCUSSION

5.1. Discussion of the lifetime components

As briefly discussed in Section 3.4, the lifetimes of free positrons in condensed matter are not expected to be much longer than 0.5 nsec. Thus, lifetime components with a mean lifetime significantly longer than 0.5 nsec are generally believed to be associated with the decay of ortho-Ps. All of the positron life-

time spectra obtained in the liquids: 5PO, 6PO, SF_6, neopentane, and hexane, contained a long-lived component with a mean lifetime significantly longer than expected for free positrons. Thus, the longest-lived components in these liquids are attributed to the decay of ortho-Ps. The two shortest-lived components are then attributed to the decay of para-Ps and free positrons. From the lifetimes of the two shortest components (for SF_6, see below) we clearly observe that these litetime components do not represent the separate decay of para-Ps ($\simeq$ 0.12 nsec) and free positrons, respectively.

In an angular correlation experiment we measure the center-of-mass momentum distribution of the positrons and the annihilation electrons. The normal decay mode of ortho-Ps is the pick-off annihilation by which the positron in ortho-Ps annihilates into two photons with an electron of opposite spin on the surrounding molecules. Thus, both free positrons and the positron in ortho-Ps annihilate with electrons of energies of about 10-20 eV. Hence, the angular correlation curves attributed to free positrons and ortho-Ps are expected to be quite broad with a FWHM of about 6-10 mrad. On the other hand, due to the fast intrinsic decay of para-Ps, the positron in para-Ps decays mainly with its own electron. Hence, in contrast to that of ortho-Ps, the angular correlation curve attributed to the decay of para-Ps can be directly associated with the center-of-mass wave function (or rather its Fourier transform) of Ps. As it is normally assumed that para-Ps is in thermal equilibrium with its surroundings prior to annihilation we expect the width of the angular correlation curve attributed to the decay of para-Ps to be strongly correlated to the degree of localization of the center-of-mass wave function. In cases of almost complete delocalization of Ps, the width of the angular correlation curve of para-Ps reflects the "thermal energy" of Ps, and the curve would consequently be close to a Dirac function (see Douglas, Eldrup, Lupton, and Stewart, 1979). In most liquids, the width of the narrow component of angular correlation curves is of the order of 2-3 mrad (Mogensen, 1980). Thus, the narrow component of the angular correlation curve associated with the decay of para-Ps is usually fairly easy to extract from the total curve. It is generally believed that the

yield of ortho-Ps is about three times that of para-Ps. Hence, a comparisor of the intensity of the narrow component as measured in an angular correlation experiment to the intensity of the longest-lived component associated with the decay of ortho-Ps can serve partly as a test of the interpretation of the lifetime components. Although, usually not in exact agreement in many liquids it is found that one-third of the intensity ($I_3/3$) of the longest lifetime component (in liquids for which it is possible to resolve the positron lifetime spectrum into at least two lifetime components) is close to the intensity (I_n) of the narrow component of the angular correlation curve. In liquid neopentane and hexane at room temperature the values of ($I_3/3$, I_n) are, respectively, (17.3%, 19.98%) and (13.8%, 17.34%).

In liquid SF_6 all the lifetime spectra were resolved into four lifetime components. The lifetimes of the two longest components (τ_3, τ_4) are both significantly larger than expected for free positrons. Hence, we have associated these two components with the decay of ortho-Ps. The lifetime of τ_2 is close to that observed for free positrons in most non-conducting condensed matter, and is thus associated with the decay of free positrons. As mentioned in Section 4 the shortest-lived component, τ_1 = 0.125 nsec, is associated with the decay of para-Ps. The fixed lifetime of para-Ps corresponds to the intrinsic lifetime. It could be argued that the pick-off annihilation mode is also active in the case of para-Ps and, hence, that this annihilation channel should be taken into account. However, there seems to be no reason to believe that the pick-off annihilation rate of para-Ps should be faster than that of ortho-Ps. The fastest pick-off annihilation rate of ortho-Ps in SF_6 is close to 0.5 $nsec^{-1}$ (τ_3). If the pick-off rate of para-Ps equals the faster pick-off rate for ortho-Ps, this will reduce the para-Ps lifetime to 0.118 nsec. However, qualitatively, the analyses of the lifetime spectra would not depend very much on whether the lifetime of para-Ps is fixed to 0.118 nsec or to 0.125 nsec. It should also be mentioned that we do not know the fraction of para-Ps which annihilates at this possible fast pick-off rate (0.5 $nsec^{-1}$). Furthermore, it could be expected that the pick-off annihilation rate is lower for para-Ps than for ortho-Ps due to the repulsion (exchange

forces) between the electron in para-Ps and electrons on the surrounding molecules having the same spin direction (Mogensen and Eldrup, 1977). Hence, by taking the above into account, a fixed lifetime of para-Ps of 0.125 nsec seems to be a reasonable value to use.

Figure 27 shows I_1 and $1/3(I_3+I_4)$ and the Ps formation all as functions of temperature. The latter is calculated simply as $4/3(I_3+I_4)$. On bearing in mind that the intensity I_1 can be very sensitive to any uncertainties in the time resolution, the approximate equality of I_1 and $1/3(I_3+I_4)$ seems to support the above interpretation of the lifetime components as obtained in liquid SF_6.

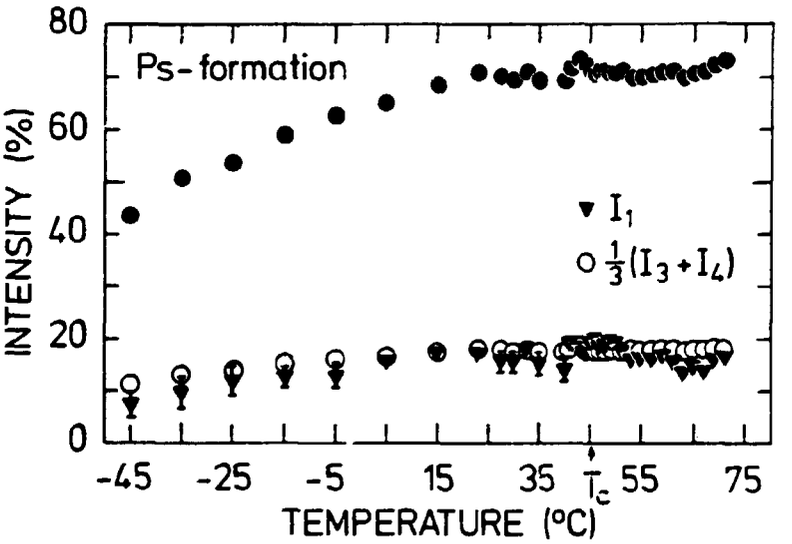

Fig.27. Temperature dependence of the Ps yield in liquid SF_6. In addition the intensity of para-Ps (I_1) and 1/3 of the intensity of the total ortho-Ps; viz. 1/3 (I_1 + I_4) are shown. T_c is the critical temperature.

Above 51°C, it was not possible to continue the four-term analyses as described in Section 4. This is probably because I_3 becomes low and that τ_3 is an intermediate lifetime. The effect of this is that the correlation between the three shortest-lived components becomes stronger, resulting in an unacceptable increase in the uncertainties of the fitting parameters. However,

the analyses of the lifetime spectra obtained in SF_6 above 51°C still gave evidence of the existence of two ortho-Ps states. In order to extract as much information as possible about the short-lived ortho-Ps component we decided to fix the free positron lifetime τ_2. The fixed value used for τ_2 corresponds to the average lifetime of the previous ten experimental points.

The state of Ps in liquids will be discussed in Section 5.2, while in Section 5.3 we shall discuss the extra ortho-Ps lifetime in liquid SF_6. In Section 5.4 the Ps yield in the liquids will be discussed in terms of the positron spur model.

5.2. The state of Ps in liquids

As already mentioned in Section 4, the temperature dependence of the lifetime of the longest-lived component in liquid SF_6, neopentane, and hexane seems to be very similar if the temperatures are compared to the critical temperature of these liquids. In all three liquids the lifetime $\tau_3(\tau_4; SF_6)$ shows a strong temperature dependence. The behaviour of $\tau_3(\tau_4; SF_6)$ as a function of temperature agrees very well with what one would have expected from previous measurements of the ortho-Ps lifetime in various liquids at room temperature (Lévay, 1979, Gray, Cook, and Sturm, 1968, and Jansen and Mogensen, 1977) and can be explained in terms of the Ps bubble model, where Ps is assumed to "dig itself" a hole in the liquid and become localized in a bubble state (Lévay, 1979, Ferrell, 1957, and Hernandez, 1976). The bubble state of Ps, described briefly in Section 1.5, shall now be discussed in some detail.

At first let us discuss the experimental and theoretical results which favour a Ps bubble state, i.e. of the formation of a microscopic cavity around Ps resulting in large configurational changes of the liquid around Ps (see Table II in Section 1.3). The strongest experimental evidence of the Ps bubble state in a liquid is found in lifetime and angular experiments performed on liquid He (Hernandez, 1976, and Briscoe, Choi, and Stewart, 1968). The change of the pick-off lifetime in solid-to-liquid

transitions (Petersen, Eldrup, and Trumpy, 1970, Kluth, Clarke, and Hogg, 1964, and Germagnoli, Poletti and Randone, 1966) for normal liquids strongly supports the Ps bubble theory. Even in the ice-water transition where the density increases, the pick-off lifetime is observed to increase roughly by a factor of two in going from ice to water (Petersen, Eldrup, and Trumpy, 1970). From studies of vacancies in molecular crystals we can also get experimental support for the Ps bubble model. Typical pick-off lifetimes of ortho-Ps trapped in vacancies in molecular crystals are: 1.2 nsec in ice (Mogensen and Eldrup, 1978, and Eldrup, Mogensen, and Bilgram, 1978), 2.45 nsec in succinonitrile (Eldrup, Pedersen, and Sherwood, 1979), 2.9 nsec in adamantane (Lightbody, Sherwood, and Eldrup, 1980), and 3.2 nsec in camphene (Eldrup, Mogensen, and Sherwood, 1979). If we neglect relaxation around the vacancies the corresponding vacancy radii are: $\simeq$ 2 Å (ice), $\simeq$ 3 Å (succinonitrile, $\simeq$ 3.7 Å (adamantane), and $\simeq$ 4 Å (camphene). From the molecular volume of SF_6, neopentane, and hexane we get the corresponding "molecular radii" at room temperature: $\simeq$ 3.5 Å (SF_6), $\simeq$ 3.65 Å (neopentane), and $\simeq$ 3.7 Å (hexane). Thus a comparison of the pick-off lifetime of ortho-Ps in liquid SF_6, neopentane, and hexane to that measured in vacancies in molecular crystals strongly suggests that Ps in liquids is localized in a state in which the density of the liquid molecules is substantially lower than the average density of the liquid molecules. Finally, perhaps the strongest argument for using the Ps bubble picture for the state of Ps in liquid comes about through angular correlation experiments where the momentum distribution of para-Ps is found to be consistent with a localized state of Ps (Jansen, 1976, and Mogensen, 1980).

Without going into detail we show in Fig. 28 the relation between the width of the momentum distribution of para-Ps and the pick-off lifetime as obtained in some "typical" liquids. The data have been collected from the works of Jansen and Mogensen, 1977, Gray, Cook, and Sturm, 1968, Mogensen, 1980. Qualitatively, the pick-off lifetime τ_p behaves as expected according to the bubble model, viz. τ_p decreases with increasing degree of localization of Ps. It should be mentioned that it is possible to find a few liquids in which the relation between the width of the momentum

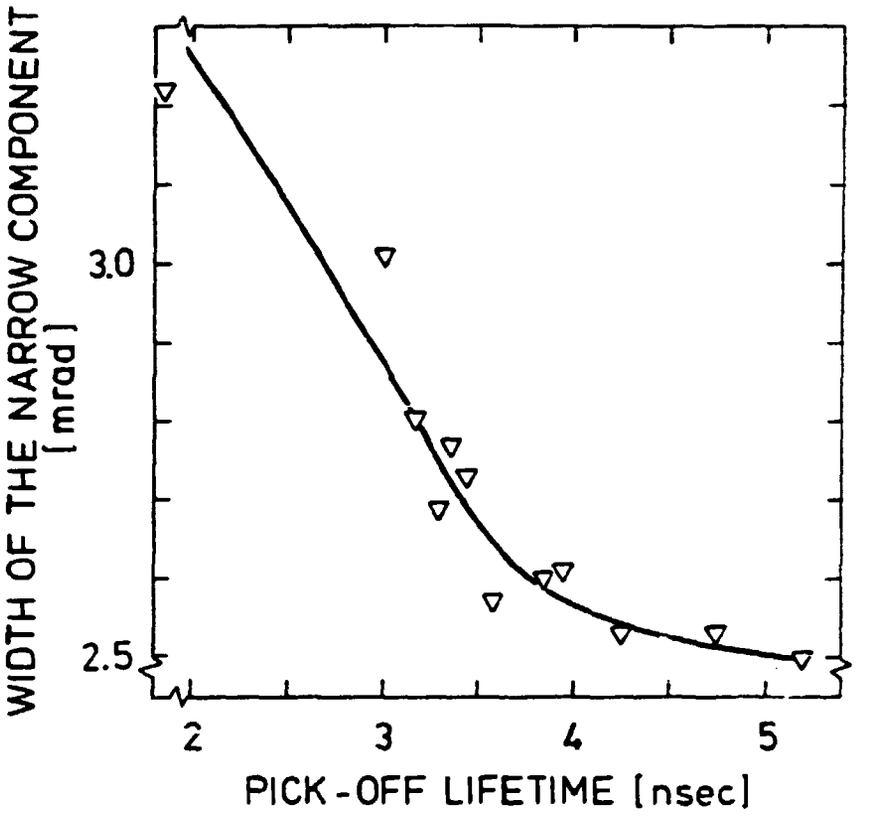

Fig.28. Correlation between the width of the momentum distribution of para-Ps and the pick-off lifetime of ortho-Ps in some selected liquids (see text).

distribution of para-Ps and the pick-off lifetime of ortho-Ps does not fit into that shown in Fig. 28.

Theoretical arguments for the existence of the Ps bubble in liquids can be found in the work on the so-called free volume model introduced by Brandt, Berko, and Walker, 1960. In this model Ps is assumed to be in the free volume between the molecules, and furthermore, that the structure of the medium is mainly unaffected by the presence of Ps. The latter infers that Ps is in an extended state such that the zero-point motion of Ps can be neglected. Using these assumptions it turns out that the lifetime of ortho-Ps is determined mainly by the free volume of the medium. In order to be able to perform a calculation of the pick-off lifetime the molecules are represented by square-well

types of potentials arranged according to the symmetry of the molecules of the medium; the lifetime is then determined by $\tau = \tau_o S(v_f, U)$, where $S(v_f,U)$ depends on the overlap between the Ps wave function and the molecules; v_f and U are, respectively, the free volume and the energy barrier height of the potential representing the molecules. The constant τ_o is usually taken to be 0.35 nsec which is not far from the lifetime of Ps^- (Ferrante, 1968).

In ice in which Ps is in an extended state in the bulk (Mogensen and Eldrup, 1978) the free volume model explains the temperature dependence of ortho-Ps at low temperatures fairly well. At higher temperatures the free volume model predicts lifetimes of ortho-Ps which are too low, very probably due to the presence of vacancies (Eldrup, Mogensen, and Bilgram, 1978, and Mogensen and Eldrup, 1978). However, for normal liquids with pick-off lifetimes of the order of 3-5 nsec or longer it is probably not possible to fit the temperature dependence of the pick-off lifetime by means of the free volume model. Merely to fit a single point will demand high values of τ_o and U, which probably are physically unreasonable. The lack of success of the free volume model in explaining the pick-off lifetime of ortho-Ps in liquids strongly suggests that Ps is situated in a cavity which is appreciably larger than the average free volume per molecule. This together with the momentum distribution of para-Ps in liquids strongly seems to favour the idea of the Ps bubble in liquids. Furthermore, in the case of polymers it has been necessary to increase τ_o by roughly a factor of three in order to get agreement between theory and experiment (Brandt, Berko, and Walker, 1960). In a polymer Ps is very probably trapped in pre-existing cavities which are larger than the average one and which perhaps are further enlarged due to the zero-point motion of Ps. Also it should be mentioned that delocalized Ps has been observed only in solids such as ice (Mogensen and Eldrup, 1977), quartz (Brandt, Coussot, and Paulin, 1969), etc., while in softer molecular solids the angular correlation curves do not indicate that para-Ps annihilates from an extended state.

Altogether, the presently available data on the Ps state in liquids and solids strongly favour the Ps bubble state in normal liquids. Thus, the longest-lived components in the liquids: SF_6, neopentane, and hexane will be interpreted in terms of the Ps bubble model. The Ps bubble state in liquids is still not universally accepted, probably partly because a clear definition of the state has not been given. We recommend the use of the definition given by Jortner and Gaathon, 1977; see Table II, Section 1.4.

The detailed processes which occur during the formation of the Ps bubble are not very well understood at present. Furthermore, the presently available knowledge of Ps-molecule interactions, etc. does not allow a detailed calculation of the structure of the Ps bubble. In addition, the detailed structure of the bubble cannot be derived from positron annihilation results at present. Thus, the situation is roughly similar to that encountered in the studies of electrons in various states in liquids where, in particular, lack of detailed experimental information limits the usefulness of complex mathematical models of the electron states in many cases. Hence, fairly simple models of the Ps bubble are normally used in the interpretation of the experimental results. The mathematical model commonly used to calculate the properties of the Ps bubble is one in which the Ps bubble is represented by a spherical square-well potential and in which the liquid molecules outside the bubble are treated as a continuum (Buchikhin, Goldanskii, and Shantarovich, 1971a, and 1971b, and Lévay and Vértes, 1976). Recently, a more detailed bubble model based on density- functional theory has been formulated by Nieminen, Välimaa, Manninen and Hautojärvi, 1980, and used to calculate the structure of the Ps bubble in liquid He. Although, while perhaps successful in He and in other atomic liquids, it is probably not useful, at present, to apply this new theory to cases of the Ps bubble in molecular liquids.

However, as the spherical square potential is often used as a model of the Ps bubble in normal liquids we shall discuss it in some detail.

The size of the Ps bubble is determined by minimizing the free energy of the system, $E_t(r)$, which is given by:

$$E_t(r) = E_{Ps}(r) + E_s(r) \tag{18}$$

where E_{Ps} and E_s are the zero-point energy of Ps localized in the bubble state and the work necessary to create the bubble, respectively. Furthermore, the following approximation is used for the pick-off lifetime τ_p:

$$\tau_p^{-1} = \lambda_p = \pi r_o^2 c n z_{eff} P(kr_b) \tag{19}$$

where r_o, c, n, z_{eff}, $P(kr_b)$, k, r_b are, respectively, the classical radius of the electron, the speed of light, the density of molecules, the average number of annihilation electrons per molecule, the quantum mechanical probability of finding Ps outside the bubble, the quantum number, and the bubble radius. The value of z_{eff} is usually taken to be the number of valence electrons. As most of the previous lifetime experiments have been performed at temperatures of low vapour pressure, E_s has usually been set equal to $4\pi r^2\sigma$, where σ is the macroscopic surface tension. By taking the vapour pressure into account and by assuming the potential energy of Ps to be -U inside the bubble and zero elsewhere we obtain, by minimizing (18):

$$\begin{aligned}&\{kr_b(\tan(kr_b)-kr_b)\}^{-1}\sin^4(kr_b)\\ &= -\pi\hbar^2\sigma/(m_eU^2) - \pi\hbar^3 kr_b P_v/(4m_e^{3/2}U^{5/2}\sin(kr_b))\end{aligned} \tag{20}$$

where P_v is the vapour pressure. Furthermore, by use of the model we can calculate the probability, $P(kr_b)$, of finding Ps outside the bubble:

$$P(kr_b) = \{1 - kr_b\cot(kr_b)\}^{-1}\sin^2(kr_b) \tag{21}$$

Thus, by knowing the pick-off annihilation rate, τ_p, $P(kr_b)$ can be determined from (19), kr_b from (21), and U from (20), whereas k and r_b are determined from the relation:
$k = (4m_eU/\hbar^2)^{\frac{1}{2}}\sin(kr_b)$.

Of course, the simple square-well model of the Ps bubble can be criticized for several reasons: Some of the calculated bubble parameters can be judged in only a rather subjective way, and the relation (19) is not obvious. Furthermore, the use of the macroscopic surface tension is incorrect for two reasons: 1) comparing the range of the forces between the liquid molecules (5-15 Å) to the calculated bubble radii (typical 3-8 Å), it is easy to see that the use of the macroscopic surface tension in E_s is not reasonable both because of the bubble size and the surface curvature, and 2) the surface tension of a liquid in equilibrium with its own vapour pressure is not expected to be the same as the surface tension of a liquid in equilibrium with the Ps bubble. Concerning only the second component, the use of the macroscopic surface tension can perhaps be justified at temperatures of low vapour pressure, while at high vapour pressure it may turn out to be a very bad approximation.

In order to gain insight into the model let us apply it to liquid SF_6 at room temperature, where we have $n = 5.5 \cdot 10^{21}$ cm^{-3}, $\sigma = 2.78$ dyn/cm, $P_v = 22.5$ atm, and $\tau_p = 11.4$ nsec. At first, we have to decide upon the number z_{eff}. Assuming that roughly three of the fluorides are sticking into the bubble we have taken $z_{eff} = 12$. However, qualitatively, the following does not depend very much on the actual value of z_{eff}. From Eq. (19) we obtain $P(kr_b) = 0.18$, from (21) $kr_b = 2.3$, and from (20) $U = 0.367$ eV. By using the relation between k, kr_b, and U given above, we obtain $r_b = 7$ Å. The energy function versus radius can be calculated by assuming U to be independent of r, and by using:

$$E_t(r) = E_{Ps}(r) + 4\pi r^2\sigma + 4/3\pi r^3 P_v$$

$$E_{Ps}(r) = -U\cos^2\{(4m_e/\hbar^2)^{\frac{1}{2}}(E_{Ps} + U)^{\frac{1}{2}}r\} \qquad (22)$$

The various energy terms are shown in Fig. 29. As observed from this figure the energy minimum of E_t is not very pronounced when compared to the thermal energy. Changes in the energy of $\pm$ kT correspond to changes in the radius of roughly 25%. Hence, the use of the model suggests that the Ps bubble is a very dynamic state and it is therefore probably not reasonable to treat the

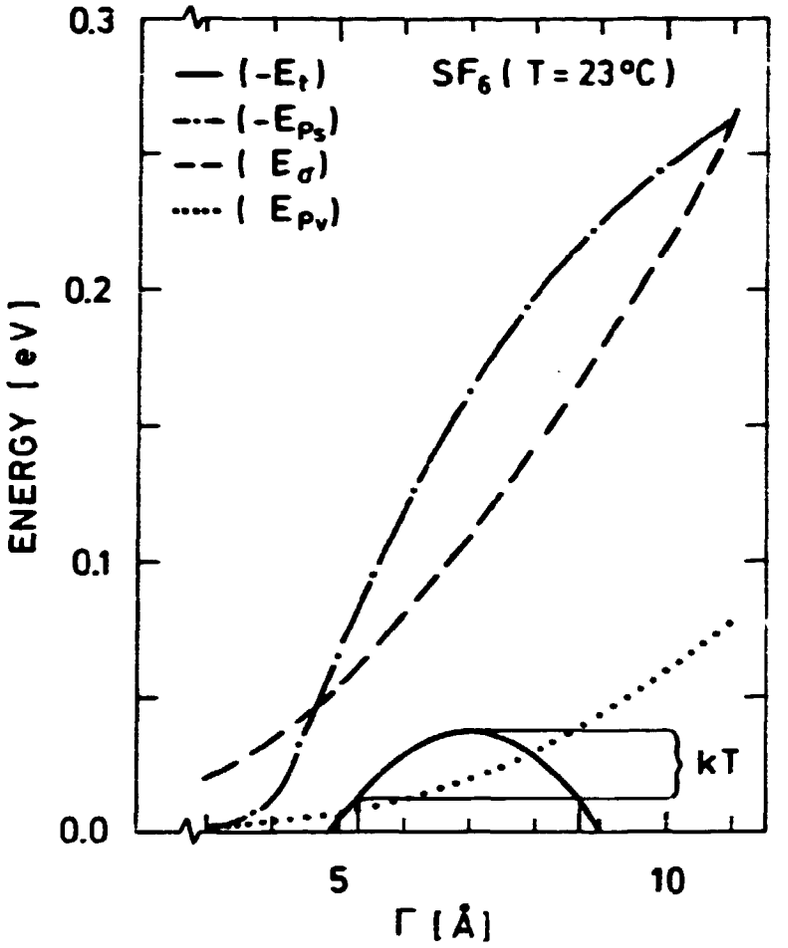

Fig. 29. The total energy E_t of the Ps bubble state as function of the bubble radius. Furthermore, the radius dependence of the various energy terms contributing to the total energy are shown. Note that the total energy, E_t, and the zero-point energy of Ps, E_{Ps}, are displayed as $-E_t$ and $-E_{Ps}$, respectively.

Ps bubble within a static continuum picture. Furthermore, small changes in the energy versus radius relation $E_t(r)$ caused by the use of different approximations may correspond to fairly large changes in the bubble radius.

Taking the above into account, it seems to be more reasonable at present to be satisfied with a qualitative model for the Ps bubble rather than a quantitative one that gives numerical values for various physical properties with very probably large uncertainties.

In many previous lifetime experiments performed on various liquids a very simple semi-empirical relationship between the pick-off lifetime τ_p and the macroscopic surface tension has been found (Tao, 1972, and Lévay and Vértes, 1976):

$$\tau_p^{-1} = 0.062\sigma^{0.51} \quad (\text{nsec})^{-1} \tag{23}$$

with σ in CGS units. Furthermore, based on a semi-empirical relationship between the solubility parameter and the surface tension, Tao, 1972, predicted that the pick-off annihilation rate should be proportional to the solubility parameter ($\lambda_p \propto \delta$). The solubility parameter is given by $\delta^2 = (\Delta H_v - RT)/V_m$, the cohesive energy density. Such a correlation is, of course, expected if the bubble picture is used to interpret the state of Ps in liquids. In a study by Skytte Jensen, 1976, it was shown, however, that the correlation between λ_p and δ fails, except for non-polar liquids. However, by using only the dispersive part (δ_D) of the solubility parameter a fairly good correlation was obtained (except for water). The correlation between τ_p and δ_D indicates that the Ps bubble in liquids is formed in or diffuses to configurations for which the interactions between the molecules are weakest. Thus, the use of an average surface energy in the interpretation of the Ps state might be misleading in cases in which the liquids comprise molecules which interact through several types of interactions.

However, for liquid SF_6, neopentane, and hexane it seems reasonable to believe that the pick-off lifetime can be correlated to the average surface energy. However, relation (23) cannot be used in the present case since it is found for liquids in a temperature region of low vapour pressure. It is, therefore, reasonable to introduce here a new semi-empirical formula for τ_p versus the surface tension σ and the vapour pressure P_v.

Let us assume that the Ps wave function outside the Ps bubble is: $\psi = A' r^{-1} \exp(-\alpha' r)$, where A' and α' are constants. In a continuum model and by neglecting electron density variation with temperature we get by use of Eq. (19):

$$\tau_p^{-1} \propto 2\pi(A')^2(\alpha')^{-1}\exp(-2\alpha' r_b) \tag{24}$$

To estimate the bubble radius r_b an infinitely deep square-well potential is used as the Ps potential. Hence, by minimizing the total energy (18) we get the bubble radius:

$$r_b = (\hbar^2/16m_e)^{1/4}\{\sigma + \tfrac{1}{2}r_b P_v\}^{-1/4} \tag{25}$$

where m_e is the mass of the electron. Because of the exponent -1/4 we can assume that r_b is roughly constant on the rhs of Eq. (25). Hence, $r_b \propto (\sigma+\beta P_v)^{-1/4}$. In that way we can make our new semi-empirical expression plausible:

$$\tau_p^{-1} = A\exp\{-\alpha(\sigma + \beta P_v)^{-1/4}\} \tag{26}$$

where A, α, and β are fitting constants. By fitting Eq. (26) to the longest lifetime in liquid SF_6, neopentane, and hexane the full lines shown in Figs. 19, 21, and 24 are obtained. As observed from the figures relation (26) fits the experimental results very well. The temperature dependence of the vapour pressure in SF_6, neopentane, and hexane was taken from the work of Mears, Rosenthal, and Sinka, 1969, Dawson, Silberberg, and McKetta, 1973, and Handbook of Chemistry and Physics (CRC 1972-73), respectively. The temperature dependence of the surface tension was determined by assuming a linear temperature dependence of σ and that σ = 0.0 dyn/cm at T_c. For liquid SF_6, neopentane, and hexane we used σ = 11.63 dyn/cm at -50°C (Gmelin Handbuch der Anorganischen Chemie, 1963), σ = 14 dyn/cm at 23°C (authors estimate), and σ = 18.43 dyn/cm (Handbook of Chemistry and Physics, CRC 1972-73), respectively. The values of the parameters used to fit the longest lifetimes of ortho-Ps in the three liquids are shown in Table VI. As observed, the values of the fitting parameters differ somewhat from liquid to liquid. However, it is probably not worthwhile to discuss these differencies, taking into account the basis of relation (26), the uncertainties of the temperature dependence of the surface tension used in the fits, etc.

Table VI. Values of the parameter in Eq.(26) as used to fit the pick-off lifetime in SF_6, neopentane and hexane.

Liquid	A ($nsec^{-1}$)	α $(dyn/cm)^{1/4}$	β $(dyncm^{-1}atm^{-1})$
SF_6	1.65	4.2	o.o56
neopentane	1.65	4.2	0.100
hexane	1.77	4.1	0.110

As is noted in Figs. 19 and 21 the lifetime of the longest-lived component in liquid SF_6 and neopentane continues to increase with rising temperature beyond the critical temterature T_c. This behaviour of $\tau_3(\tau_4, SF_6)$ could seem a little surprising. However, although the surface tension of a liquid in equilibrium with its own vapour pressure becomes zero at the critical point this need not necessarily be the case for the microscopic surface tension of a liquid in the equilibrium state of the Ps bubble. At higher temperatures $\tau_3(\tau_4, SF_6)$ decreases slightly with increasing temperature. This is explained by the increase in vapour pressure.

In the following we shall discuss the temperature dependence of the ortho-Ps lifetime in the liquids: 5PO and 6PO (see Figs. 16 and 17). As the behaviour of τ_3 as a function of temperature is very similar in both liquids we shall discuss the lifetime results without differentiating between 5PO and 6PO.

Below the temperature T_g the lifetime of ortho-Ps is independent of temperature, probably reflecting the equilibrium defect distribution of the glass state. Similar organic structures may be expected to possess similar entropies in the glassy state and possibly also similar defect densities. To some extent this hypothesis is supported by the closely similar values of the ortho-Ps lifetime observed in the two liquids.

Above T_g the lifetime of ortho-Ps increases markedly with increasing temperature. It is of interest that the T_g value obtained from the positron studies is lower than that observed

from viscoelastic measurements [T_g]$_v$. One reason may be that whereas the viscosity reflects the mean distribution of the free volume, the ortho-Ps lifetime is very probably sensitive to fluctations in the defect distribution. For energetical reasons Ps is probably trapped in pre-existing cavities (defects) which are larger than the average cavity. Such fluctuations in the defect distribution will not necessary lead to mass transport and therefore not influence the viscosity. On the other hand, they will significantly influence the overlap between the Ps wavefunction and the molecules and, hence, the pick-off lifetime of ortho-Ps. Further, the pressure which Ps exerts on its surroundings may tend to lower the glass transition temperature of the material around it.

Supercooling has been studied in a large number of liquids and the nature of this mesophase is well established. Molecular motion in the supercooled state is cooperative viz. motion of a particular molecular unit requires the motion of neighbouring molecular units. Cooperative relaxation can be described in terms of a defect diffusion model by which the motion of a particular thermally-activated molecule is controlled by the free volume in its neighbourhood. Measurements on a wide variety of liquids have indicated that there is good correlation between the shift in the dielectric relaxation frequency and the viscosity. In the high viscosity region, the viscosity is known to be influenced by variation of the free volume.

Fig. 30 shows the lifetime of ortho-Ps versus the viscosity η (Logη) for the two liquids. The variation of Log(η) and the ortho-Ps lifetime is linear over nearly eight decades of the viscosity, implying a fundamental connection between the lifetime of ortho-Ps and the free volume in the high viscosity region. The loss of the linear correlation at a viscosity of $\sim 10^8$P suggests that a new effect may begin to be important. As discussed above, Ps is very probably trapped in pre-existing cavities. At viscosities higher than $\simeq 10^8$P the Ps cavity is probably determined mainly by the pre-existing holes. They may be enlarged somewhat due to the presence of Ps by primarily elastic processes in the surrounding structure. Due to the pressure which Ps

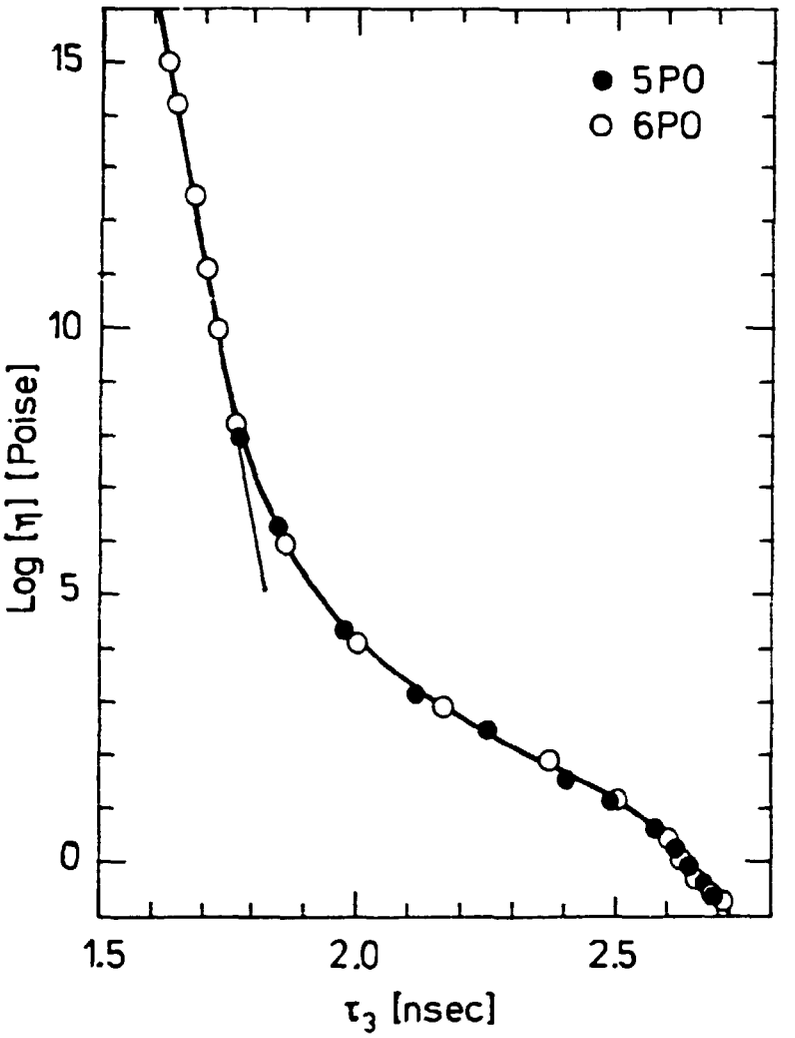

Fig.30. Correlation between the viscosity and the pick-off lifetime of ortho-Ps as measured in the liquids: 6PO and 5PO.

exerts on its surroundings it seems reasonable to assume that the loss of linearity between Log(η) and the ortho-Ps lifetime is caused by a further relaxation enlargement of the pre-existing cavities which trap Ps. At viscosities below approximately 10^8P a long range relaxation of the surrounding structure due to the pressure of Ps may begin to be rapid enough to take place before ortho-Ps decays.

Above temperature T_r the ortho-Ps lifetime becomes less sensitive to increasing temperature. Above T_r the two liquids behave

roughly similar to normal liquids. Thus it is reasonable to assume that at temperatures above T_r the ortho-Ps cavity can relax into its equilibrium size before ortho-Ps annihilates. Hence, it is expected that the lifetime of ortho-Ps can be interpretated in terms of the Ps bubble model. By using the semi-empirical relation between the pick-off lifetime and the surface tension given by Tao (1972) Equation (23), we obtain τ_3=2.85 nsec (2.46 nsec), i.e. roughly the measured lifetimes, for σ=30 dyn/cm (40 dyn/cm). Preliminary measurements (Barlow, Erginsav and Lamb, 1969) gave σ=30-40 dyn/cm for both liquids just above T_r.

Thus, according to the discussion given above, the lifetime of ortho-Ps at temperatures between T_g and T_r, is very probably closely related to the time it takes to form the Ps bubble in its equilibrium state. At temperatures close to T_g the Ps bubble formation time is probably much longer than the lifetime of ortho-Ps, while at temperatures close to T_r the bubble formation time and the lifetime of ortho-Ps are probably of similar order. However, due to the lack of detailed information about the structure and the distribution of the pre-existing cavities we do not consider it possible to obtain more detailed information of the time aspect of the Ps bubble-formation process.

5.3. The extra ortho-Ps lifetime component in liquid SF_6

Perhaps the most important result of the lifetime experiment performed on liquid SF_6 was the appearance of a short-lived ortho-Ps component with the lifetime τ_3. Of course, we did not expect to find such a component, and hence, we measured the spectra several times and checked carefully for the possibility that this component was caused by impurity effects, etc. (see below). However, we had to conclude that this component is an intrinsic property of SF_6 and Ps.

As observed from Fig. 19 the lifetime τ_3(2-2.5 nsec) of this new short-lived ortho-Ps component depends only weakly on the temperature in the main part of the temperature range studied. Due to the lack of detailed information of the spur properties in

liquid SF_6 (no radiation chemistry experiments have yet been performed on liquid SF_6) and on Ps-SF_6 interaction it is not an easy task to interpret the short-lived ortho-Ps component. However, in principle, we can imagine two possible causes for the appearance of the short-lived ortho-Ps component: 1) a reaction of ortho-Ps with some of the spur species in the positron spur, and 2) the possibility that ortho-Ps can annihilate from two different states in liquid SF_6.

In the former case it should be emphasized that the kinetics of reactions between spur species (recombination, Ps formation, Ps reaction with other spur species, etc.) are expected to be highly non-homogeneous in nature. In general, the reactions between the various spur species are believed to depend strongly on space and time. If homogeneous kinetics were applied to possible reactions between Ps and some of the other spur species it would turn out that the decay of ortho-Ps can be expressed in terms of a single lifetime component with a lifetime given as $\tau^{-1} = \tau_p^{-1} + k_n[X_n]$, where τ_p is the pick-off lifetime and the [X]'s are average densities of the spur species; k_n is a rate constant which depend on the diffusion properties of Ps and X_n as well as specifically on X_n. However, if the reactions between Ps and some of the spur species depend on space and time it is not very hard to imagine that the decay of ortho-Ps is not very well described by a single decaying exponential function. Typical spur species which may react with Ps are: the positive ions (of which at least one must exist in the spur in the whole lifetime of Ps), the excess electrons which have not yet recombined with the positive ions, etc. A reaction between a positive ion and Ps will probably lead to an oxidation of Ps, while a reaction with one of the excess electrons might result in the formation of Ps^- (Mogensen, 1981). Furthermore, possible formation of triplet states during the recombination of the excess electrons and the positive ions could be expected to have an influence of the lifetime of ortho-Ps (exchanges of electrons, spin flip, etc.). Intuitively, we expect some of the above-mentioned Ps reaction processes to take place in the spur, e.g. it is not very difficult to imagine that the Ps-positive ion reaction must be important in cases where Ps is formed close to the positive ions while in cases of Ps forma-

tion at larger distance from the positive ions this process is probably of no importance. However, generally, the present knowledge of the distribution of Ps as function of space and time does not allow us to estimate, quantitatively, the importance of such Ps reactions. On the other hand, the strong temperature dependence of the Ps yield in the temperature range from -45°C to 23°C indicates changes in spur porperties such as changes of the distribution of excess electrons/positron. Such changes would be expected to have an influence on Ps reactions with other spur species and thus cause changes in both the lifetime τ_3 and the fraction of ortho-Ps in the short-lived ortho-Ps component. Although the fraction of ortho-Ps in the short-lived component is sensitive to changes in temperatures, the lifetime τ_3 is almost constant in the range from -45°C to the critical point. The temperature independence of τ_3 can perhaps be taken as an indication that Ps reactions with other spur species are not the main cause of the appearance of the short-lived orhto-Ps component.

However, the two ortho-Ps lifetime components can be well understood if it is assumed that ortho-Ps can annihilate from two different states in liquid SF_6. Hence, the value of the short-lived ortho-Ps lifetime (2.-2.5nsec) indicates that this part of ortho--Ps is localized in a free volume corresponding to a radius of roughly 3-4 Å. This estimate is derived from measured pick-off lifetimes of ortho-Ps trapped in molecular crystals (see section 5.2). This estimate is also in agreement with the experience of the pick-off lifetime versus the degree of localization of Ps as derived from angular correlation experiments in a number of liquids (Jansen, 1976, and Mogensen, 1980). Similar short pick--off lifetimes have been measured for other liquids (Gray, Cook, and Sturm, 1968, and Jansen and Mogensen, 1977). However, in those cases only one ortho-Ps lifetime component was found and in most cases the lifetime could be explained by reference to a high surface tension. In a previous work (Jacobsen, Eldrup, and Mogensen, 1980) CS_2 was mentioned as a specific example of such a liquid (τ_p=2.2 nsec). However, the short pick-off lifetime in CS_2 cannot be explained simply by reference to the surface tension (σ≈33dyn/cm). By use of the semi-empirical relation between the pick-off decay rate (Eq. 23) we obtain τ_p=2.7 nsec in CS_2.

Furthermore, the width of the narrow component of the angular correlation curve (FWHM=2.6 mrad) associated with the decay of para-Ps is not in agreement with the relationship between that and the pick-off lifetime (see Fig. 28).

Although the size of the free volume corresponding to τ_3 is not much larger than the average free volume per molecule at higher temperatures it still seems to be justified to call this Ps state a bubble state with reference to Table II in Section 1.3. Apparently, the short-lived ortho-Ps state can be explained by assuming that the energy-versus-radius relation of the Ps bubble has two minima, one corresponding to a radius of roughly 3-4 Å and a deeper minimum which in principle can be determined as described in Section 5.2. The kind of interaction which causes the minimum corresponding to the state of the short-lived ortho-Ps is, however, not known at present. On the other hand, two properties of SF_6, viz. its rather high polarizability, $\alpha \approx 16$ Å^3 (Tiipton, Dea, and Boogs, 1964) and its electron affinity, EA≈0.6 eV (Nyikos, van der Ende, Warman, and Hummel, 1980) make SF_6 different from other "normal" liquids studied before. Thus, it seems reasonable to connect the short-lived ortho-Ps state with one of these properties, perhaps both. As mentioned previously, a repulsion is found between most "normal" molecules and Ps. The reason is very probably 1) the Coulomb and exchange interaction between the electron in Ps and the molecules, and 2) the neutrality of Ps which strongly reduces the polarization attraction of any of the two particles. A positron can penetrate the valence shell and is repelled only by the positive atomic cores. However, due to the high electron affinity of SF_6, repulsion between the electron in Ps and the SF_6 molecules might be reduced compared with a "normal" molecule case while the high polarizability of SF_6 increases the strength of the attractive induced dipole - induced dipole interaction between Ps and the nearest SF_6 molecules. Concerning the van der Waals forces it should be noted that the polarizability of Ps is roughly eight times that of hydrogen. Thus, the inclusion of these two effects in the energy-versus-radius relation of the Ps bubble might result in an extra minimum in the SF_6 case compared with the "normal" liquid case. Some support for the explanation is found

in the measured pick-off lifetime in gaseous SF_6 (Osmon, 1965) which is shorter than that in other normal gases at a given pressure. This indicates a stronger overlap of Ps with the SF_6 molecules than with other "normal" molecules. The weak temperature dependence of the lifetime of the short-lived ortho-Ps component is not in conflict with the above interpretation of this lifetime component as non of these attractive energy terms are expected to be very sensitive to temperature.

We also performed some measurements to investigate the influence of impurities on the short-lived ortho-Ps component. The number and amount of impurities was analysed by means of gas chromatography and mass spectrometry. The sample used in these analyses was taken from the vapour phase of the original sample that was studied in the lifetime experiment. The results of these analyses gave 0.02% mole fraction of O_2 and 0.16% of N_2. The concentration of O_2 and N_2 was then increased to 0.08% and 0.4%, respectively. The lifetime parameters of ortho-Ps obtained in the two cases are shown in Fig. 31. The effect of the increased impurity level is clearly demonstrated by the quenching of the lifetime τ_4. A quenching effect on the short-lived ortho-Ps lifetime is also observed at room temperature while no effect is observed at 35°C and 40°C. However, the most important result shown in Fig. 31 is that within the experimental uncertainties the intensities I_3 and I_4 remain fixed upon changes of the concentration of O_2 and N_2, which were the only impurities detected. Thus, the results displayed in Fig. 31 strongly indicate that the appearance of the short-lived ortho-Ps component is an intrinsic property of liquid SF_6 and, hence, that the formation of the short-lived ortho-Ps state is caused mainly by the interaction between Ps and the bulk molecules (SF_6).

If it is assumed that only O_2 causes quenching of τ_4 and that the concentration ratio of O_2 also in the liquid in the two cases is four as in the vapour phase, the true pick-off lifetime of the long-lived ortho-Ps component, the product of the quenching constant (k), and the concentration ($[O_2]$) can be calculated using:

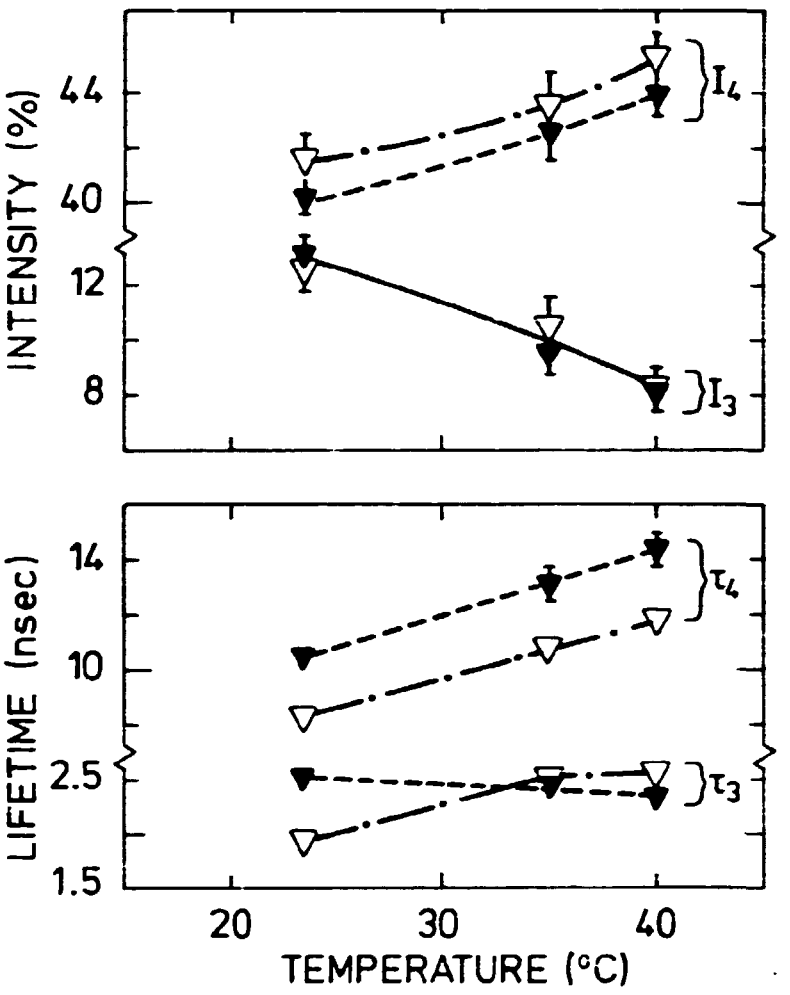

Fig.31. Impurity dependence of the ortho-Ps lifetime parameters in liquid SF_6. The concentration in mole fractions were: O_2(0.02%) and N_2(0.16%) (▼), and O_2(0.08%) and N_2(0.4%) (▽), respectively, as measured in the vapour phase.

$$\lambda = \lambda_p + \lambda_{in} + k[O_2] \qquad (27)$$

where λ, λ_{in}, and λ_p are the measured, intrinsic, and pick-off decay rate, respectively. The values obtained for λ_p are 12.7 nsec, 15.8 nsec, and 17.5 nsec, respectively, at 23.5°C, 35°C, and 40°C. The values for $k[O_2]$, given for 0.08% of O_2 in the vapour phase, are on the same order, $3.5 \cdot 10^7 sec^{-1}$, $2.3 \cdot 10^7 sec^{-1}$, and $2.1 \cdot 10^7$, respectively. At present, however, it is not possible to explain the behaviour of $k[O_2]$ as a function of temperature as the solubility of O_2 in liquid SF_6 is unknown.

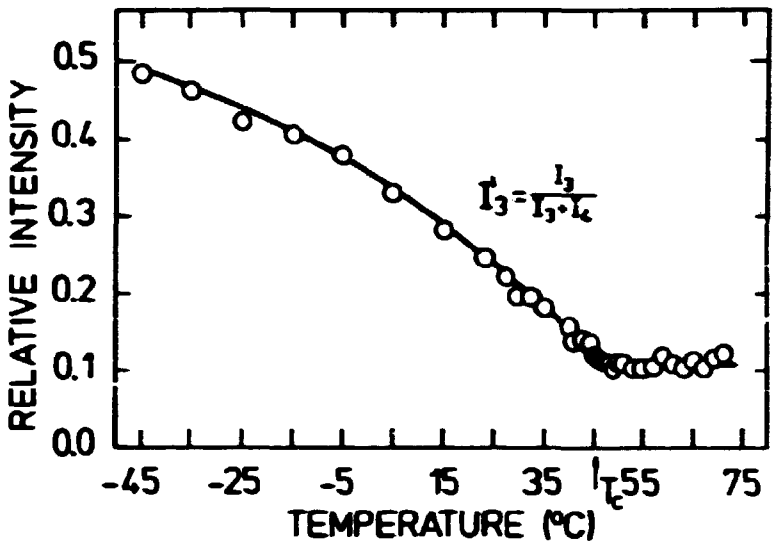

Fig.32. Temperature dependence of the fraction of ortho-Ps in liquid SF_6 which annihilates from the small bubble state. T_c is the critical temperature.

In Fig. 32 the fraction of the total intensity of ortho-Ps that annihilates from the short-lived ortho-Ps state is shown ($I_3' = I_3/(I_3 + I_4)$). An interesting question that cannot be answered from the present work is the following: Is the measured distribution of ortho-Ps in the two states formed within a short time compared with τ_3 or does the main part of the Ps formed enter the short-lived state during or after its formation? In the latter case ortho-Ps must have a certain probability of making a transition to the normal bubble state depending on e.g. the energy barrier separating the two states, the dynamics of the liquid, the availability of nearby free volume, etc. In the former case, the intensity I_3' can probably be correlated to the density of the liquid. In a qualitative manner both models can explain the decrease of I_3' with rising temperature up to the critical point. Above the critical point the behaviour of I_3' suggests that the formation of the short-lived ortho-Ps state correlates to the density of the liquid. Due to the difference in lifetime of para-Ps and ortho-Ps it should be possible to distinguish between the two cases if results from angular correlation experiments are compared to the lifetime results. We hope to be able to perform such an experiment.

In liquid neopentane and hexane the positron lifetime spectra were mathematically well described in terms of three exponentially decaying lifetime components. However, as briefly discussed in Section 3.4 the mathematical goodness of the description of a positron lifetime spectrum is perhaps not always an accurate measure of the number of states from which the positron can decay in a medium. Due to this argument we decided to analyse the positron lifetime spectra measured in hexane and neopentane in terms of four lifetime components with a constant lifetime of para-Ps (0.125 nsec). In the hexane case the analyses did not indicate the presence of an extra lifetime component. However, in neopentane at temperatures higher than 100^{o}C the analyses indicated the appearance of an extra lifetime component with a lifetime close to $\simeq$ 2 nsec. At lower temperatures the analyses displayed a rather large correlation between the two longest--lived components. In order to decrease the number of freedoms of the analyses we decided (on non-physical grounds) to repeat the four-term analyses but with two lifetimes fixed to 0.125 nsec and 2 nsec, respectively. The lifetimes and intensities of such analyses are shown in Figs. 33 and 34, respectively. The variance of the fits are comparable to that obtained in the free three--term analyses. In Section 3.4 we discussed the analyses of a computer-generated experimental lifetime spectrum consisting of three purely exponentially decaying lifetime components with values of the lifetimes and intensities similar to that obtained from free three-term analyses of measured lifetime spectra in liquid neopentane. It was concluded from this computer experiment that it was not possible to force the POSITRONFIT to extract an extra lifetime component. Of course the situation in analysing a real spectrum could be expected to be different for reasons given in Section 3.4. However, let us assume that the results shown in Figs. 33 and 34 represent an accurate way of describing the positron lifetime spectra as measured in liquid neopentane. Without repeating the arguments we then interprete the two longest-lived components as resulting from the decay of ortho-Ps, while the (τ_2, I_2) component is caused by the decay of free positrons. The dashed line shown in Fig. 34 is one-third of the combined intensities I_3 and I_4. The approximately equality of this combination and the intensity of para-Ps at lower temperatures

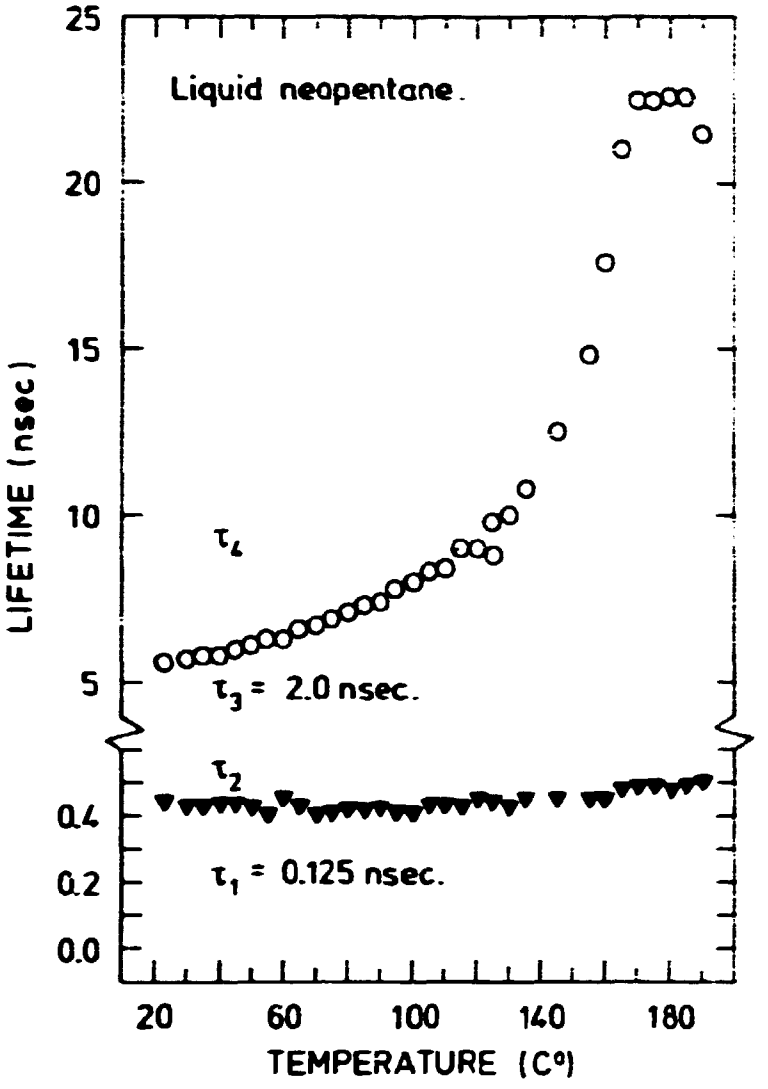

Fig.33. Temperature dependence of positron lifetimes in liquid neopentane as obtained from lifetime spectra resolved into four components using a constant lifetime of para-Ps equal to 0.125 nsec. T_c is the critical temperature.

(140°C) seems to support the interpretation. Fig. 35 shows the fraction of the total ortho-Ps included in the short-lived ortho--Ps component. Thus, apart from the absolute value of I_3, these results seem very similar to those obtained in liquid SF_6. Whether or not we can believe in them is difficult to answer and perhaps the best we can do is to note that the analyses indicate the possible presence of two ortho-Ps components. On the other

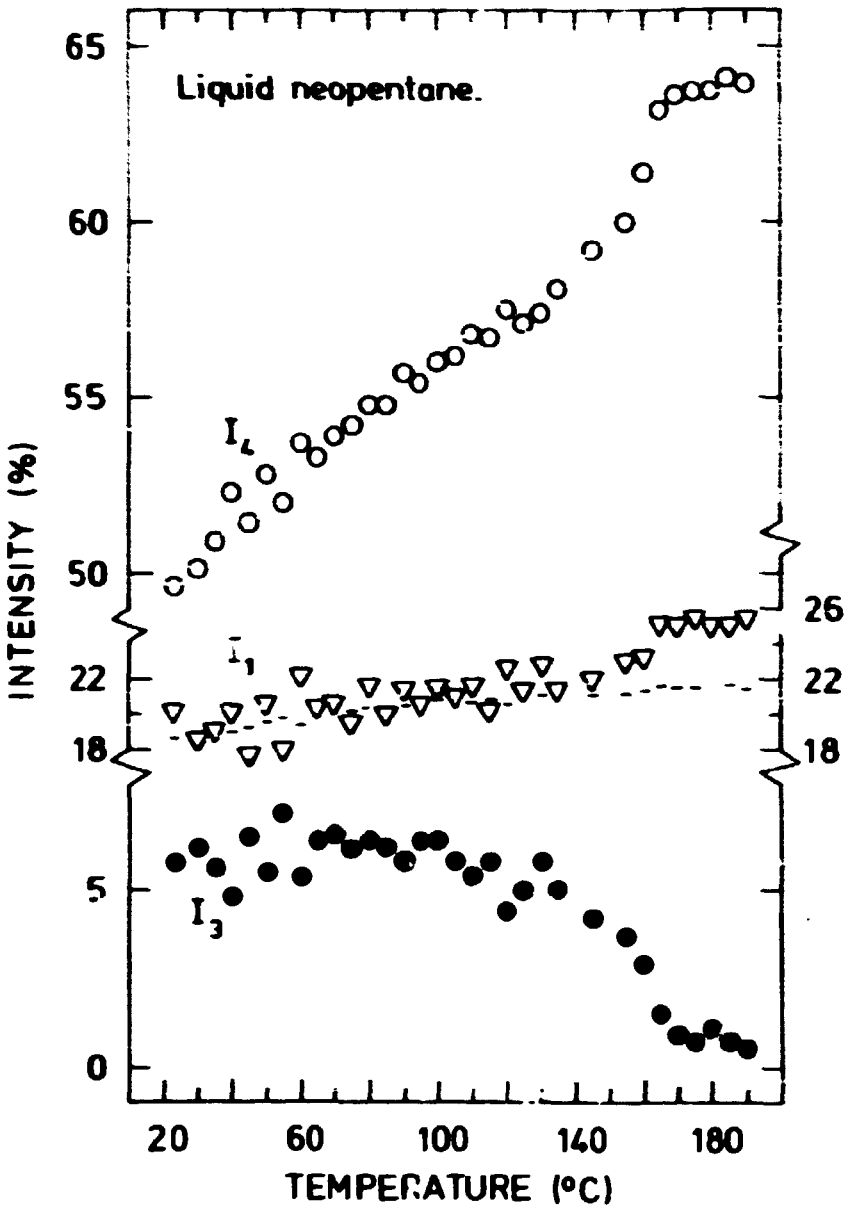

Fig.34. Temperature dependence of the intensities I_1, I_3, and I_4 in liquid neopentane. The dashed line corresponds to $1/3(I_3 + I_4)$. T_c is the critical temperature.

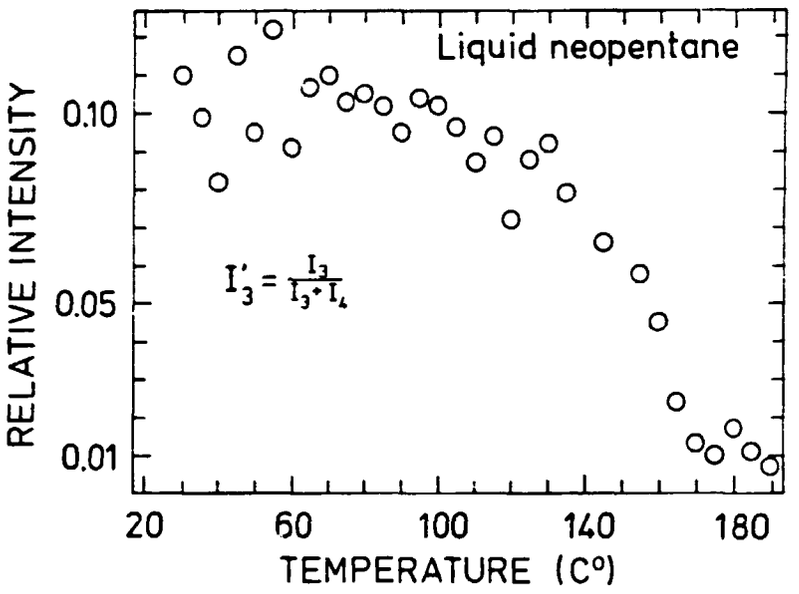

Fig.35. Temperature dependence of $I'_3 = I_3/(I_3 + I_4)$ in liquid neopentane. T_c is the critical temperature.

hand, the analyses clearly illustrate the dilemma: How detailed is it possible to perform an analysis on a positron lifetime spectrum, in order to extract maximum information without risking that the analysis turn into a meaningless computer game.

5.4. The yield of Ps in liquids

Recent experimental studies of the Ps yield and formation processes in a wide variety of solutions strongly favour the ideas of the positron spur-reaction model (Mogensen, 1974, Lévay, 1979, and Molin and Anisimov, 1979). Although, other models of the Ps formation processes are still used (see e.g. Ache, 1979, and Para and Lazzarini, 1978) it seems that the spur model is the model used mostly today in the interpretation of the Ps yield in solutions. Phenomena such as inhibition of Ps formation (Wikander, 1979 and 1981, Abbe, Duplatre, Maddock, and Haessler, 1980, Mogensen, 1979, and Lévay and Mogensen, 1980), and anti-inhibition (Anisimov and Molin, 1975, Ito and Tabata, 1979a, and Lévay and Mogensen 1980) are well interpreted by means of the

spur model. Furthermore, the use of the spur model in the interpretation of the measured Ps yields in solutions also provide information of the behaviour of the excess electrons. Based on measured Ps yield in various solutions (Lévay and Mogensen, 1980) it was predicted that the mobility of excess electrons in "shallow-trap" electron attachment liquids such as pure CS_2, SF_6, C_6F_6, etc. is much higher than that of the massive ions. Recent mobility measurements by Nyikos, van den Ende, Warman, and Hummel, 1980, have confirmed a high mobility of excess electrons in the cases of liquid C_6F_6 and CS_2. The success of the spur model in interpreting the measured Ps yield in various solutions strongly favours the reaction between a mainly thermalized positron and one of the excess electrons created during the slowing down of the positron, as being the most significant channel of Ps formation. As in solution, we, of course, expect the Ps yield in pure liquids to depend strongly on the positron spur properties, viz. the time and space distribution of the excess electrons, the positron, and the positive ions, and furthermore on the solvent properties in relation to the positron and the excess electrons, etc. Typical experimental results which substantiate the ideas of the spur model as being important in the Ps formation processes in pure liquid are: 1) the influence of a high positive ion (positive hole) mobility (see e.g. de Haas, Hummel, Infelta, and Warman, 1977) on the Ps yield (see e.g. Lévay, Lund, and Mogensen, 1980), and 2) the influence of an electric field on the Ps yield (Mogensen, 1975, and Ito and Tabata, 1979b). Furthermore, very often it is observed that the measured Ps yield in pure liquids correlates strongly with properties of the excess electrons such as mobility, work function, thermalization range of secondary electrons, etc. However, in general, it is far more difficult to interprete the measured Ps yield in pure liquids compared with solutions. The reason for this is that only meagre experimental knowledge exists on the properties of the spur species in the time scale of interest. Thus, quite often empirical relations between the measured Ps yield and various radiation chemistry data are used in the interpretation of the measured results. In this connection, it should be emphasized that the data obtained in radiation chemistry experiments on various spur properties represent properties of

mainly single pair spurs, while the positron spur is the terminal spur of the positron track. Thus, it is very likely that the positron spur is a multi-pair spur (high LET at energies below 100-200 eV), and perhaps some of the spur reactions in a multi-pair spur are somewhat different with respect to time and space to that taking place in a single pair spur.

Although it cannot be done on the basis of very detailed experimental knowledge of the positron spur properties, we shall discuss the measured Ps yield and the Ps formation processes in some detail. We will especially discuss some of the empirical relations between the measured Ps yield and various spur properties that are used to interprete the measured results. Several of these spur properties are interrelated and the correlation between the measured Ps yield to a specific property of, e.g., the excess electrons, can perhaps be misleading in some cases.

The property of the excess electron most often used in the interpretation of measured Ps yield in non-polar liquids is the excess electron mobility (see e.g. Jansen and Mogensen, 1977, and Lévay and Mogensen, 1980). From previous experiments it seems that there exists a nearly universal relation between measured Ps yield and excess electron mobility in similar non-polar liquids, viz. increase of the measured Ps yield with increasing excess electron mobility. By comparing the mobility results in neopentane (Fig. 23) and hexane (Fig. 26) to the measured ortho-Ps yield (I_3) in these liquids (Figs. 22 and 25), we see that the present work substantiats this relation (μ-I_3). On the other hand it should be noted that in neopentane the mobility changes approximately by a factor of four within the temperature range studied while the absolute changes of I_3 corresponds to roughly 6.5% ($I_3(23^oC)$ = 52.2%). Thus, although the I_3-μ correlation appears to be quite clear, the correlation is not specifically strong within the range of the excess electron mobility studied. In Fig. 36, we plot I_3 versus the mobility of the excess electrons in hexane. From this figure it seems that the I_3-μ correlation can be divided into two regions. At mobilities above roughly 0.07 cm^2/Vs the correlation is rather weak compared to that at mobilities below this value.

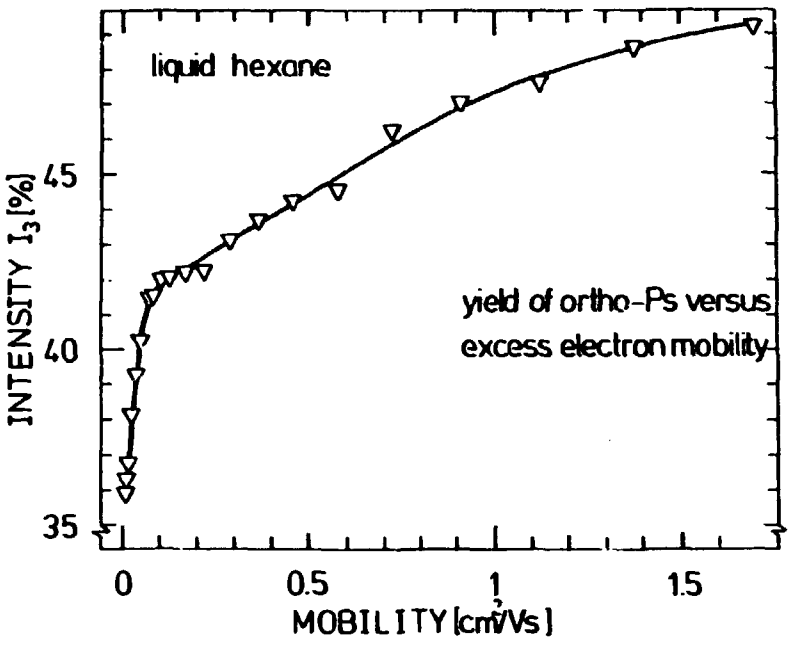

Fig.36. Correlation between the ortho-Ps yield(I_3) and the excess electron mobility in liquid hexane.

Based on considerations of simple chemical kinetics it is quite difficult to understand the I_3-μ correlation. In this picture the Ps formation rate constant (k_{Ps}) (Weston and Schwarz, 1972) is given by:

$$k_{Ps} \simeq 4\pi (kT/e)(\mu_e + \mu_p) r_c \qquad (28)$$

where e is the numerical electron change, μ_e and μ_p are, respectively, the mobility of the excess electron and the positron, and r_c is the critical distance at which the potential energy of a charge pair becomes equal to the thermal energy. Typical values of r_c in non-polar liquids are 250-300 Å at room temperature. The positive ion - excess electron recombination rate constant is given by the same expression (Eq. 28), but with μ_p replaced by μ_+. Hence, although the rate of the Ps formation process increases with increasing mobility of the excess electron so does the recombination rate, and as the Ps formation process competes with that of the recombination, the increase of μ_e is expected to speed up the spur processes, but not favour those of Ps formation.

On the other hand, the measured Ps yield - excess electron mobility correlation can perhaps be explained by refering to some of the following properties: 1) In addition to the competition of the positive ion - excess electron recombination, the Ps formation process also competes with the decay of the free positron. 2) Perhaps the correlation in space between the last created excess electron and positron increases with increasing mobility of the excess electron so that the distance between the positron and one of the excess electrons, when thermalized, decreases with increasing excess electron mobility. 3) The overlap between the wave function of the positron and that of the excess electrons might favour Ps formation compared with the effect of the overlap between the excess electrons wave function and the positive ions on the recombination process. 4) As the behaviour of the positron in non-polar liquids is generally not very well known, an easy hypothesis would be to state the behaviour of the positron mobility as functions of temperature, density, etc. to be similar to that of the excess electrons. Other phenomena could be suggested in the interpretation of the I_3-μ_e such as polarization effects of the positron/electron in trapped states. Although, some of the above-mentioned effects may favour the Ps formation process compared with other excess electrons reactions it is, however, in general very difficult to obtain an estimate on their contribution to the measured Ps yield. On the other hand, a rough estimate can be made on typical Ps formation times and hence on whether or not the decay of the free positrons can explain the I_3-μ_e correlation. If we assume the spur size b as measured in radiation chemistry to represent a typical distance between the positron and one of the excess electrons at the time of the positron spur formation (t = 0), we can express the time it takes the two particles to reach each other roughly as:

$$t = e(3\mu kTr_c)^{-1}b^3 \quad \text{(sec)} \tag{29}$$

In the above expression we neglected the diffusion term and assumed the sum (μ) of the mobility of the two particles to be independent of the Columb field. As an example, let us consider hexane at room temperature. The values of b, μ_e, and r_c are, respectively, 70 Å (Schmidt and Allen, 1970), 0.07 cm^2/Vs, and

≈ 300 Å. Thus, if we do not take positron mobility into account we obtain a typical Ps formation time of 20 - 25 psec. Typical lifetimes of free positrons in non-conducting condensed matter are 0.4-0.5 nsec. Within the time interval of 20-25 psec roughly 5% of the free positrons are lost due to annihilation. The temperature dependence of the thermalization range of secondary electrons follows roughly that of the molecular volume (V_m), viz. $b \approx \text{constant} \cdot V_m$. Thus, from the simple calculation we will expect the Ps formation time to decrease with increasing temperature in hexane (see Fig. 26).

In liquid neopentane the spur size changes within the interval b ≈ 200-400 Å (Holroyd and Cipolline, 1979); hence, the Ps formation time in neopentane at all temperatures is expected to be considerably shorter than that in hexane at room temperature. Thus, apart from hexane below roughly room temperature it seems reasonable to assume that the decay of the free positron does not explain the I_3-μ_e correlation in hexane and neopentane. According to the excess electron mobility in hexane these electrons are believed to be mainly in trapped states (see Table II). However, during the slowing down of the secondary electrons these have to pass through the conduction band. In the conduction band the excess electron mobility is perhaps several orders of magnitude greater than the measured mobility. Since it is likely that the excess electron reactions can start to take place before the electrons are fully solvated, the estimated Ps formation time in hexane is probably an upper limit. Further, it could be expected that the probability of encounter pair reactions in the conduction band is of significance.

However, the transition in the measured Ps yield - excess electron mobility correlation at roughly 0.07 cm^2/Vs to a stronger correlation below 0.07 cm^2/Vs might result from a decrease of the reaction rate of the excess electrons. Hence the decay of the free positrons play a more important role in the measured Ps yield at these low excess electron mobilities.

As mentioned above, the behaviour of positrons in non-polar liquids is generally not very well known. However, preliminary studies of

Ps inhibition/antiinhibition in hexane as functions of temperature (Jacobsen, Mogensen and Eldrup, 1981) seem to indicate that the mobility of the positron in hexane is somewhat lower than that of the excess electron. Thus, although it cannot be excluded, it seems at present that the temperature dependence of the measured Ps yield in hexane cannot be explained simply by referring to changes of the positron mobility.

From radiation chemistry experiments it is often observed that the thermalization range of secondary electrons correlates to the excess electron mobility (Shinsaka, Dodelet and Freeman, 1975 and Dodelet, Shinsaka and Freeman, 1973). The reason for the correlation between the thermalization range of secondary electrons and excess electron mobility is very probably caused by the determination of the thermalization range mainly by the distance the electrons have to travel in order to lose the last $\sim$ 0.5 eV of their kinetic energies (Bullot, Cordier and Gauthier, 1980), and also that the excess electron mobility can be taken as a measure of the efficiency of the energy loss processes at these secondary electrons energies, viz. increase of the thermalization distance of the secondary electron with increasing excess electron mobility. It should be noted that during the thermalization of the secondary electrons they always spend some time in the conduction band; perhaps the thermalization range then correlates more strongly to the behaviour of the electron in the conduction band than to the measured mobilities in liquids in which the excess electron mobility is determined mainly by properties of trapped electron states.

Many of the spur properties as measured in radiation chemistry experiments are often fairly well explained by assuming that the probability of the thermalization distance of a secondary electron from its parent positive ion can be approximated by a three dimensional gaussian with the parameter b (spur size) as the most probable thermalization distance (Schmidt and Allen, 1970). As mentioned above, the positron spur is the terminal spur of the positron track, and hence it is believed to be a multi-pair spur. Without proof, we will assume that the positron spur at its formation (t = 0) can be described as a number of positive ions (3-5) situated fairly close to each other compared with the spur size.

Further, we shall assume that the probability of finding one of the thermalized secondary electrons/positron can be approximated by a three-dimensional gaussian (or a similar function) with the parameter b_e/b_p as the most probable distance of finding the electrons/positron at t = 0. In general, $b_e \neq b_p$.

Although the above picture of the positron spur at its formation is an idealization of reality, it is believed to reflect qualitatively some important properties of the positron spur. Due to the inhomogeneous initial distribution of the spur species the probabilities of various spur reactions will depend strongly on space and time. Furthermore, in a detailed model it should be taken into account that the "diffusion" properties of the excess electrons and the positron depend on time (solvation of electrons/positron) and perhaps also on space (field dependence of the solvation time?). However, without going into too detailed a discussion, it seems reasonable to assume that the strength of the competitive positive ion - excess electron recombination process on the Ps formation process depends strongly on the initial probability distribution of the excess electrons as well as that of the positron. Let us first assume that b_e is comparable to b_p. In this case it might be reasonable to believe that the initial strength of the recombination process decreases with increasing b_e. On the other hand, at very large $b_e(b_p)$ the Coloumb forces between the positron and the excess electrons become weaker; thus, the probability that an electron and a positron will diffuse out of their mutual field increases with increasing $b_e(b_p)$. In the case of $b_e \approx b_p$, it then seems reasonable to expect that the measured Ps yield increases rather strongly with increasing $b_e(b_p)$ at smaller b_e. On the other hand, at larger b_e (comparable to r_c) the Ps yield will probably only depend weakly on $b_e(b_p)$, while at very large $b_e(b_p)$ the Ps yield very likely decreases with increasing $b_e(b_p)$. In the case of $b_e > b_p$ almost the same arguments can be used to explain the dependence of the measured Ps yield on b_e. However, in this case the outermost secondary electrons will feel a stronger electric field from the inner part of the spur, on the average, and hence the probability that they can escape the spur will be lower compared with the $b_e \approx b_p$ case. Furthermore, the outermost electrons which do not escape the spur have to pass -

so to speak - the probability function of the positron before possible recombination with one of the positive ions. Thus, in the case of $b_e > b_p$ the Ps yield dependence on b_e may perhaps be expected to be stronger; furthermore the decrease of the Ps yield with increasing b_e is expected to set in at a larger b_e compared with the case of $b_e = b_p$.

If it is qualitatively correct to treat the positron spur as an essentially isolated multi-pair spur it seems that the third case, viz. $b_e < b_p$, can be excluded at least for cases of b_e considerably less than b_p, since, otherwise, Ps yield well above 50% (as measured in many non-polar liquids) would be very hard to interprete. On the other hand, in a more detailed model the possible influence of ionization events outside of what we have defined as the positron spur should be considered.

By using the above picture of the initial distribution of the spur species it is clear that Ps is not formed with an equal probability as a function of space in the positron spur. Generally, it might be expected that on the average Ps is formed at a greater distance from the positive ions with increasing b_e and/or b_p. As was briefly discussed in Section 5.3 it could very well be expected that Ps that are formed close to the positive ions (of which at least one exists in the whole lifetime of Ps) have high probability of reacting with one of the positive ions; for Ps formed at larger distance from the positive ions, on the other hand, this secondary reaction can probably be neglected. A reaction between Ps and a positive ion will very probably lead to oxidation of Ps. Hence, to complicate further the interpretation of the Ps yield in liquids, we also have to discuss whether it is reasonable to directly associate the measured Ps yield with that actually formed. The problem arising is: If ortho-Ps which is formed close to the positive ions reacts fast enough with one of the positive ions then the lifetime of the positron initially bound in Ps will be mainly a property of free positrons in the liquid. Thus, in analysing the decay spectrum, it could be expected that the lifetime component associated with the decay of free positrons also include a fraction of the formed ortho--Ps which have taken part in this secondary reaction. Furthermore, other secondary reactions could be expected to take place such

as the formation of Ps^- (Mogensen, 1981), which perhaps can react further with one of the positive ions (the "reaction radius" of a charged pair is roughly two orders of magnitude greater than that of a reaction between a neutral and charged particle). Because the lifetime of ortho-Ps is much longer than that of para-Ps the probability of ortho-Ps forming Ps^- could be expected to be much higher than that of para-Ps forming Ps^-. The product resulting from a reaction of Ps^- and one of the positive ions is a neutral molecule plus Ps. However, the probability of transferring either one of the two electrons in Ps^- to the positive ion is probably the same. Thus, the ratio of para-Ps and ortho-Ps formed from this possible reaction is unity while, in general, it is believed that this ratio is 1/3 when Ps is formed by a reaction between a "free" electron and positron. Furthermore, possible formation of triplet states during the excess electron - positive ion recombination could also be expected to influence Ps formed close to the positive ions, and perhaps have an influence on the measured Ps yield.

In the cases of possible secondary, tertiary, etc. positron reactions it is important to note that because of the highly inhomogeneous nature of the positron spur these reaction do not in any way lead to a simple modification of the decay rates of positrons annihilating as free particles or as initially bound in Ps. Of course, we do not generally expect these Ps reactions to play a major role in the decay kinetics of the positrons in liquids. However, in e.g. neopentane, we discuss relative changes in the Ps yield of roughly 10%, while in hexane above room temperature relative changes of roughly 20%. Thus, possible Ps reactions could be expected to contribute to changes of the measured ortho-Ps yield with a non-negligible strength. In this connection it is perhaps worthwhile to note that the Ps yield as determined in angular correlation experiments in liquid hexane and neopentane at room temperature is higher than that determined in the present lifetime experiments.

In summing up the discussion of the influence of the spur properties on the measured Ps yield in liquid neopentane and hexane, the following interpretation is probably reasonable: In liquid neopentane and hexane (at temperatures above roughly room temperature)

it is probably impossible to distinguish between whether the changes of the measured Ps yield are caused mainly by changes of the excess electron mobility, or by the thermalization range of the secondary electrons. However, qualitatively it seems reasonable to expect that the competition between the recombination process and that of the Ps formation is influenced by the thermalization distance; nonetheless, it is considered impossible to give a quantitative estimate. If possible Ps reactions with other of the spur species are important then it seems very likely that the measured Ps yield in a lifetime experiment is not necessarily equal to that actually formed. Thus, the most we can state is that all of the above-mentioned spur properties probably have to be taken into acccunt in interpreting the measured Ps yield. Although this is quite a pessimistic conclusion to reach there seems to be a glimmer of light ahead. Due to the different lifetime of para-Ps and orhto-Ps it is perhaps possible to distinguish experimentally between the influence of some of the above-mentioned spur properties on the measured Ps yield; e.g. it seems reasonable to believe that the probability of para-Ps reactions with other spur species is considerably less compared with that of ortho-Ps. However, in order to study the behaviour of para-Ps in liquids it is necessary to do that by performing angular correlation experiments. The presently available amount of angular correlation data obtained in liquids are insufficient to be useful in the present discussion.

In hexane at temperatures roughly below room temperature, it is perhaps reasonable to expect that the Ps formation process, in addition, feels the competition caused by the decay rate of free positrons.

Finally, it should be strongly emphasized that the behaviour of the positron in non-polar liquids is not very well known, so perhaps changes of the positron states in liquids also play a role in the measured changes of the Ps yield.

In Section 4, it was mentioned that it was quite diffecult to reproduce the intensity I_3 in neopentane above 140°C. The reason could very well be that small amounts of impurities from the wall of the autoclave became solvated in the liquid. The Ps yield in

neopentane at room temperature is very sensitive to addition of electron acceptor molecules at a concentration level of p.p.m. (Mogensen, 1979); very likely because of a very large positron spur in liquid neopentane.

The Ps yield in liquid SF_6 shows a strong temperature dependence. The Ps yield (4/3 of the ortho-Ps yield) increases from about 43% at -45°C to about 70% at room temperature. Between 23°C and 71°C the Ps yield is roughly independent of the temperature. However, no radiation chemistry experiments have been performed on liquid SF_6 so it is impossible to discuss the measured Ps yield in SF_6 in any detail. However, because of the relatively strong temperature dependence of the Ps yield and the high measured Ps yield at temperatures above room temperature, liquid SF_6 could perhaps from a radiation chemistry point of view be an interesting liquid to study. Although SF_6 is one of the best and most often used electron scavengers in radiation chemistry experiments, the present work could indicate a rather high mobility of the excess electron compared to that of the massive ions.

In the two viscolastic liquids (6PO and 5PO) the Ps yield increases with increasing temperature. At present it is not possible to interprete the Ps yield in these liquids. However, the increase of the Ps yield with decreasing viscosity is not surprising, but very likely not the only reason for the increase of the Ps yield with increasing temperature.

6. SUMMARY AND CONCLUSIONS

The aims of the present work were to make a detailed study of the state of Ps and to study the Ps formation processes in molecular liquids. Positron lifetime measurements have been performed on liquid SF_6, neopentane, hexane and on two viscoelastic liquids (6PO and 5PO), respectively, as function of temperature over quite broad temperature ranges. The experimental results showed that Ps is formed in all of these liquids.

The longest-lived lifetime component in these liquids was attributed to the decay of ortho-Ps. From a rather detailed discussion of the state of ortho-Ps in condensed matter we conclude that the ortho-Ps lifetime in liquid neopentane, hexane and SF_6 (the longest-lived ortho-Ps component) as function of temperature is fairly well explained by assuming that Ps is localized in a microscopic cavity, viz. the Ps bubble in these liquids.

The Ps bubble in molecular liquids is not generally accepted today partly because 1) sometimes very doubtful references have been made to the de Broglie wave length of Ps in condensed matter in the existing literature and/or 2) a clear definition of the bubble state has not been given. We recommened the definition of the Ps bubble given in Section 1.3.

The behaviour of the ortho-Ps lifetime in the liquids 6PO and 5PO as function of temperature displays qualitatively the dynamics in the Ps bubble formation process. It was concluded that by changing the temperature the Ps state in these liquids could be continuously changed from a typical bubble state at high temperatures to a Ps state which mainly depends on pre-existing cavities (defects) at low temperatures. Qualitatively, the viscosity of these liquids was related to the Ps bubble formation time.

Quantitative calculations of the properties of the Ps bubble state in liquids were discussed in some detail. From our point of view it seems that the presently available knowledge of the Ps - molecule interactions are very probably too limited to make such calculation useful in most cases. The use of the simple Ps bubble model in which the Ps bubble is approximated by a spherical square well potential and where the surrounding molecules are treated as a continuum may even be a very bad approximation in some cases. Indeed the use of the model indicates that the Ps bubble is a very dynamic state which cannot be treated in a static continuum picture. Thus, we conclude that it is perhaps more useful, at present, to use a qualitative description of the Ps bubble state rather than a quantitative model which gives numerical values of the Ps bubble properties with very likely large uncentainties.

In order to show qualitatively how the ortho-Ps lifetime in the bubble state depends on the surface work and the vapour pressure a semi-empirical expression is provided which fits the temperature dependence of the lifetime of ortho-Ps in neopentane, hexane and SF_6 (the longest-lived ortho-Ps component) fairly well.

In liquid SF_6 the analyses of the positron lifetime spectra displayed two ortho-Ps lifetime components. The longest-lived ortho--Ps component was similar to that observed in hexane and neopentane (see above) while the state of the shortest-lived ortho-Ps component ($\tau_3 \simeq 2 - 2.5$ nsec) was mainly independent of temperature. The appearance of this new extra ortho-Ps component in liquid SF_6 was discussed with reference to possible secondary positrons reactions and to the possibility that ortho-Ps can become localized in two different states in liquid SF_6. Due to the temperature independence of τ_3 it seems most likely to assume that the extra ortho-Ps component in liquid SF_6 is caused by ortho-Ps annihilation from a small "bubble" (cavity) state of a radius of 3 -4 Å. This was tentative explained in terms of a second minimum around 3 - 4 Å in the energy-versus-radius relation of the Ps bubble apart from the normal minimum at larger radius. As the main differences between SF_6 and other "normal" molecules are the large electron affinity and polarizability of SF_6, it has been suggested that the second minimum, and hence the formation of the short--lived ortho-Ps state in liquid SF_6 is connected to these properties.

The analyses of the positron lifetime spectra obtained in liquid neopentane indicated the possibility that two ortho-Ps components were included in these spectra. However, it should be strongly emphasized that the mathematical accuracy of the analyses in which two ortho-Ps components were assumed was not improved compared to those in which only one ortho-Ps components was assumed to be included in the positron lifetime spectra.

The measured Ps yield in liquid neopentane and hexane has been discussed in some detail. The results showed a quite strong correlation between the measured Ps yield and the excess electron mobility, viz. increase of the measured Ps yield with increasing

excess electron mobility. Generally, this correlation is very difficult to interpret and from a simple chemical kinetic point of view this correlation cannot be understood. On the other hand, in cases of very low mobility of both the excess electrons and positron the Ps formation process compete with the annihilation of free positrons and it was concluded that this could be the explanation of the measured Ps yield dependence on the excess electron mobility in liquid hexane below roughly room temperature. However, at higher temperatures in hexane and at all temperatures in neopentane we concluded that the decay rate of the free positron probably not could be expected to influence the measured Ps yield. Other phenomena correlated to the excess electron mobility have been suggested in the interpretation of the measured Ps yield - excess electron mobility correlation such as the overlap between the wave function of excess electrons and that of the positron might favour the Ps formation compared to the effect of the overlap between the excess electron wave function and the positive ions on the recombination process, etc.

Based on perhaps a somewhat naive view of the initial distribution of the spur species in the positron spur we discussed the possible influence of the spur size on the measured Ps yield. It was concluded that at spur sizes less than the critical distance at which the potential energy of a charge pair becomes equal to the thermal energy it could be expected that the Ps yield increases with increasing spur size. Furthermore, the influence of possible Ps reactions with other spur species on the measured results was discussed and in cases of such reactions we concluded that the measured Ps yield is not necessarily equal to that actually formed.

Thus, it could be expected that some part of the measured Ps yield - excess electron mobility correlation is caused by the correlation between the mobility of excess electrons and the thermalization range of the secondary electrons.

ACKNOWLEDGEMENTS

The work present in this report was carried out in partial fulfilment of the requirements for obtaining the "licentiat grad" (equivalent to the Ph.D.). The work was carried out at the Chemistry Department, Risø National Laboratory under supervision of prof. G. Trumpy, Laboratory of Applied Physics II, Technical University of Denmark and lic. tech. O.E. Mogensen, from Februar 1978 to September 1980.

I would like to thank prof. Trumpy for his interest and support, and for a number of valuable discussions. I would very much like to express my gratitude to O.E. Mogensen and M. Eldrup for their continual interest and support, and for many very interesting and stimulating discussions from which I have learned a lot about positrons and physics in general. Further, I very much wish to thank N.J. Pedersen and D. Platz for their interet and invaluable support during this work and to S.J.G. Lund who introduced me to the details of the lifetime spectrometer. Also I want to thank D. Lightbody for many interesting discussions.

Furthermore, I would like to thank Dr. R.A. Pethrick for his collaborative stay at Risø in august 1978. I also want to express my thanks to prof. G.R. Freeman for the very interesting discussions we had during his visit to Risø in march 1980. Furthermore, I very much appreciate the discussions I had with Dr. J. Warman and collaborators in Delft, april 1980. Thanks are also due to H. Egsgaard who did the impurity analysis of liquid SF_6 and to A. Berman who has done much to improve my english. Also many thanks are due to A. Andersen and I. Pedersen who typed the manuscript.

The kind and efficient assistance of many people fron the Departments of Electronics, Service, Computer, Construction, Workshop, and the Library is gratefully acknowledged.

Finally I would like to thank the many people in the Chemistry Department who have provided special working conditions which have proved to be continually stimulating.

February 1981

Finn M. Jacobsen

REFERENCES

ABBE, J.-CH., DUPLATRE, G., MADDOCK, A.G. and HAESSLER, A. (1980). Radiat. Phys. Chem. 15, 617-622.

ACHE, H.J. (1979). In Positronium and Muonium Chemistry. Edited by H.J. ACHE (Advances in Chemistry Series 175) (American Chemical Society, Washington, D.C.) 1-50.

AKHIEZER, A.I. and BERESTETSKII, V.B. (1965). Quantum Electrodynamics 2.ed. (Interscience, New York) 868 pp.

ANDERSON, C.D. (1932). Science, New Series 76, 238.

ANISIMOV, O.A. and MOLIN, Yu.N. (1975). Khim. Vys. Energ. 9, 539-540 (English translation: High Energy Chem. 9 (1975) 471-472).

BARLOW, A.J., ERGINSAV, A. and LAMB J. (1969). Proc. R. Soc. A309, 473-496.

BENGTSON, B. (1980). private communication.

BERESTETSKII, V.B. (1949). Zh. éksp. teor. Fiz. 19, 1130-1135.

BLACKETT, P.M.S. and OCCHIALINI, G.P.S. (1933). Proc. R. Soc. A139, 699-727.

BRANDT, W., BERKO, S. and WALKER, W.W. (1960). Phys. Rev. 120, 1289-1295.

BRANDT, W., COUSSOT, G. and PAULIN, R. (1969). Phys. Rev. Lett. 23, 522-524.

BRISCOE, C.V., CHOI, S.-I. and STEWART, A.T. (1968). Phys. Rev. Lett. 20, 493-496.

BUCHIKHIN, A.P., GOLDANSKII, V.I. and SHANTAROVICH, V.P. (1971a). Soviet Phys. JETP 33, 615-617; (1971b). JETP Lett. 13, 444-447.

BULLOT, J., CORDIER, P. and GAUTHIER, M. (1980). J. Phys. Chem. 84, 3516-3521.

Chemical Rubber Co. (1972) Handbook of Chemistry and Physics. 53rd edition.

COCHRANE, J. and HARRISON, G. (1972). J. Phys. E 5, 48-51.

DANNEFÆR, S. (1980). Private communication.

DAWSON, P.P., SILBERBERG, I.H. and MCKETTA, J.J. (1973). J. chem. Engng. Data 18, 7-15.

DEUTSCH, M. (1951). Phys. Rev. 82, 455-456.

DIRAC, P.A.M. (1930). Proc. Camb. phil. Soc. 26, 361-375.

DIRAC, P.A.M. (1930). Proc. R. Soc. A126, 360-365.

DODELET. J.-P. and Freeman, G.R. (1977). Can. J. Chem. 55, 2264-2277.

DODELET, J.-P., SHINSAKA, K. and FREEMAN, G.R. (1973). J. Chem. Phys. 59, 1293-1297.

DOUGLAS, R.J., ELDRUP, M., LUPTON, L. and STEWART, A.T. (1979). Proc. of the 5th. Int. Conf. on Positron Annihilation. Edited by R.R. HASIGUTI and K. FUJIWARA. Lake Yamanaka, April 8-11, 1979. (The Japan Inst. of Metals, Sendai) 621-624.

EASTWOOD, A.E., COCHRANE, J., HARRISON, G., LAMB, J. and PHILLIPS, D.W. (1980). Glasgow University, unpubl. data.

EINSTEIN, A. (1905). Annln. Phys. 17, 891; 18, 639.

ELDRUP, M., MOGENSEN, O.E. and BILGRAM, J.H. (1978). J. Glaciol. 21, 101-113.

ELDRUP, M., PEDERSEN, N.J. and SHERWOOD, J.N. (1979). Phys. Rev. Lett. 43, 1407-1410.

ELDRUP, M., MOGENSEN, O.E. and SHERWOOD, J.N. (1979). Proc. of the 5th Int. Conf. on Positron Annihilation, Edited by R.R. HASIGUTI and K. FIJIWARA. Lake Yamanaka, April 8-11, 1979. (The Japan Inst. of Metals, Sendai) 465-469.

ELDRUP, M. and KIRKEGAARD, P. (1973). unpubl.

FERRANTE, G. (1968). Phys. Rev. 170, 76-80.

FERRELL, R.A. (1951). Phys. Rev. 84, 858-859.

FERRELL, R.A. (1957). Phys. Rev. 108, 167-168.

FOCK, V.A. (1926). Z. Phys. 38, 242-250; 39, 226-232.

GERMAGNOLI, E., POLETTI, G. and RANDONE, G. (1966). Phys. Rev. 141, 419-422.

GMELIN Handbuch der Anorganischen Chemie. Schwefel 8. Aufl. (WEINHEIM/BERGSTR., 1963).

GOLDANSKII, V.I. (1968). At. Energy Rev. 6, 3-148.

GORDON, W. (1926). Z. Phys. 40, 117-133.

GRAY, P.R., COOK, C.F. and STURM, G.P. (1968). J. Chem. Phys. 48, 1145-1157.

HARDY, W.H. and LYNN, K.G. (1976). IEEE Trans. Nucl. Sci. 23, 229-233.

HERNANDEZ, J.P. (1976). Phys. Rev. A14, 1579-1582.

HOLROYD, R.A. and CIPOLLINI, N.E. (1979). Proc. of the 6th Int. Congress on Radiation Research. Edited by S. OKADA, M. IMAMURA, T. TERASHIMA and H. YAMAGUCHI. Tokyo, May 13-19, 1979. 228-235.

HUANG, S. S.-S. and FREEMAN, G.R. (1978). Can J. Chem. 56, 2388-2395.

IKARI, H. and FUJIWARA, K. (1979). J. Phys. Soc. Jpn. 46, 92-96.

ITO, Y. and TABATA, Y. (1980). Radiat. Phys. Chem. 15, 329-336.

ITO, Y. and TABATA, Y. (1979). Proc. of the 5th Int. Conf. on Positron Annihilation. Edited by R.R. HASIGUTI and K. FUJIWARA. Lake Yamanaka, April 8-11; 1979. (The Japan Inst. of Metals, Sendai) 321-324.

JACOBSEN, F.M., ELDRUP, M. and MOGENSEN, O.E. (1980). Chem. Phys. 50, 393-403.

JACOBSEN, F.M., MOGENSEN, O.E. and ELDRUP, M. (1981). to be publ.

JANSEN, P. (1976). Thesis, Risø-Rep. 333. 81 pp.

JANSEN, P. and MOGENSEN, O.E. (1977). Chem. Phys. 25, 75-86.

JORTNER, J., KESTNER, N.R., RICE, S.A. and COHEN, M.H. (1965). J. Chem. Phys. 43, 2614-2625.

JORTNER, J. and GAATHON, A. (1977). Can J. Chem. 55, 1801-1819.

KIRKEGAARD, P. and ELDRUP, M. (1972). Comput. Phys. Commun. 3, 240-255.

KIRKEGAARD, P. and ELDRUP, M. (1974). Comp. Phys. Commun. 7, 401-409.

KIRKEGAARD, P., ELDRUP, M., MOGENSEN, O.E. and PEDERSEN, N.J. (1981). Submitted to Comp. Phys. Commun.

KLEIN, O. (1926). Z Phys. 37, 895-906.

KLUTH, E.L.E., CLARKE, H. and HOGG, B.G. (1964). J. Chem. Phys. 40, 3180-3182.

KÖGEL, G. (1979). Proc. of the 5th. Int. Conf. on Positron Annihilation. Edited by R.R. HASIGUTI and K. FUJIWARA. Lake Yamanaka, April 8-11, 1979. (The Japan Inst. of Metals, Sendai) 383-386.

LÉVAY, B. and MOGENSEN, O.E. (1980). Chem. Phys. 53, 131-139.

LÉVAY, B., LUND, S.J.G. and MOGENSEN, O.E. (1980). Chem. Phys. 48, 97-104.

LÉVAY, B. (1979). At. Energy Rev. 17, 413-476.

LÉVAY, B. and VÉRTES, A. (1976). J. Phys. Chem. 80, 37-40.

LIGHTBODY, D., SHERWOOD, J.N. and ELDRUP, M. (1980). Chem. Phys. Lett. 70, 487-491.

LOVELAND, R.J., LE COMBER, P.G. and SPEAR, W.E. (1972). Phys. Lett. 39A, 225-226.

LUND, S.J.G. (1978). unpubl.

MARQUARDT, D.W. (1963). J. Soc. Ind. Appl. Math. 11, 431-441.

MEARS, W.H., ROSENTHAL, E. and SINKA, J.V. (1969). J. Phys. Chem. 73, 2254-2261.

MERRIGAN, J.A., GREEN, J.H. and TAO, S.J. (1972) In: Techniques of Chemistry, Vol. 1. Physical Methods of Chemistry, Part III D. Ed. by A. WEISSBERGER and B.W. ROSSITER. (Wiley, New York) 501-586.

MICHELSON, A.A. and MORLEY, E.W. (1887). Amer. J. Sci. 34, 333.

Mobility data

RYAN, T.G. et al. (1978). J. Chem. Phys. 68, 5144-5150. HUANG, S.S.-S. et al. (1980). J. Chem. Phys. 72, 2849-2855. GEE, N. et al. (1980). Phys. Rev. A 22, 301. BAKELE, G. et al. (1973). Z. Naturforsch. A 28, 511-518. DODELET, J.-P. et al. (1977). Can. J. Chem. 55, 2264-2277. CIPOLLINI, N.E. (1977). J. Chem. Phys. 67, 131-133. ROBINSON, M.G. et al. (1974). Can. J. Chem. 52, 440-446. YOSHINO, K. et al. (1976). SCHMIDT, W.E. (1977). Can. J. Chem. 55, 2197-2210.

MOGENSEN, O.E. (1981). private communication.

MOGENSEN, O.E. (1980). to be publ.

MOGENSEN, O.E. and LÉVAY, B. (1980). J. Phys. Chem. 84, 1296-1298.

MOGENSEN, O.E. (1979). Chem. Phys. Lett. 65, 511-514.

MOGENSEN, O.E. and ELDRUP, M. (1978). J. Glaciol. 21, 85-99.

MOGENSEN, E.O. and ELDRUP, M. (1977). Risø-Rep.-366, 72 pp.

MOGENSEN, O.E. (1975). Appl. Phys. 6, 315-322.

MOGENSEN, O.E. (1974). J. Chem. Phys. 60, 998-1004.

MOHOROVICIC, S. (1934). Astr. Nachr. 253, 94-

MOLIN, Y.N. and ANISIMOV, O.A. (1979). Positronium and Muonium Chemistry (Edited by H.J. ACHE) (Advances in Chemistry Series 175) (American Chemical Society. Washington D.C.) 179-202.

MOSZYNSKI, M. and BENGTSON, B. (1979). Nucl. Instrum. & Methods 158, 1-31.

NIEMINEN, R.M., VÄLIMAA, I., MANNINEN, M. and HAUTOJÄRVI, P. (1980). Phys. Rev. A 21, 1677-1686.

NYIKOS L., VAN DER ENDE, C.A.M., WARMAN, J.M. and HUMMEL, A. (1980) J. Phys. Chem. 84, 1154-1155.

ORE, A. (1950). Universitetet i Bergen. Årbok, Naturvidenskabelig Rekke 9, 15 pp.

OSMON, P.E. (1965). Phys. Rev. 140, A8 - A11.

PARA, A.F. and LAZZARINI, E. (1978). J. Inorg. Nucl. Chem. 40, 1473-1481.

PETERSEN, K., ELDRUP, M. and TRUMPY, G. (1970). Phys. Lett. A31, 109-110.

PIRENNE, J. (1947). Arch. Sci. Phys. Nat. 29, 121-150; 207-238.

RUARK, A.E. (1945). Phys. Rev. 68, 278

SCHMIDT, W.F. and ALLEN, O.A. (1970). J. Chem. Phys. 52, 2345-2351.

SHINSAKA, K., DODELET, J.-P. and FREEMAN, G.R. (1975). Can. J. Chem. 53, 2714-2728.

SKYTTE JENSEN, B. (1976). The 4th Int. Conf. on Positron Annihilation, Helsingør, August 23-26, 1976, preprint G16, 67-69.

TAO, S.J. (1972). J. Chem. Phys. 56, 5499-5510.

TIPTON, A.B., DEAM, A.P. and BOGGS, J.E. (1964). J. Chem. Phys. 40, 1144-1147.

WARMAN, J.M., INFELTA, P.P., DE HAAS, M.P. and HUMMEL, A. (1977). Can. J. Chem. 55, 2249-2257.

WEST, R.N. (1973). Advan. Phys. 22, 263-383.

WESTON, R.E. and SCHWARZ, H.A. (1972). Chemical Kinietics. (Prentice - Hall, New Jersey) 275 pp.

WHEELER, J.A. (1946). Ann N.Y. Acad. Sci. 48, 219-236.

WIKANDER, G. (1981). Chem. Phys. Lett. 77, 120-126.

WIKANDER, G. (1979). Chem. Phys. 39, 309-323.

Sales distributors:
Jul. Gjellerup, Sølvgade 87,
DK-1307 Copenhagen K, Denmark

Available on exchange from:
Risø Library, Risø National Laboratory,
P. O. Box 49, DK-4000 Roskilde, Denmark

ISBN 87-550-07!
ISSN 0106-2840